CHAPTER

Loudspeaker systems

7

CHAPTER OUTLINE

Acoustics: Sound Fields and Transducers. DOI: 10.1016/B978-0-12-391421-7.00007-5

PART XXI: SIMPLE ENCLOSURES

Loudspeaker enclosures are the subject of more controversy than any other item connected with modern high-fidelity music reproduction. Even though the behavior of enclosures is well understood, opinions and pseudo theories as to the effects of enclosures on loudspeaker response still persist. For instance, the very mention of directivity is guaranteed to spark a lively debate amongst audio engineers, with some favoring a wide pattern while others prefer a narrow pattern, although virtually all agree that a constant pattern is desirable to ensure that the room reflections produced by the off-axis sound have the correct frequency balance. Personal preferences aside, it could be that the choice depends on the program material. A narrow pattern with fewer room reflections allows the listener to hear the acoustics of the recording location more clearly, as well as the positions of the individual performers on the stage. Hence we might expect a narrow pattern to favor recordings made in a natural acoustic space such as a concert hall, church, or theatre. On the other hand, for close-miked studio recordings, a greater sense of presence and listener envelopment may be created by employing a wide pattern that produces many reflections around the room in order to produce some sense of a live performance, albeit in a flawed domestic listening space. After all, unlike the majority of loudspeakers, musical instruments do not generally fire in one direction only at higher frequencies. One thing that we cannot control is the fact that at low frequencies, where the wavelength is much larger than the diaphragm, loudspeakers are invariably omnidirectional, except for a few dipole/cardioid designs. More directive patterns at low frequencies come at the cost of reduced efficiency.

The design of an enclosure should be undertaken only with full knowledge of the characteristics of the loudspeaker and of the amplifier available, but fortunately most reputable manufacturers now provide the Thiele–Small parameters in their data sheets along with other useful figures such as sensitivity, $x_{\max}$, and power rating.

A large part of the difficulty of selecting a loudspeaker and its enclosure arises from the fact that the psychoacoustic factors involved in the reproduction of speech and music are not understood. Listeners will rank-order differently four apparently identical loudspeakers placed in four identical enclosures. It has been remarked that if one selects his own components, builds his own enclosure, and is convinced he has made a wise choice of design, then his own loudspeaker sounds better to him than does anyone else's loudspeaker. In this case, the frequency response of the loudspeaker seems to play only a minor part in forming a person's opinion.

Many working in the field of loudspeaker design believe that it is as much an art as a science because it involves many choices which reflect personal preferences such as maximum loudness versus bass extension, physical size, directivity characteristics, and so forth. In this chapter, we shall discuss only the physics of the problem. Designers should be able to achieve, from this information, any reasonable frequency-response curve that they may desire. Further than that, they will have to seek information elsewhere or to decide for themselves which shape of frequency-response curve will give greatest pleasure to themselves and to other listeners.

With the information of this chapter, the high-fidelity enthusiast should be able to calculate, if he or she understands AC circuit theory, the frequency-response curve for his or her amplifier-loudspeaker-baffle combination. Design graphs are presented to simplify the calculations, and three complete examples are worked out in detail. Unfortunately, the calculations are sometimes tedious, but there is no short cut to the answer.

7.1 BRIEF SUMMARY OF COMMON LOUDSPEAKER SYSTEMS

In the sections that follow, information is given on the detail design of loudspeaker systems. A brief summary of the four most common systems is given here as an aid to understanding the relative advantages of each of those that are discussed.

Loudspeaker in closed box. It is not practical to mount a loudspeaker in the wall of a residence. Alternatively, an unbaffled speaker would behave like a dipole radiator and at low frequencies would radiate little power. To eliminate radiation from the rear side, all loudspeakers before 1950 were mounted in a simple box. In the equivalent circuit, see Fig. 7.1a, the presence of the box appears as a series compliance C_{MB} which equals $S_D{}^2V_B/1.4P_0$, where V_B is the volume of the box. Its presence raises the speaker's resonance frequency above that if it were in an infinite baffle. Obviously, to minimize this increase, the volume of the box must be made very large. Historically, increasing the compliance C_{MS} to compensate would result in too large an excursion of the voice coil at low frequencies.

Air-suspension loudspeaker system. A unique solution to box size came with the perception that if the suspension compliance C_{MS} were made very large, the compliance of the box C_{MB} (i.e., its volume) could be made much smaller, actually equaling the magnitude of the C_{MS} of the usual loudspeaker, A different method of suspending the cone was used and, after about 1950, box volumes were often as small as 20 liters.

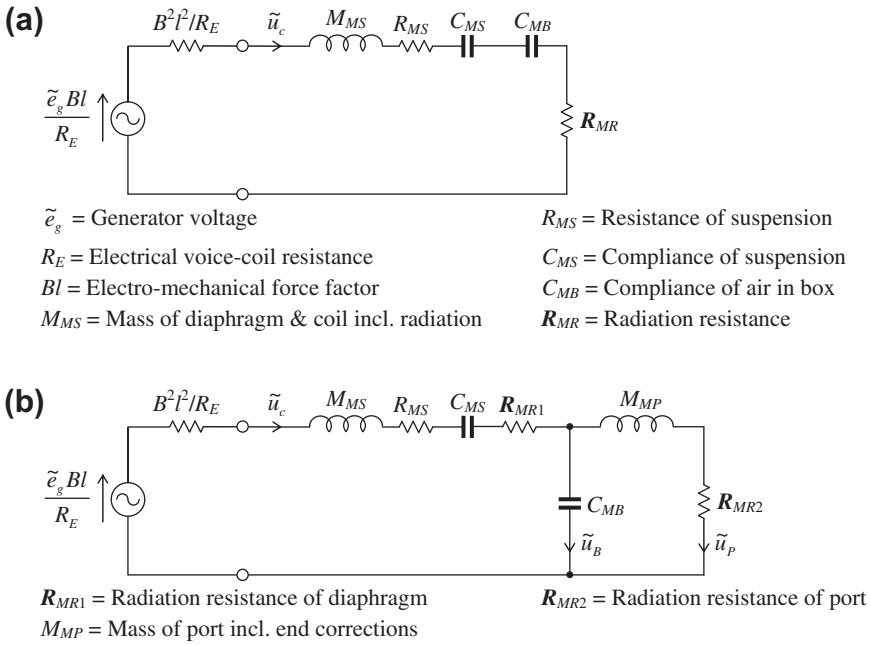

FIG. 7.1 Low-frequency analogous circuits for (a) a closed-box loudspeaker and (b) a bass-reflex loudspeaker with electrical quantities referred to mechanical side.

For simplicity, generator, box, leakage, and port resistances are omitted.

Bass-reflex loudspeaker system. The bass-reflex system is a means for obtaining a greater response at low frequencies than that from the same loudspeaker in a closed box. Actually, it is often used to boost the output at low frequencies from a system using a relatively small box. Its special feature is a port in the box from which sound emerges that adds to that directly radiated by the loudspeaker. The port is a tube with a cross-section area about equal to the area of the loudspeaker cone and a length that is chosen to give the desired resonance frequency.

The simplified equivalent circuit is shown in Fig. 7.1b. Two resonant frequencies occur: that of the loudspeaker (ω_0) and that of the box/port. Usually, $M_{MS}C_{MS} = M_{MP}C_{MB} = 1/\omega_0$. At ω_0, $\tilde{u}_c$ approaches zero and $\tilde{u}_P$ becomes very large. Below ω_0, $\tilde{u}_c$ and $\tilde{u}_P$ are out of phase and the response is not enhanced by the addition of the port. But, for one to two octaves above ω_0 the response is usually enhanced by about 5 dB.

Transmission-line enclosures. A transmission-line enclosure is the result of research leading to a small box containing a small loudspeaker and yet producing a strong bass sound. The box may have a volume as little as 2 liters. The loudspeaker-drive unit usually has a stiff cone with a diameter between 5 cm and 12 cm and its voice coil is capable of large excursions without generating appreciable distortion. The front side of the cone radiates directly into the listening space. Connected to the rear side is a tube whose length is 1/4th that of the lowest desired bass frequency, and the open end of which also radiates into the listening space. A small displacement of the cone will result in a large displacement of the air particles at the end of the tube. For strong bass at 100 Hz this means a length of 86 cm. The difficulty in the overall design of the system, is that the tube also resonates at frequencies higher than the 100 Hz. Their strength at the opening end of the tube is diminished by tapering the tube and filling it with a porous acoustical material of low flow resistance.

7.2 UNBAFFLED DIRECT-RADIATOR LOUDSPEAKER

A baffle is a structure for shielding the front-side radiation of a loudspeaker diaphragm from the rear-side radiation which can potentially cancel it at low frequencies. The necessity for shielding the front side from the rear side can be understood if we consider that an unbaffled loudspeaker at low frequencies is the equivalent of a pair of simple spherical sources of equal strength located near each other and pulsing out of phase (see Fig. 7.2). The rear side of the diaphragm of the loudspeaker is equivalent to one of these sources, and the front side is equivalent to the other.

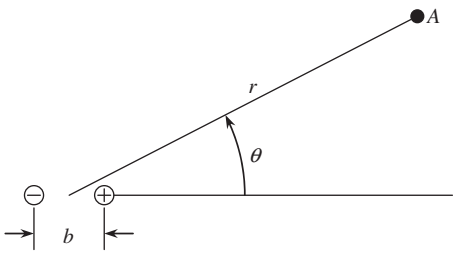

FIG. 7.2 Doublet sound source equivalent at low frequencies to an unbaffled vibrating diaphragm.

The point *A* is located a distance *r* and at an angle θ with respect to the axis of the loudspeaker.

If we measure, as a function of frequency f, the magnitude of the rms sound pressure p at a point A, fairly well removed from these two sources, and if we hold the volume velocity of each constant, we find from Eq. (4.117) that

$$\left|\tilde{p}\right| = -\frac{\rho_0 f^2 \left|\tilde{U}_0\right| b\pi}{rc} \cos\theta \tag{7.1}$$

where

$|\tilde{U}_0|$ is strength of each simple source in m^3/s.
b is separation between the simple sources in m.
ρ_0 is density of air in kg/m^3 (1.18 kg/m^3 for ordinary temperature and pressure).
r is distance in m from the sources to the point A. It is assumed that $r >> b$.
θ is angle shown in Fig. 7.2.
c is speed of sound in m/s (344.8 m/s, normally).

In other words, for a constant-volume velocity of the loudspeaker diaphragm, the pressure $\tilde{p}$ measured at a distance r is proportional to the square of the frequency f and to the cosine of the angle θ and is inversely proportional to r. In terms of decibels, the sound pressure $\tilde{p}$ increases at the rate of 12 dB for each octave (doubling) in frequency.

In the case of an actual unbaffled loudspeaker, below the first resonance frequency where the system is stiffness-controlled, the velocity of the diaphragm is not constant but doubles with each doubling of frequency. This is an increase in velocity of 6 dB per octave. Hence, the pressure $\tilde{p}$ from a loudspeaker *without* a baffle increases $12 + 6 = 18$ dB for each octave increase in frequency. Above the first resonance frequency, where the system is mass-controlled, the velocity of the diaphragm decreases 6 dB for each octave in frequency. Hence, in that region, the pressure $\tilde{p}$ increases $12 - 6 = 6$ dB for each octave increase in frequency and we can use the curve shown in Fig. 13.22 for an unbaffled circular piston ($b = a$), which turns out to be the magnitude of the radiation impedance shown in Fig. 4.38.

The unbaffled loudspeaker has the same analogous circuit as that shown in Fig. 6.4 for a loudspeaker in an infinite baffle except that the radiation impedance is given by Fig. 4.38 and the on-axis pressure is proportional to the total radiation *force* $\tilde{f}_R$ as opposed to the *volume acceleration*. The on-axis pressure is given by Eq. (13.128) if we let $\tilde{p}_0 = \tilde{f}_R/S_D$. Although this is an expression for a resilient disk (uniform pressure), it will be shown in Sec. 13.10 that it is the same as that for a rigid disk (uniform velocity) if we let $\tilde{p}_0 = 2Z_{AR}\tilde{U}_0$. Hence we find that the on-axis pressure is the same as that given by Eq. (6.31) multiplied by $S_D Z_{AR}/(\rho_0 c)$. In other words, if the diaphragm acceleration is constant, the on-axis response is simply the magnitude of the radiation impedance shown in Fig. 4.38.

The absence of a baffle makes the loudspeaker more directional because, in the plane of the baffle, the sound pressure tends to reduce to zero. Hence there are fewer reflections from side walls. This figure 8 directivity pattern may be used to extend the width of the stereo "sweet spot" in a room. If the listener moves towards one side of the listening area, he or she will move further off the main axis of the nearest loudspeaker than that of the furthest one. Hence the sound pressure of the nearest loudspeaker will be reduced automatically relative to that of the furthest one, which will compensate for its proximity.

Certain kinds of loudspeaker that have very low moving mass, such as electrostatic or planar magnetic types, are used almost exclusively without a baffle because the extra stiffness provided by a closed box would push the fundamental resonance frequency up too high. The problem of low-frequency cancellation is compensated for by using a very large radiating area. Full-range electrostatic or planar magnetic loudspeakers have radiating areas of at least 0.5 m^2.

7.3 INFINITE BAFFLE

In the previous chapter we talked about direct-radiator loudspeakers in infinite baffles. Reference to Fig. 6.7 reveals that with an infinite baffle, the response of a direct-radiator loudspeaker is enhanced over that just indicated for no baffle. It was shown that if one is above the suspension resonance frequency, but below the first diaphragm break-up mode, usually the response is flat with frequency (unless the *Bl* product is very large) and that if one is below the first resonance frequency the response decreases at the rate of 12 dB per octave instead of 18 dB per octave. Hence, the isolation of the front side from the back side by an infinite baffle is definitely advantageous.

In practice, the equivalent of an infinite baffle is a very large enclosure, well damped by absorbing material. One practical example is to mount the loudspeaker in one side of a closet filled with clothing, allowing the front side of the loudspeaker to radiate into the adjoining listening room.

Design charts covering the performance of a direct-radiator loudspeaker in an infinite baffle are identical to those for a closed box. We shall present these charts in Sec. 7.6.

7.4 FINITE-SIZED FLAT BAFFLE

The discussion above indicated that it is advisable to shield completely one side of the loudspeaker from the other, as by mounting the loudspeaker in a closet. Another possible alternative is to mount the loudspeaker in a flat baffle of finite size, free to stand at one end of the listening room. The worst shape for such a baffle is circular because sound from the rear arrives at the front at the same time whichever radial path is taken. Hence at some frequencies, where the radial path length is a multiple of the wavelength λ, the front radiation is partially canceled and we have a comb filter effect, as shown in Fig. 13.22. The effect is considerably smeared if we use a rectangular baffle with the drive unit offset from the center as is the case with the IEC 268-5 baffle. [38]

The performance of a loudspeaker in a free-standing flat baffle leaves much to be desired, however. If the wavelength of a tone being radiated is greater than twice the smallest lateral dimension of the baffle, the loudspeaker will act according to Eq. (7.1). This means that for a finite flat baffle to act approximately like an infinite baffle at 50 Hz, its smallest lateral dimension must be about 3.5 m (11.5 ft), which limits its use to mid-range units or above. However, even above this frequency, sound waves traveling from behind the loudspeaker reflect off walls and meet with those from the front and cause alternate cancellations and reinforcements of the sound as the two waves come into phase or out of phase at particular frequencies in particular parts of the room. Hence, the loudspeaker must be located away from walls or reflecting objects in order to minimize this effect.

7.5 OPEN-BACK CABINETS

An open-back cabinet is simply a box with one side missing and with the loudspeaker mounted in the side opposite the open back. Many portable stereos are of this type. Such a cabinet performs nearly the same as a flat baffle that provides the same path length between the front and back of the loudspeaker. One additional effect, usually undesirable, occurs at the frequency where the depth of the box approaches a quarter wavelength. At this frequency, the box acts as a resonant tube, and more power is radiated from the rear side of the loudspeaker than at other frequencies. Furthermore, the sound from the rear may combine in phase with that from the front at about this same frequency, and an abnormally large peak in the response may be obtained.

7.6 CLOSED-BOX BAFFLE [1,2]

The most commonly used type of loudspeaker baffle is a closed box in one side of which the loudspeaker is mounted. In this type, discussed here in considerable detail, the back side of the loudspeaker is completely isolated from the front. A customary type of closed-box baffle is shown in Fig. 7.3. The sides are made as rigid as possible using some material like 5-ply plywood or MDF, 0.75 to 1.0 inch thick and braced to prevent resonance. A slow air leak must be provided in the box so that changes in atmospheric pressure do not displace the neutral position of the diaphragm.

When selecting a loudspeaker, the first two questions that arise are how loud must it go and what bass cut-off frequency can be tolerated? This of course will depend on the application and the radiated sound pressure will need to be greater for an auditorium than for a domestic living room. For a cell-phone ring tone, it must be possible to hear it in a noisy street environment. In general, the low-frequency sound pressure is limited by the displacement limit x_{max} and the high-frequency sound pressure is limited by the power rating. In fact, at higher frequencies the situation is worse because at least the larger low-frequency displacement pumps air through the magnetic gap, which helps to cool the voice coil. If the suspension alone is not stiff enough to limit the full-power displacement at low

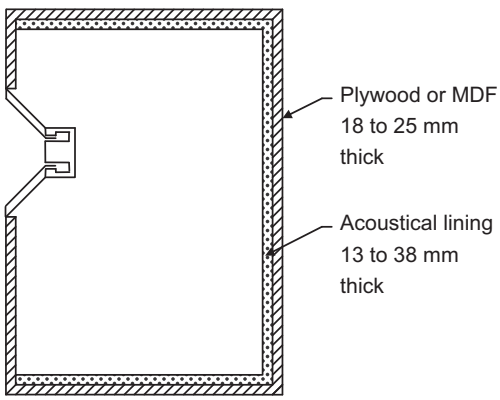

FIG. 7.3 Typical plywood box with loudspeaker mounted off center in one side and lined with a layer of soft absorbent acoustical material.

frequencies, then part of the function of the box is to provide the extra stiffness needed to keep the displacement in check. Otherwise, an auxiliary high-pass filter must be employed. As more stable suspension materials have been developed, the trend has been towards more compliant suspensions so that an ever greater proportion of the stiffness can be provided by air in the box which in turn makes the volume of the box correspondingly smaller. This principle is known as *air suspension* [37].

Summary of closed-box baffle design

To determine the volume of the closed box and the − 3 dB cut-off frequency:

If the Thiele-Small parameters (R_E, Q_{ES}, Q_{MS}, f_S, S_D, and V_{AS}) of the chosen drive unit are not supplied by the manufacturer, they may be measured according to Sec. 6.10. Then $Q_{TS} = Q_{ES}Q_{MS}/(Q_{ES} + Q_{MS})$.

From Table 7.2, select the frequency-response shape, taking into account that the closed-box Q_{TC} value must be higher than the infinite-baffle Q_{TS} of the drive unit. The effect of various Q_{TC} values upon the frequency-response shape can be seen from Fig. 7.16. Further advice regarding Q_{TC} is given in the paragraph following Eq. (7.56).

Estimate the volume of air in the box V_A using Eq. (7.61). However, if the box is filled or has a thick lining, then the Q_{TC} value will be modified. Using the manufacturer's or measured value of flow resistance R_f for the lining material, compute R_{AB} from Eq. (7.7) and Q_{MB} from Eq. (7.58). Determine the volume V_A from Eq. (7.60). The total internal volume is then $V_B = V_A + V_M$, where V_M is the volume of the lining material.

Determine the closed-box resonance frequency f_C from Eq. (7.28). From the value of f_{3dB}/f_C given in Table 7.2, compute the cut-off frequency f_{3dB}.

To determine the maximum sound pressure level (SPL):

If the loudspeaker is to be used near a wall or a rigid planar surface, which is large compared to the longest wavelength to be reproduced, then the maximum sound pressure SPL_{max} is obtained from Eq. (6.34) to give

$$\text{SPL}_{\text{max}} = 20 \log_{10} \left(\frac{1}{rc \times 20 \times 10^{-6}} \sqrt{\frac{Z_{\text{nom}} W_{\text{max}} 2\pi f_S^3 V_{AS} \rho_0}{R_E Q_{ES}}} \right) \text{ dB SPL @ 1 m}$$

where W_{max} is the maximum rated input power. Otherwise, if it is to be used in the free field, subtract 6 dB from SPL_{max}.

To determine the excursion limit:

The maximum peak diaphragm displacement at frequencies well below the closed-box resonance is obtained from Eq. (7.64) to give

$$\eta_{\text{max}} = \frac{1}{S_D c(1 + V_{AS}/V_{AB})} \sqrt{\frac{Z_{\text{nom}} W_{\text{max}} V_{AS}}{R_E Q_{ES} \pi f_s \rho_0}}$$

However, we see from Fig. 7.17 that at frequencies below the closed-box resonance, the displacement peaks at a higher value in the case of Chebyshev alignments. For example, the displacement peaks at $1.4\eta_{\text{max}}$ in the case of the 3-dB Chebyshev alignment or $2\eta_{\text{max}}$ in the case of the 6-dB Chebyshev alignment. If this peak value is greater than the rated x_{max} limit of the drive unit, then it should be arranged for the box resonance frequency f_C to be placed below the lower limit of the frequency range of the program material to be reproduced. If this is not possible, a high-pass filter should be employed to remove all content below the box resonance frequency. If this is not possible either, then an alternate drive unit with a greater x_{max} limit should be considered.

Fig. 7.4 shows the effective diameter of a drive unit required to achieve a given sound pressure level, with a peak displacement of 1 mm, when radiating omnidirectionally into free space from a closed-box enclosure. This is obtained from Eq. (6.35), but adjusted by a factor of $\sqrt{2}$ for free-space omnidirectional radiation. Hence, for loudspeakers which are to be placed near a wall, the required

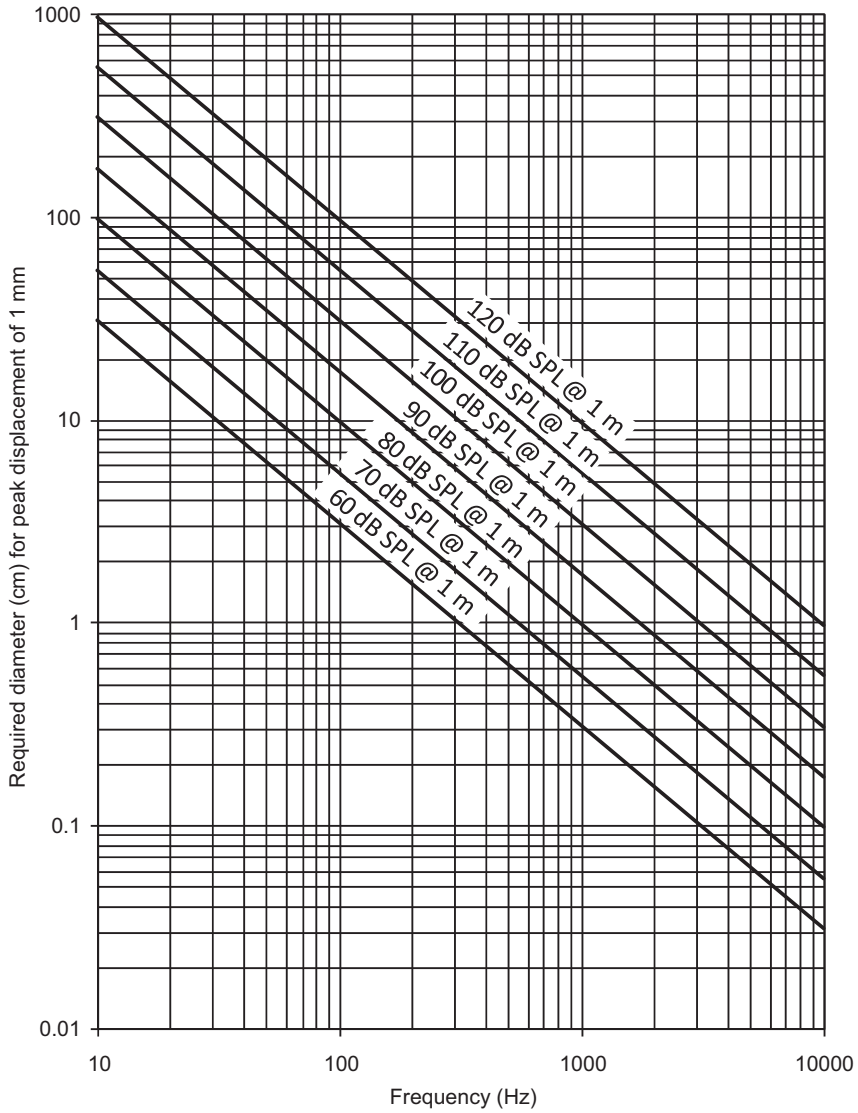

FIG. 7.4 Drive unit effective diameter required to produce a given sound pressure level, with a peak displacement of 1 mm, when radiating omnidirectionally into free space from a closed-box enclosure.

If the peak displacement is quadrupled (say a peak displacement of 4 mm is allowed), then the required diameter is halved.

diameter should be divided by $\sqrt{2}$. Because the diameter has an inverse square-root relationship with the displacement, quadrupling the peak displacement halves the required diameter. Hence there has been a trend towards smaller drive units with greater $x_{\max}$ values, usually achieved by extending the coil beyond the magnetic gap, although this reduces sensitivity and efficiency. Considering that the maximum effective diameter of an individual drive unit is around 40 cm, the difficulty of producing very low frequencies at high sound pressures is evident. For large auditoriums, the very large diameters are made up by stacking multiple loudspeakers.

Analogous circuit. A closed box reacts on the back side of the loudspeaker diaphragm. This reaction may be represented by an acoustic impedance which at low frequencies is a compliance operating to stiffen the motion of the diaphragm and to raise the resonance frequency. At high frequencies, the reaction of the box, if unlined, is that of a multiresonant circuit. This is equivalent to an impedance that varies cyclically with frequency from zero to infinity to zero to infinity, and so on. This varying impedance causes the frequency-response curve to have corresponding peaks and dips.

If the box is lined with a sound-absorbing material, these resonances are damped and at high frequencies the rear side of the diaphragm is loaded with an impedance equal to that for the diaphragm in an infinite baffle radiating into free space. The acoustical circuit for the box and radiation load on the diaphragm is given in Fig. 7.5. The reactance and resistance of the box are X_{AB} and R_{AB}. The radiation mass and resistance on the front of the diaphragm are M_{AR} and R_{AR} respectively.

At low frequencies, where the diaphragm vibrates as one unit so that it can be treated as a rigid piston, a complete electro-mechano-acoustical circuit can be drawn that describes the behavior of the box-enclosed loudspeaker. This circuit is obtained by combining Fig. 6.4(b) and Fig. 7.5. To do this, the acoustical radiation element of the circuit labeled "$2M_{M1}$" in Fig. 6.4(b) is removed, and the circuit of Fig. 7.5 is substituted in its place. The resulting circuit with the transformer removed and everything referred to the acoustical side is shown in Fig. 7.6.

Some interesting facts about loudspeakers are apparent from this circuit. First, the electrical generator (power amplifier) resistance R_g and the voice-coil resistance R_E appear in the denominator of one of the resistances shown. This means that if one desires a highly damped or an overdamped system, it is possible to achieve this by using a power amplifier with very low output impedance. Second, the

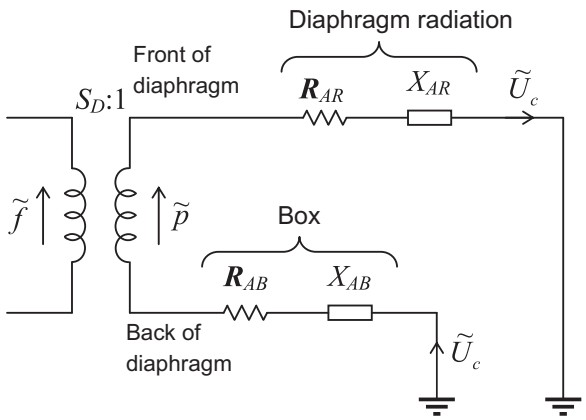

FIG. 7.5 Analogous acoustical circuit for a loudspeaker box. The volume velocity of the diaphragm is $\tilde{U}_C$.

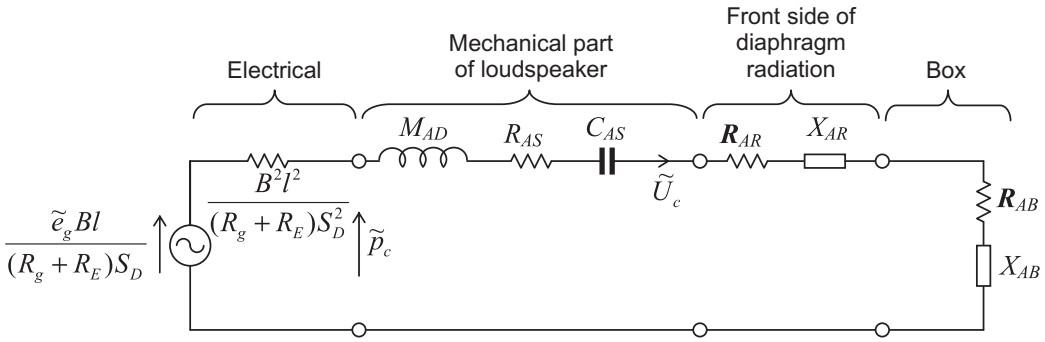

FIG. 7.6 Circuit diagram for a direct-radiator loudspeaker mounted in a closed-box baffle. This circuit is valid for frequencies below about 400 Hz.

circuit is of the simple resonant type so that we can solve for the voice-coil volume velocity (equal to the linear velocity times the effective area of the diaphragm) by the use of universal resonance curves. Our problem becomes, therefore, one of evaluating the circuit elements and then determining the performance by using standard theory for electrical series *LRC* circuits.

Values of electrical-circuit elements. All the elements shown in Fig. 7.6 are in units that yield acoustic impedances in $\mathrm{N \cdot s/m^5}$, which means that all elements are transformed to the acoustical side of the circuit. This accounts for the effective area of the diaphragm S_D appearing in the electrical part of the circuit. The quantities shown are:

$\tilde{e}_g$ is open-circuit voltage in V of the audio amplifier driving the loudspeaker.
B is flux density in the air gap in T ($1\ \mathrm{T} = 10^4$ gauss).
l is length of the wire wound on the voice coil in m.
R_g is output electrical impedance (assumed resistive) in Ω of the audio amplifier.
R_E is electrical resistance of the wire on the voice coil in Ω.
a is effective radius in m of the diaphragm.
$S_D = \pi a^2$ is effective area in $\mathrm{m^2}$ of the diaphragm.

Values of the mechanical-circuit elements. The elements for the mechanical part of the circuit differ here from those of Part XIX in that they are transformed over to the acoustical part of the circuit so that they yield acoustic impedances in $\mathrm{N \cdot s/m^5}$.

$M_{AD} = M_{MD}/{S_D}^2$ is acoustic mass of the diaphragm and voice coil in $\mathrm{kg/m^4}$.
M_{MD} is mass of the diaphragm and voice coil in kg.
$C_{AS} = C_{MS}{S_D}^2$ is acoustic compliance of the diaphragm suspensions in $\mathrm{m^5/N}$.
C_{MS} is mechanical compliance in m/N.
$R_{AS} = R_{MS}/{S_D}^2$ is acoustic resistance of the suspensions in $\mathrm{N \cdot s/m^5}$.
R_{MS} is mechanical resistance of the suspensions in $\mathrm{N \cdot s/m}$.

These quantities may readily be measured with a simple setup in the laboratory, as described in Sec. 6.10. It is helpful, however, to have typical values of loudspeaker constants available for rough computations, and these are shown in Fig. 7.7 and Fig. 7.8. The average value of R_E for a drive unit

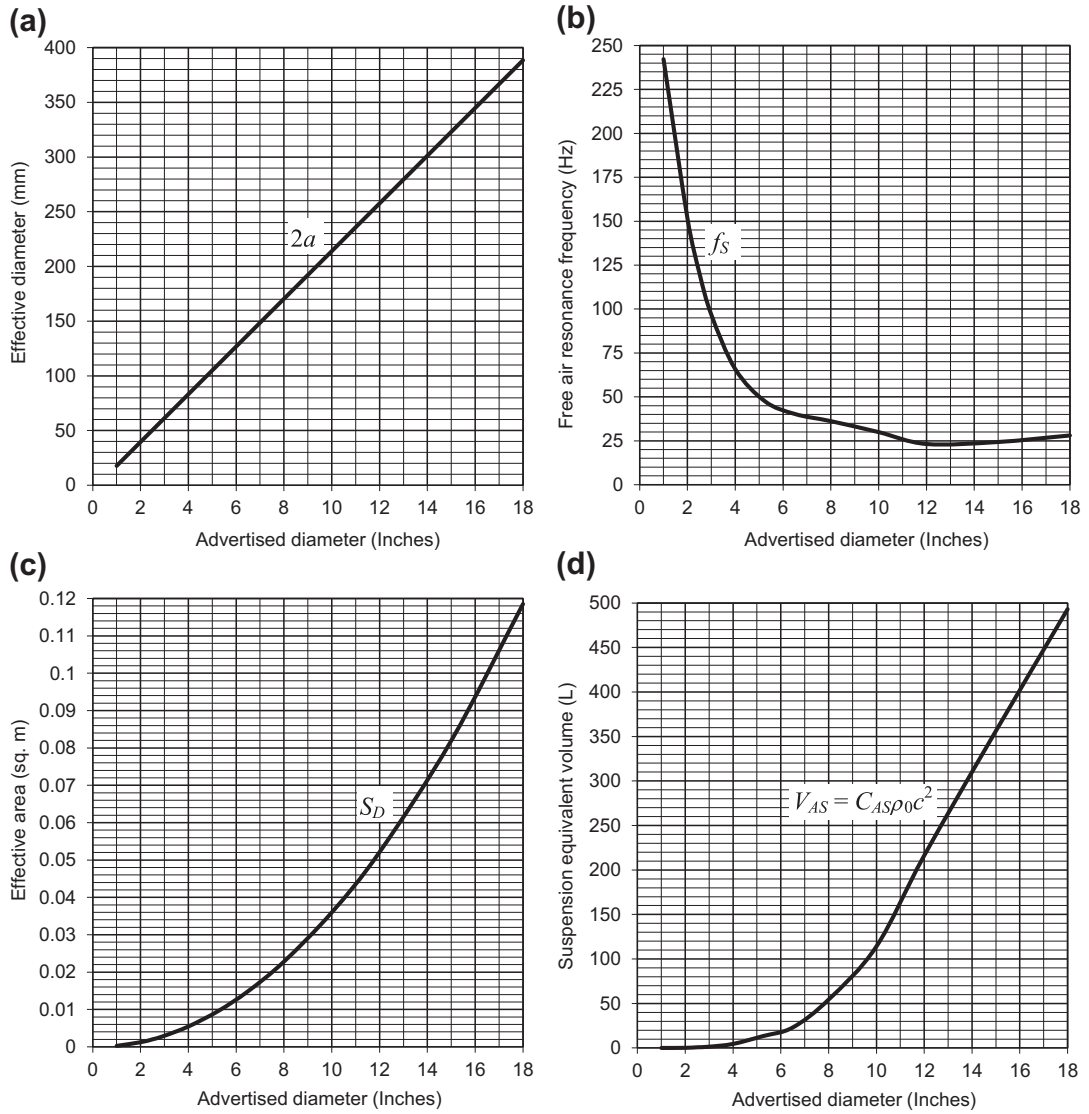

FIG. 7.7 (a) Relation between effective diameter of a loudspeaker and its advertised diameter. (b) Average resonance frequencies of direct-radiator loudspeakers when mounted in IEC 268-5 baffles [38] vs. the advertised diameters. (c) Average effective radiating areas of loudspeakers vs. the advertised diameters. (d) Average compliances of suspensions of loudspeakers vs. the advertised diameters, where the compliance is expressed as an equivalent volume in liters.

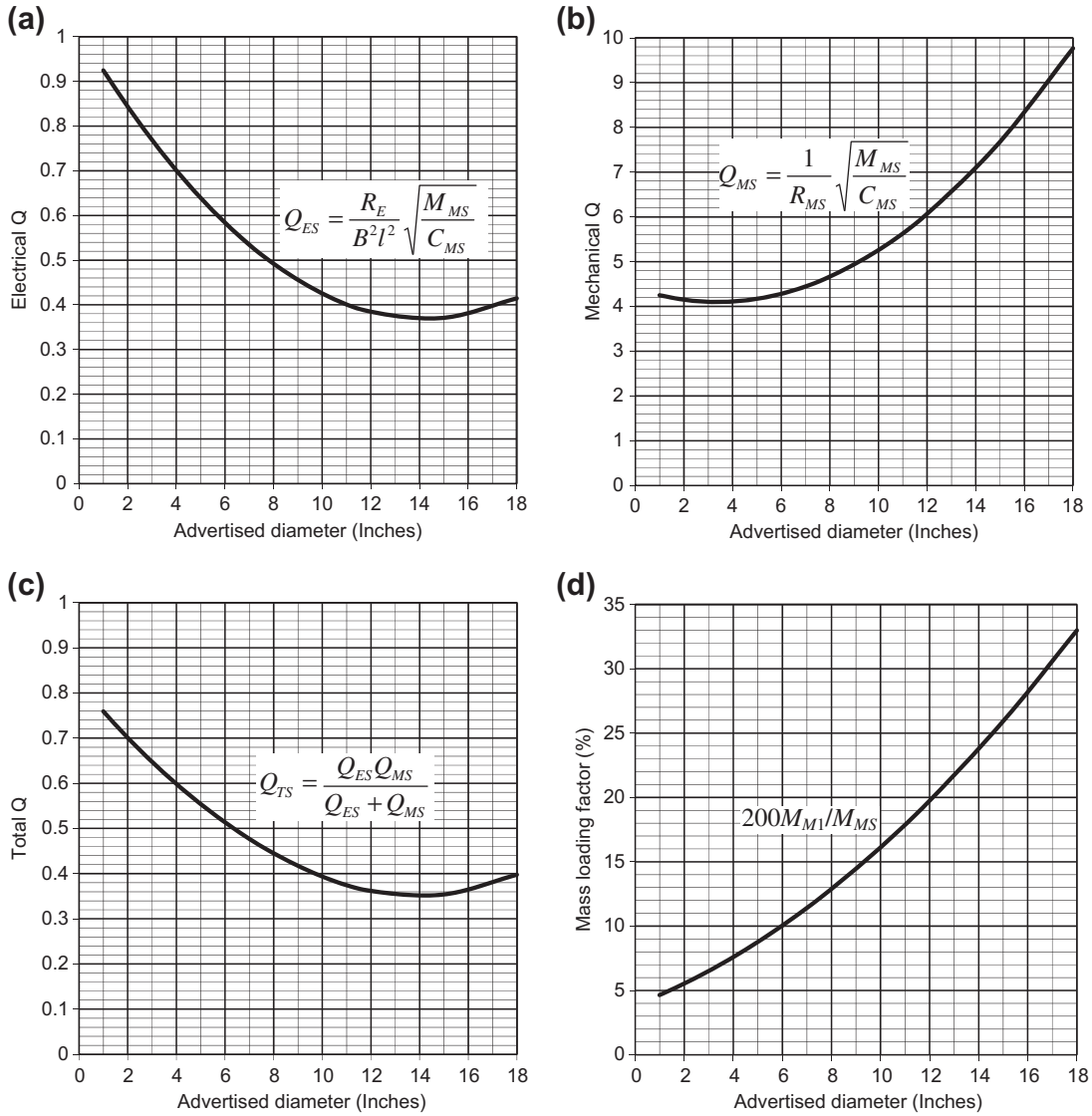

FIG. 7.8 (a) Average electrical Q_{ES} values of loudspeaker drive units vs. the advertised diameters. (b) Average mechanical Q_{MS} values of loudspeaker drive units vs. the advertised diameters. (c) Average total Q_{TS} values of loudspeaker drive units vs. the advertised diameters. (d) Average mass loading factors of loudspeaker drive units vs. the advertised diameters, where the mass loading factor is the ratio of the radiation mass on *both sides* in an infinite baffle ($2M_{M1}$) to the total moving mass of the drive unit (M_{MS}), where $M_{MS} = M_{MD} + 2M_{M1}$.

with an advertised impedance of 8 Ω is around 6.3 Ω. The magnitude of the air-gap flux density B varies from 0.6 to 1.4 T depending on the cost and size of the loudspeaker.

Impedance of closed box with absorbent lining. The type of reactance function shown in Fig. 7.12 without absorbent lining is not particularly desirable because of the very high value that X_{AB} reaches at the first normal mode of vibration (resonance) for the box, which occurs when the depth of the box equals one-half wavelength. A high reactance reduces the power radiated to a very small value. To reduce the magnitude of X_{AB} at the first normal mode of vibration, an acoustical lining is placed in the box. This lining should be highly absorbent at the frequency of this mode of vibration and at all higher frequencies. For normal-sized boxes, a satisfactory lining is a 25 mm-thick layer of bonded mineral wool, bonded Fiberglass, bonded hair felt, Cellufoam (bonded wood fibers), etc. For small cabinets, where the largest dimension is less than 0.5 m, a 12.5 mm-thick layer of absorbing material may be satisfactory.

At low frequencies, where the thickness of the lining is less than 0.05 wavelength, the impedance of the box presented to the rear side of the diaphragm is represented by the analogous circuit of Fig. 7.9 and equals

$$Z_{AB} = \boldsymbol{R}_{AB} + jX_{AB} \tag{7.2}$$

where

$$X_{AB} \approx \omega M_{AB} - \frac{1}{\omega(C_{AA} + C_{AM})} \tag{7.3}$$

and C_{AA} and M_{AB} are the acoustic compliance and mass respectively of the air inside the box given by

$$C_{AA} = \frac{V_A}{\gamma P_0} \tag{7.4}$$

$$M_{AB} = \frac{B\rho_0}{\pi a} \tag{7.5}$$

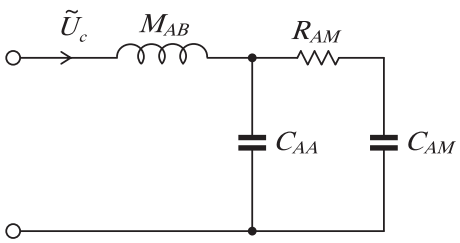

FIG. 7.9 Analogous circuit for the acoustic impedance Z_{AB} presented to the rear side of the diaphragm at low frequencies where the smallest dimension of the box is less than one-sixteenth wavelength.

The volume velocity of the diaphragm = $\tilde{U}_c$; M_{AB} = acoustic mass of the air load on the rear side of diaphragm; C_{AA} = acoustic compliance of the air in the box excluding the lining; C_{AM} = acoustic compliance of the air in the pores of the lining, R_{AM} = acoustic resistance of the lining.

where

V_A is volume of air in the box in m^3 excluding that contained within the pores of the lining material. The volume of the loudspeaker should also be subtracted from the actual volume of the box in order to obtain this number. To a first approximation, the volume of the speaker in m^3 equals $0.4 \times$ the fourth power of the advertised diameter in m.
$\gamma = 1.4$ for air for adiabatic compressions.
P_0 is atmospheric pressure in Pa (about 10^5 on normal days).
$\pi a = \sqrt{S_D \pi}$ if the loudspeaker is not circular.
B is a constant, given in Fig. 7.10 for a box of the type shown in Fig. 7.11, which is dependent upon the ratio of the effective area of the loudspeaker diaphragm S_D to the area L^2 of the side of the box in which it is mounted.

We see from Fig. 7.10 that when the diaphragm has the same area as the cross-sectional area of the box, that is $S_D/L^2 = 1$, the box becomes a closed tube of length $L/2$ and the mass load on the rear of the diaphragm is one third of the total mass in the box, so that $B = \sqrt{\pi}/6$. On the other hand, when the area of the diaphragm is very small compared to the cross-sectional area of the box, that is $S_D/L^2 \to 0$, the mass on the rear of the diaphragm is that of a piston in an infinite baffle so that $B \to 8/(3\pi)$.

It is assumed that the pressure variations in the pores of the lining material are isothermal so that the compliance of the lining material is given by

$$C_{AM} = \frac{V_M}{P_0} \tag{7.6}$$

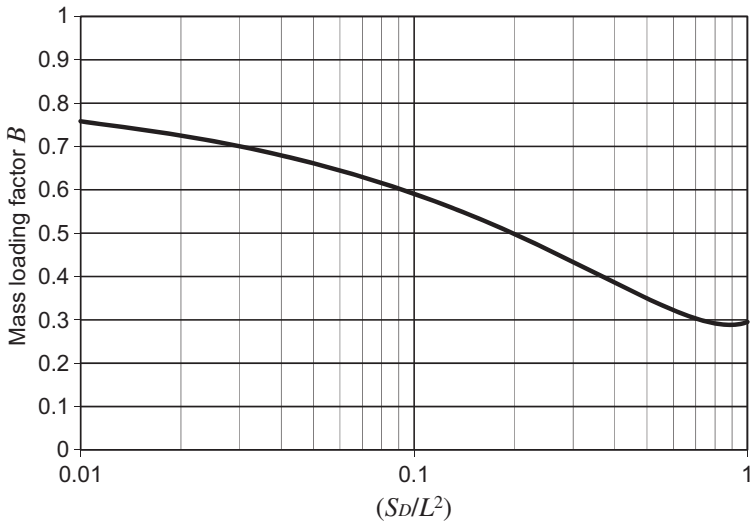

FIG. 7.10 End-correction factor *B* for the reactance term of the impedance at the rear side of the loudspeaker diaphragm mounted in a box of the type shown in Fig. 7.11.

The acoustic reactance of the box on the diaphragm is given by $X_{AB} = -\gamma P_0/\omega V_A + \omega B \rho_0/\pi a$. For a noncircular diaphragm of area S_D, $\pi a = \sqrt{S_D \pi}$.

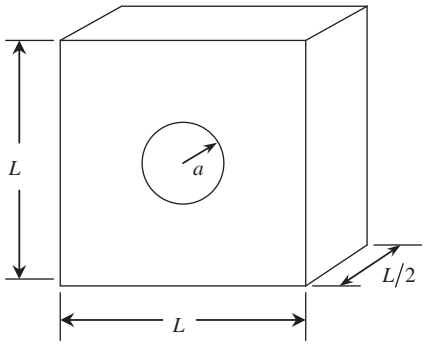

FIG. 7.11 Loudspeaker mounted in a closed box with internal dimensions $L \times L \times L/2$ when unlined and a diaphragm of area $S_D = \pi a^2$ at the center of the $L \times L$ face where $L^2/S_D = 16$.

When lining of thickness $d = L/10$ is added to the rear surface, the internal depth is increased to $0.6L$. While this type of box is convenient for analysis, the construction shown in Fig. 7.3 is more commonly used.

where V_M is the total volume of the pores. Then from Fig. 7.9 the resistance is defined by

$$\begin{aligned} \boldsymbol{R}_{AB} &= \Re\left(\left(j\omega C_{AA} + \frac{1}{R_{AM} + (j\omega C_{AM})^{-1}}\right)^{-1}\right) \\ &= \frac{R_{AM}}{\left(1 + \dfrac{V_A}{\gamma V_M}\right)^2 + \omega^2 R_{AM}^2 C_{AA}^2} \end{aligned} \tag{7.7}$$

where

$R_{AM} = dR_f/(3S_M)$ is one-third of the total flow resistance of a layer of thickness d of the acoustical material that lines the box divided by the area of the acoustical material S_M. The units are $\mathrm{N \cdot s/m^5}$. The flow resistance equals the ratio of the pressure drop across the sample of the material to the linear air velocity through it. For lightweight materials the flow resistance R_f is about 100 rayls for each 25 mm of thickness. For dense materials like PF Fiberglass board or rockwool duct liner, the flow resistance may be as high as 2000 rayls for each 25 mm of thickness of the material. For example, if the flow resistance per 25 mm of material is 500 rayls, the thickness 75 mm, and the area $0.2\mathrm{m}^2$, then $R_{AM} = 1500/(3 \times 0.2) = 2500\ \mathrm{N \cdot s/m^5}$.
It is assumed in writing this equation that the material does not occupy more than 20% of the volume of the box.

Sound propagation in homogeneous absorbent materials [3]. The sound propagation in fibrous or porous acoustical materials can be described with a relatively simple analytical model if the constituent (the solid part of the material) is assumed to be rigid [4]. A model taking into account the flexibility of the constituent [5] would better describe behavior of the relatively low-density absorbents used in loudspeakers, but such a model requires parameters that are quite difficult to obtain. A good empirical description of sound propagation in absorbents has been presented by Delany and Bazley

[6], with extensions by Miki [7]. Flow resistance is needed to compute the acoustical properties of a porous material. It can be determined, when the porosity and the average (rms) fiber diameter are known, by using an equation derived by Sides et al. [8]:

$$R_f = \frac{\Delta p}{ud} = \frac{4\mu(1-\varphi)}{\varphi r^2}\left(\frac{1-\frac{4}{\pi}(1-\varphi)}{2+\ln\frac{\mu\varphi}{2r\rho_0 u}}+\frac{6}{\pi}(1-\varphi)\right) \tag{7.8}$$

where

R_f is flow resistance of material in rayls/m.
Δp is pressure difference across material in Pa.
u is flow velocity in the material in m/s.
d is thickness of the material in m.
μ is viscosity coefficient. For air $\mu = 1.86 \times 10^{-5}$ N·s/m^2 at 20°C and 0.76 m Hg.
φ is porosity of the material.
r is fiber diameter (rms average).
ρ_0 is density of air in kg/m^3.

As Eq. (7.8) shows, the flow resistance is a function of flow velocity. Equation (7.8) is actually the equation of the static flow resistance, and so with sound the rms value of flow velocity should be used. With flow velocities associated with sound pressures of interest the variation of the flow resistance is rather small, and so this nonlinear effect can be ignored and a typical value of flow velocity can be used; Sides et al. recommend a value of $u = 0.03$ m/s. If the flexibility of the constituent were taken into account, the resistance values would be somewhat lower. The porosity φ is defined as the proportion of the constituent material to the total volume the absorbent and is defined by

$$\varphi = 1 - \frac{\rho_M}{\rho_C} \tag{7.9}$$

where

ρ_M is density of absorbent material in kg/m^3.
ρ_C is density of the constituent material (e.g. glass 2200–2900 kg/m^3).

Typical values of porosity in acoustical absorbents range from 0.95 to 0.99. When the flow resistance is determined, then the characteristic impedance Z_s can be determined by

$$Z_s = \rho_0 c\left\{\left(1+a_1\left(\frac{R_f}{f}\right)^{b_1}\right)-ja_2\left(\frac{R_f}{f}\right)^{b_2}\right\} \tag{7.10}$$

and the wave number $\boldsymbol{k}$ by

$$\boldsymbol{k} = \frac{\omega}{c}\left\{\left(1+a_3\left(\frac{R_f}{f}\right)^{b_3}\right)-ja_4\left(\frac{R_f}{f}\right)^{b_4}\right\} \tag{7.11}$$

where

ρ_0 is density of air in kg/m^3.
c is speed of sound in air in m/s.

f is frequency in Hz.
ω is angular frequency ($2\pi f$).
α is real part of the propagation coefficient.
β is imaginary part of the propagation coefficient.
and the coefficients a_1 to b_4 are given in Table 7.1

The original coefficients given by Delany and Bazley give an excellent match to experimental results when $0.01 < f/R_f < 1$, but the coefficients should not be used for extrapolation outside this range; using these coefficients with low values of flow resistance and frequency (such as those usually applied in loudspeakers) can yield negative values of attenuation. In such cases the coefficients given by Miki should be used instead. The lower limit of validity for Miki's equations is $f/R_f > 0.0005$. Other conditions for validity of these equations is that the porosity is close to unity and that the flow resistance R_f is between 20 and 800 rayls/cm. In practice the soft bulk fibrous absorbents, like natural and synthetic organic fibers and soft glass wool, used in loudspeakers meet these additional conditions. The more rigid absorbent sheets commonly used for room acoustics treatment have anisotropic acoustical characteristics and these models cannot be applied as such.

Impedance of closed box with or without absorbent lining at all frequencies. Until now we have only dealt with low frequencies using the circuit shown in Fig. 7.9, which is valid when the wavelength is greater than 8 times the smallest dimension of the box. In order to see the effect of the internal standing wave modes upon the impedance or to investigate the effect of placing lining material on the rear surface, we need a full model of the enclosed space. Such a model will be developed in Sec. 7.18 resulting in Eq. (7.131) for the self and mutual impedances of a closed box with two pistons in one wall and an impedance boundary condition on the opposite wall as shown in Fig. 7.34. The second piston is intended to represent the coupling to a bass-will reflex port. The width, length, and depth of the box are l_x, l_y, and l_z respectively. The dimensions of the pistons are $a_1 \times b_1$ and $a_2 \times b_2$. However, for a closed box with no bass-reflex port, we just use z_{11} and divide through by $a_1^2 b_1^2$ to obtain the acoustic impedance which is in the form of an eigenfunction expansion:

Table 7.1 Values of coefficients used in Eqs. (7.10) and (7.11) for characteristic impedance and wave number respectively of a homogenous absorbent material

Coefficient	Delaney & Bazley	Miki
a_1	0.0511	0.070
a_2	0.0768	0.107
a_3	0.0858	0.109
a_4	0.175	0.160
b_1	0.75	0.632
b_2	0.73	0.632
b_3	0.70	0.618
b_4	0.59	0.618

$$Z_{AB} = \rho_0 c \left\{ \frac{1}{l_x l_y} \frac{\frac{Z_s}{\rho_0 c} + j \tan kl_z}{1 + j \frac{Z_s}{\rho_0 c} \tan kl_z} + \frac{2l_x}{\pi^2 a_1{}^2 l_y} \sum_{m=1}^{\infty} \frac{k}{m^2 k_{m0}} \sin^2\left(\frac{m\pi a_1}{l_x}\right) \frac{\frac{k_{m0} Z_s}{k\rho_0 c} + j \tan k_{m0} l_z}{1 + j \frac{k_{m0} Z_s}{k\rho_0 c} \tan k_{m0} l_z} \right.$$

$$+ \frac{8l_y}{\pi^2 b_1{}^2 l_x} \sum_{n=1}^{\infty} \frac{k}{n^2 k_{0n}} \cos^2\left(\frac{n\pi y_1}{l_y}\right) \sin^2\left(\frac{n\pi b_1}{2l_y}\right) \frac{\frac{k_{0n} Z_s}{k\rho_0 c} + j \tan k_{0n} l_z}{1 + j \frac{k_{0n} Z_s}{k\rho_0 c} \tan k_{0n} l_z}$$

$$\left. + \frac{16 l_x l_y}{\pi^4 a_1^2 b_1^2} \sum_{m=1}^{\infty} \sum_{n=1}^{\infty} \frac{k}{m^2 n^2 k_{mn}} \sin^2\left(\frac{m\pi a_1}{l_x}\right) \cos^2\left(\frac{n\pi y_1}{l_y}\right) \sin^2\left(\frac{n\pi b_1}{2l_y}\right) \frac{\frac{k_{mn} Z_s}{k\rho_0 c} + j \tan k_{mn} l_z}{1 + j \frac{k_{mn} Z_s}{k\rho_0 c} \tan k_{mn} l_z} \right\} \tag{7.12}$$

where k_{mn} is given by

$$k_{mn} = \sqrt{k^2 - \left(\frac{2m\pi}{l_x}\right)^2 - \left(\frac{n\pi}{l_y}\right)^2} \tag{7.13}$$

Although this expansion looks complicated, it is highly amenable to numerical computation and the impedance can be used as part of a matrix expression for the equivalent circuit, as will be demonstrated in Examples 7.2 and 7.3. The first term is simply that of a tube with the same depth l_z as that of the box and a termination impedance Z_s. The impedance of a tube was given by Eq. (2.60). For the impedance of the lining we set

$$Z_s = \frac{R_f d}{3} + \frac{P_0}{j\omega d} \tag{7.14}$$

where d is the thickness of the lining and we are assuming that the material is so porous that it is mainly air. For simplicity we will let $l_z = L/2$, $l_x = l_y = L$, $a_1 = b_1 = \sqrt{S_D}$, and $y_1 = L/2$. In Fig. 7.12 the specific impedance is plotted for the box of Fig. 7.11 with acoustic lining on the rear surface only to a depth of $d = L/10$ in addition to the box depth of $L/2$. Hence the air volume is $V_A = L^3/2$ and the material volume $V_M = L^3/10$. The flow resistance of the lining is $R_f d = 3\rho_0 c$ in order maximize absorption at high frequencies.

We see from Fig. 7.12 that at high frequencies the unlined box impedance varies dramatically with frequency between zero reactance and very high reactance. With lining, the box resonances (normal modes of vibration) are damped out so that R_{SB} has a constant value of around $\rho_0 c$ and X_{SB} approaches zero. If this behaved simply like an acoustic transformer (see Eq. (4.38)), we might expect the high-frequency value of R_{SB} to be $\rho_0 c/16$, that is, the impedance of the lining divided by the ratio of the area of the lining to that of the diaphragm. However the transformer model is only valid when the wavelength is large compared to the depth $L/2$. Instead we see a much higher value of R_{SB} because, as the size of the box is increased, the impedance seen by the diaphragm approaches that of a piston in an infinite baffle, which is $\rho_0 c$.

Acoustical material may also be used to enlarge effectively the volume of enclosed air. Gaseous compressions in a sound wave are normally adiabatic. If the air space is completely filled with a soft,

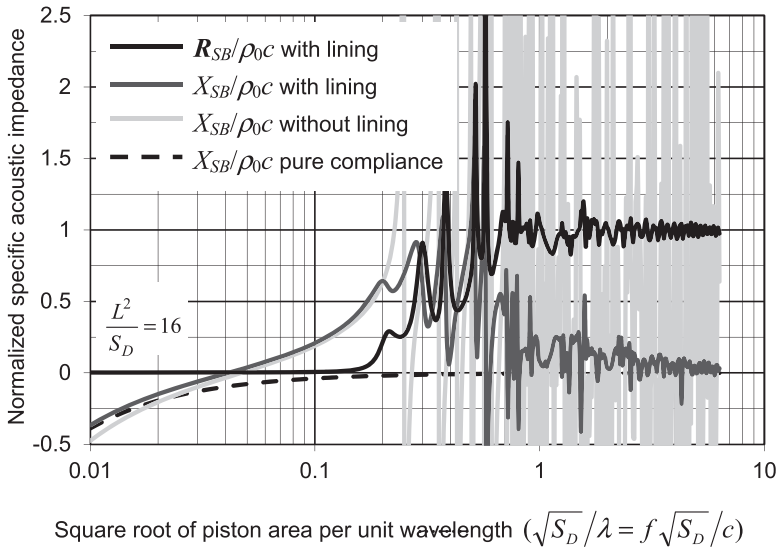

FIG. 7.12 Normalized specific acoustic impedance ($Z_{SB}/\rho_0 c = Z_{MB}/(S_D \rho_0 c) = Z_{AB} S_D/\rho_0 c$) of the closed box shown in Fig. 7.11.

The lining has a specific flow resistance of $R_f d = 3\rho_0 c$ which provides optimum sound absorption at higher frequencies. The position of the first normal mode of vibration occurs when $L/2 = \lambda/2$, that is, it occurs at $\sqrt{S_D}/\lambda = 0.25$ for $L^2/S_D = 16$. Without the lining, $R_{SB} = 0$.

lightweight material such as kapok or Cellufoam (foamed wood fibers), the compressions become isothermal. This means that the speed of sound decreases from $c = 344.8$ m/s to $c = 292$ m/s. Reference to Fig. 7.12 shows that this lowers the reactance at low frequencies just as does an increase in box dimension L. This also means that in Eq. (7.4) the value of γ is 1.0 instead of 1.4. In some designs, activated carbon is used to increase the apparent volume of the box even further. The pores within the material have a vast internal surface area on which air molecules are adsorbed when the pressure increases. When the pressure decreases, they are released again, the effect of which is to reduce the stiffness of the air in the box. However, the flow resistance of the material will have the effect of reducing the Q of the closed-box resonance which may or may not be a good thing depending on what the value was to begin with. [40,41]

Unlined closed box at low frequencies. In an unlined box, X_{AB} is not well behaved for wavelengths shorter than 8 times the smallest dimension of the box [9], as is seen from Fig. 7.12. If the dimension behind the loudspeaker is less than about $\lambda/4$, the reactance is negative (compliance dominated). If that dimension is greater than $\lambda/4$, the reactance is usually positive (mass dominated). When that dimension is equal to $\lambda/2$, the reactance becomes very large and the sound pressure radiated from the loudspeaker is attenuated. However, in many applications, such as tweeters, cellphones and MP3-player docking stations, the box is small compared to the wavelength over most of the working frequency range and so these typically have unlined enclosures. For those frequencies where the wavelength of sound is greater than eight times the smallest dimension of the box, the acoustic reactance presented to the rear side of the loudspeaker is a series mass and compliance as given by Eq. (7.3), but with $C_{AM} = 0$. For example if the depth of the box is

2 cm, then the maximum frequency for Eq. (7.3) is 2.18 kHz and the reactance will become very large at 8.72 kHz. The impedance at all frequencies is given by Eq. (7.12), but with $Z_s \rightarrow \infty$, so that

$$\frac{\dfrac{k_{mn}Z_s}{k\rho_0 c} + j\tan k_{mn}l_z}{1 + j\dfrac{k_{mn}Z_s}{k\rho_0 c}\tan k_{mn}l_z} = -j\cot k_{mn}l_z \tag{7.15}$$

In order to determine the end-correction factor B used in Eq. (7.5) and for the plot of Fig. 7.10 (where for simplicity we let $l_z = L/2$, $l_x = l_y = L$, $a_1 = b_1 = \sqrt{S_D}$, and $y_1 = L/2$), we make the following low-frequency ($k \rightarrow 0$) approximations:

$$\cot\frac{kL}{2} \approx \frac{2}{kL} - \frac{kL}{6} \tag{7.16}$$

$$k_{mn} \approx j\frac{2\pi}{L}\sqrt{m^2 + n^2} \tag{7.17}$$

and

$$\frac{k}{k_{mn}}\cot\frac{k_{mn}L}{2} \approx -\frac{kL}{2\pi\sqrt{m^2 + n^2}} \tag{7.18}$$

Noting that $Z_{AB} = jX_{AB}$, where X_{AB} is given by Eq. (7.3), we obtain the following expression for the end-correction factor B:

$$\begin{aligned} B = \frac{\sqrt{\pi S_D}}{\rho_0} M_{AB} = \Bigg\{ &\frac{\pi^{1/2}\sqrt{S_D}}{6L} + \frac{2L}{\pi^{5/2}\sqrt{S_D}} \sum_{m=1}^{\infty} \frac{\sin^2\left(m\pi\sqrt{S_D}/L\right)}{m^3} \\ &+ \frac{2}{\pi^{9/2}}\left(\frac{L}{\sqrt{S_D}}\right)^3 \sum_{m=1}^{\infty}\sum_{n=1}^{\infty} \frac{\sin^2\left(m\pi\sqrt{S_D}/L\right)\sin^2\left(n\pi\sqrt{S_D}/L\right)}{m^2 n^2\sqrt{m^2 + n^2}} \Bigg\} \end{aligned} \tag{7.19}$$

which is valid for lined or unlined boxes.

Location of loudspeaker drive unit in box. The results shown in Fig. 7.12 for the reactance of the closed box apply to a loudspeaker mounted in the center of one of the L by L sides, This location of the loudspeaker leaves something to be desired, because waves traveling outward from the diaphragm reach the outside edges of the box simultaneously and in combination set up a strong diffracted wave in the listening space. To reduce the magnitude of the diffracted wave, the loudspeaker should be moved off center by several inches—preferably in the direction of one corner. The use of rounded corners also helps to mitigate diffraction effects.

Note that if an ideal flat drive unit occupies the whole of one wall, no modes will occur between the adjacent walls, only between the drive unit and opposite (rear) wall. This is because the drive unit itself and the opposite wall are both reflected in the adjacent walls which act like mirrors. Hence the drive unit behaves like an infinite piston facing an infinite reflective surface.

The front face of the box of Fig. 7.11 need not be square. It is possible to make the ratio of the two front edges vary between 1 and 3 without destroying the validity of the charts, for the same total volume. In hi-fi loudspeaker enclosures it is not unusual for all the sides to be of different lengths with a "golden ratio" of $2^{1/3}$ (= 1.26) between the two smallest sides and the two largest ones so that the largest side is $2^{2/3}$ (= 1.6) times longer than the shortest one. The purpose of this is to interleave the internal vibration modes so that they do not reinforce each other. It is also common to make the width of the front panel as narrow as possible (hence there will be little in the way of modes between the side walls) and also to extend the height of the box so that the loudspeaker is floor standing. It is advisable to locate the drive unit at about one third of the internal height from either the top or bottom so as not to coincide with the anti-nodes of the first or second vertical modes.

***Effect of box compliance on resonance frequency and* Q.** Let us analyze the effect of the closed-box baffle on the lowest resonance frequency of a direct-radiator loudspeaker. For convenience, let us define a net compliance C_{AB} for a lined box:

$$C_{AB} = C_{AA} + C_{AM} \tag{7.20}$$

where C_{AM} is the compliance of the air in the lining material (we assume that it is highly porous so that it is mainly air) given by Eq. (7.6) and C_{AA} is the compliance of the remaining free space given by Eq. (7.4). Let us define an apparent box volume V_{AB} for a lined box in terms of the volume of the lining material V_M and the remaining internal free space V_A so that

$$V_{AB} = V_A + \gamma V_M \tag{7.21}$$

However, the total physical internal volume of the box V_B is

$$V_B = V_A + V_M \tag{7.22}$$

which is smaller than the apparent volume V_{AB} due to the isothermal pressure fluctuations within the lining material. For a loudspeaker mounted in an infinite baffle, the frequency for zero reactance is

$$f_{SB} = \frac{1}{2\pi\sqrt{C_{AS}(M_{AD} + 2M'_{A1})}} \tag{7.23}$$

where we have assumed that the radiation reactance X_{AR} from each side of the diaphragm equals $\omega M'_{A1}$ and that $M'_{A1} = 0.27\rho_0/a$.

From Fig. 7.6 we see that the resonance frequency f_C for the loudspeaker in a closed-box baffle with a volume less than about 200 L is

$$f_C = \frac{1}{2\pi}\sqrt{\frac{C_{AS} + C_{AB}}{C_{AS}C_{AB}(M_{AD} + M_{A1} + M_{AB})}} \tag{7.24}$$

where C_{AB} and M_{AB} are given by Eqs. (7.20) and (7.5) and M_{A1} is the radiation mass of a closed-back piston given by $M_{A1} = {}^3\!/_4 M'_{A1} \approx 0.2\rho_0/a$.

The ratio of (7.24) to (7.23) is equal to the ratio of the resonance frequency with the box to the resonance frequency with an infinite baffle. This ratio is

$$\frac{f_C}{f_{SB}} = \sqrt{\left(1 + \frac{C_{AS}}{C_{AB}}\right)\left(1 + \frac{2M'_{A1} - M_{A1} - M_{AB}}{M_{AD} + M_{A1} + M_{AB}}\right)} \tag{7.25}$$

Let us assume that M_{AB} is approximately the radiation mass of a piston in an infinite baffle and that $M'_{A1} \approx 0.043 M_{AD}$ so that Eq. (7.25) is approximately:

$$\frac{f_C}{f_{SB}} = \sqrt{1.01\left(1 + \frac{C_{AS}}{C_{AB}}\right)} \tag{7.26}$$

Hence the 1% difference in mass loading alone of the loudspeaker in a closed box compared to in an infinite baffle will produce a 0.5% increase in resonance frequency.

Often, it is difficult to find an "infinite" baffle in which to determine the resonance frequency. If the loudspeaker is held in free space without a baffle, the mass loading M''_{A1} on the diaphragm will be exactly one-half its value in an infinite baffle, that is, $M''_{A1} = 0.135\rho_0/a$. Hence, the ratio of the resonance frequency in the closed box f_C to the resonance frequency without baffle f_{SA} is approximately

$$\frac{f_C}{f_{SA}} = \sqrt{0.97\left(1 + \frac{C_{AS}}{C_{AB}}\right)} \tag{7.27}$$

Ignoring the mass loading effect, the above equations for the frequency shift due to a lined box can be conveniently expressed in terms of the Thiele–Small parameters f_S, and V_{AS} (IEC-baffle [38] resonance frequency and equivalent suspension volume respectively), and the apparent box volume V_{AB}:

$$\frac{f_C}{f_S} = \sqrt{1 + \frac{V_{AS}}{V_{AB}}} \tag{7.28}$$

This equation is plotted in Fig. 7.13.

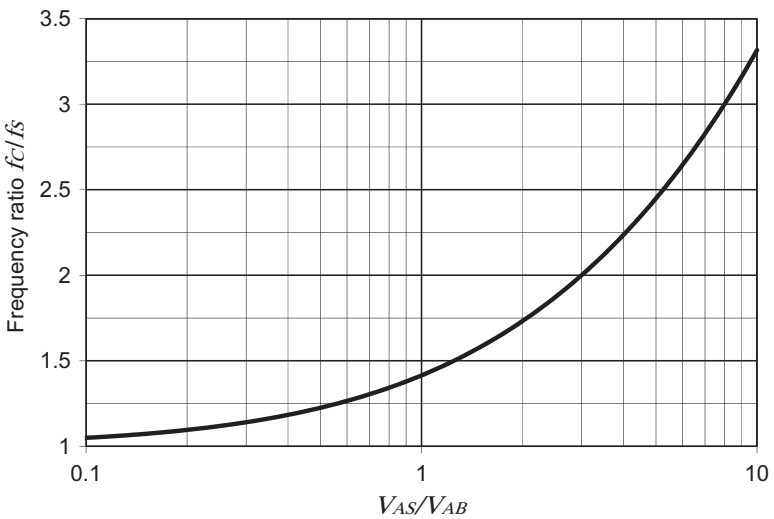

FIG. 7.13 Frequency ratio f_C/f_S = ratio of the resonance frequency for a loudspeaker in a closed-box baffle to the resonance frequency for the same loudspeaker in an IEC 268-5 baffle.[38]

Values of radiation (front-side) impedance. Acoustical elements always give the newcomer to the field of acoustics some difficulty because they are not well behaved. That is to say, the resistances vary with frequency, and, when the wavelengths are short, so do the masses.

The radiation impedance for the radiation from the front side of the diaphragm is simply a way of indicating schematically that the air has mass, that its inertia must be overcome by the movement of the diaphragm, and that it is able to accept power from the loudspeaker. The magnitude of the front-side radiation impedance depends on whether the box is very large so that it approaches being an infinite baffle or whether the box has dimensions of less than about 0.6 by 0.6 by 0.6 m (7.6 ft^3), in which case the behavior is quite different.

Very large box (approximating infinite baffle)

$\boldsymbol{R}_{AR}$ is radiation resistance for a piston in an infinite baffle in $N \cdot s/m^5$. This resistance is determined from the ordinate of Fig. 4.35 multiplied by $407/S_D$. If the frequency is low, so that the effective circumference of the diaphragm ($2\pi a$) is less than λ, that is, $ka < 1$ (where $k = 2\pi/\lambda$), $\boldsymbol{R}_{AR}$ may be computed from

$$\boldsymbol{R}_{AR} \approx \frac{0.159\omega^2\rho_0}{c} \approx 0.0215\, f^2 \tag{7.29}$$

X_{AR} is radiation reactance for a piston in an infinite baffle. This reactance is determined from the ordinate of Fig. 4.35, multiplied by $407/S_D$. For $ka < 1$, X_{AR} is given by

$$X_{AR} = \omega M_{A1} \approx \frac{0.270\omega\rho_0}{a} \approx \frac{2.0\, f}{a} \tag{7.30a}$$

and

$$M_{A1} = \frac{0.270\rho_0}{a} \approx \frac{0.318}{a} \tag{7.30b}$$

Small to medium-sized box (less than 200 L)

$\boldsymbol{R}_{AR}$ is approximately the radiation impedance for a one-sided piston in free space. This resistance is determined from the ordinate of Fig. 4.39 multiplied by $407/S_D$. If the frequency is low so that the effective circumference of the diaphragm ($2\pi a$) is less than λ, $\boldsymbol{R}_{AR}$ may be computed from

$$\boldsymbol{R}_{AR} = \frac{\pi f^2 \rho_0}{c} \approx 0.01076\, f^2 \tag{7.31}$$

X_{AR} is approximately the radiation reactance for a one-sided piston in free space. This reactance is determined from the ordinate of Fig. 4.39 multiplied by $407/S_D$. For $ka < 1$, X_{AR} is given by

$$X_{AR} = \omega M_{A1} \approx \frac{\omega(0.2026)\rho_0}{a} \approx \frac{1.5\, f}{a} \tag{7.32a}$$

and

$$M_{A1} = \frac{0.2026\rho_0}{a} \approx \frac{0.239}{a} \tag{7.32b}$$

Radiation equation. At very low frequencies where the diaphragm has not yet become a directional radiator (i.e., its circumference is less than about a wavelength), the loudspeaker in a closed-box baffle may be treated as though it were a simple spherical source of sound. We find from Eq. (4.71) that the sound pressure a distance r away from such a source in a free field is given by

$$\tilde{p}(r) = -jf\rho_0\tilde{U}_c \frac{e^{-jkr}}{2r}, \qquad kR << 1 \tag{7.33}$$

where

$\tilde{p}$ is sound pressure in Pa at a distance r from the loudspeaker.

$\tilde{U}_c = \tilde{u}_c S_D$ is volume velocity of the diaphragm in m^3/s.
ρ_0 is density of air in kg/m^3 (about 1.18 kg/m^3 for normal room conditions).
r is distance from the loudspeaker in m.
f is frequency in Hz
$R = (3V_B/4\pi)^{1/3}$ is average dimension of the enclosure.

At higher frequencies, where the diaphragm is becoming more directional but yet is still vibrating substantially as a rigid piston, we use Eq. (13.104) for a piston in an infinite baffle. When the wavelength is small compared to the dimensions of the box, it acts as a large baffle so that the pressure at a distance r in a free field is

$$\tilde{p}(r) = -jf\rho_0\tilde{U}_c \frac{e^{-jkr}}{r}, \qquad kR >> 1 \tag{7.34}$$

Hence there is a 6 dB lift at higher frequencies due to the baffle effect. Examples of this can be seen in Fig. 12.24 and Fig. 13.30 which show the on-axis pressure responses of a piston in a sphere and a closed-back circular baffle respectively. If the corners of the box are square, the rise will be accompanied by some ripples in the on-axis response due to reflections from the corners. No exact solution exists for this kind of problem although some useful approximations can be made [10–12]. Otherwise, if the corners are rounded, the transition will be smoother like that of a point source in a sphere shown in Fig. 12.15. Let us now modify Eq. (7.33) by adding an on-axis directivity function $D(0)$ so that it covers the transition region:

$$\tilde{p}(r) = -jf\rho_0\tilde{U}_c \frac{e^{-jkr}}{2r} D(0) \tag{7.35}$$

The type of approximation we use for $D(0)$ will depend on the form of the enclosure. If it is very rounded, the following expression provides a reasonably good approximation to a point source on a sphere:

$$D(0) = \frac{1 + jkR}{1 + jkR/2} \tag{7.36}$$

where R is the radius of the sphere and $k = 2\pi f/c$, so that the pressure magnitude is

$$|p(r)| = \frac{f\rho_0|U_c|}{2r}\sqrt{\frac{1 + k^2R^2}{1 + k^2R^2/4}} \tag{7.37}$$

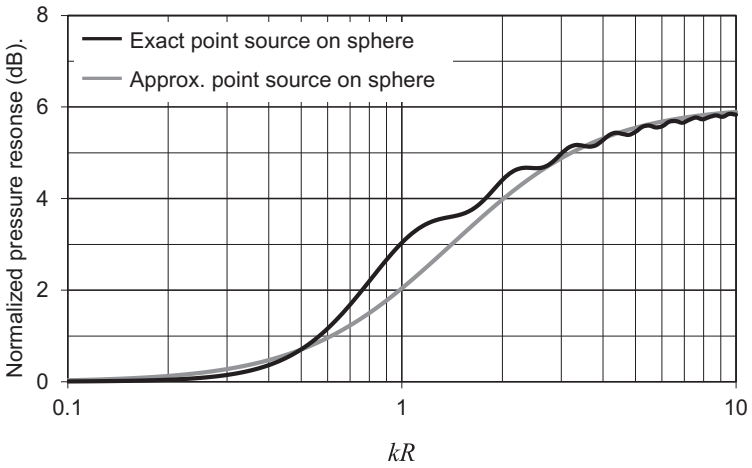

FIG. 7.14 Plot of $20\log_{10}D(0)$ for a point source in a sphere of radius R, which is used to model the baffle effect of a loudspeaker in a rounded closed-box baffle with constant diaphragm acceleration.

The black curve shows the exact result from Eq. (12.47) and the gray curve the approximation from Eq. (7.36).

The approximation of Eq. (7.36) is plotted in Fig. 7.14 along with the exact expression for a point source on a sphere from Eq. (12.47). For an enclosure in which the loudspeaker occupies the full width, a closed-back piston model is more appropriate, in which case

$$D(0) = \frac{1 - 2k^2a^2 + j2ka}{1 - k^2a^2 + jka} \tag{7.38}$$

where a is the radius of the piston so that the pressure magnitude is:

$$|p(r)| = \frac{f\rho_0|U_c|}{2r}\sqrt{\frac{(1 - 2k^2a^2)^2 + 4k^2a^2}{(1 - k^2a^2)^2 + k^2a^2}} \tag{7.39}$$

The approximation of Eq. (7.38) is plotted in Fig. 7.15 along with the exact expression for a closed-back piston in free space from Eq. (13.253). This gives a more rapid 6 dB transition than the point source on a sphere. Since most drive units are designed to have as flat a response as possible in a flat baffle, the only way to correct for this 6 dB lift is to include the inverse of the function $D(0)$ in the cross-over network as will be discussed in Sec. 7.20. At even higher frequencies, the on-axis response starts to roll off, even if the diaphragm is rigid and perfectly well behaved, because of the cone shape, which can be thought of as an approximate concave dome. See Fig. 12.32. The roll off is somewhat irregular due to "cup" resonances. The directivity pattern then becomes constant with an angle of dispersion that corresponds to the arc angle of the concave dome, as shown in Fig. 12.31.

Diaphragm volume velocity $\tilde{U}_c$. We determine the volume velocity $\tilde{U}_c$ from Fig. 7.6:

$$\tilde{U}_c = \frac{\tilde{e}_g Bl}{S_D(R_g + R_E)\left(\dfrac{B^2l^2}{(R_g + R_E)S_D^2} + R_A + jX_A\right)} \tag{7.40}$$

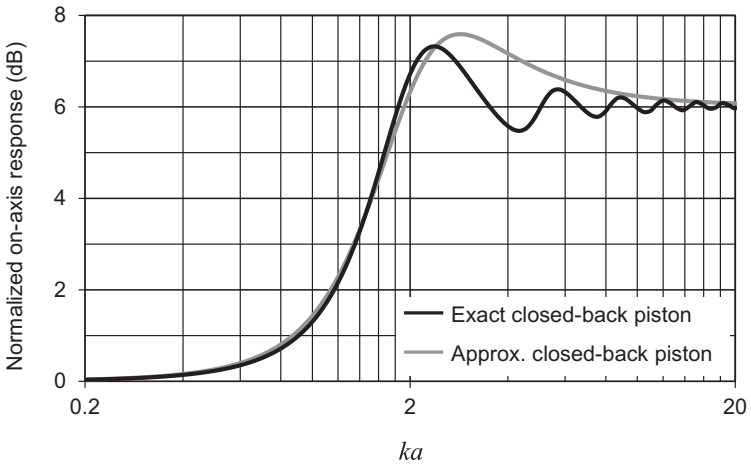

FIG. 7.15 Plot of $20\log_{10}D(0)$ for a closed-back piston of radius a in free space, which is used to model the baffle effect of a loudspeaker in a narrow closed-box baffle with constant diaphragm acceleration.

The black curve shows the exact result from Eq. (13.253) and the gray curve the approximation from Eq. (7.38). It is interesting to note that the exact on-axis response of the closed-back piston is the obtained from the sum of the on-axis responses of a free piston and a piston in an infinite baffle, where the latter is just unity under constant acceleration. The on-axis response of a free piston is simply the magnitude of its radiation impedance shown in Fig. 4.38.

where, from Fig. 7.6,

$$R_A = R_{AS} + \boldsymbol{R}_{AB} + \boldsymbol{R}_{AR} \tag{7.41}$$

$$X_A = \omega M_A - 1/(\omega C_A) \tag{7.42}$$

$$M_A = M_{AD} + M_{A1} + M_{AB} \tag{7.43}$$

$$C_A = \frac{C_{AS}C_{AB}}{(C_{AS} + C_{AB})} \tag{7.44}$$

The radiation mass and resistance $\boldsymbol{R}_{AR}$ and M_{A1} are generally given by Eqs. (7.31) and (7.32) but for very large boxes or for infinite baffles are given by Eqs. (7.29) and (7.30).

In an effort to simplify Eq. (7.40), let us define a Q_{TC} in the same manner as we do for electrical circuits. First, let us set

$$\omega_C = 2\pi f_C = \frac{1}{\sqrt{M_A C_A}} \tag{7.45}$$

where ω_C = angular resonance frequency for zero reactance. Then,

$$Q_{EC} = \frac{(R_g + R_E)S_D^2}{B^2 l^2}\sqrt{\frac{M_A}{C_A}} \tag{7.46}$$

$$Q_{MC} = \frac{1}{R_A}\sqrt{\frac{M_A}{C_A}} \tag{7.47}$$

$$Q_{TC} = \frac{Q_{EC}Q_{MC}}{Q_{EC} + Q_{MC}} \tag{7.48}$$

so that we can write

$$\tilde{U}_c = \frac{S_D\tilde{e}_g}{BlQ_{EC}}\, B_C(f) \tag{7.49}$$

where the frequency response function $B_C(f)$ is given by

$$B_C(f) = \frac{j\dfrac{f}{f_C}}{1 - \dfrac{f^2}{f_C^2} + j\dfrac{1}{Q_{TC}}\cdot\dfrac{f}{f_C}} \tag{7.50}$$

This has the same form as $\beta_c(f)$ in Eq. (6.7) for a loudspeaker in an infinite baffle, which is plotted in Fig. 6.5, except that the parameters have been modified by the enclosure.

Reference volume velocity and sound pressure. A reference diaphragm volume velocity is arbitrarily defined here by the equation

$$U_{c(\text{rms})} = \frac{e_{g(\text{rms})}BlS_D}{(R_g + R_E)\omega M_M} \tag{7.51}$$

where we have set the total mass to $M_A = M_M/{S_D}^2$. This reference volume velocity is equal to the actual volume velocity above the resonance frequency under the special condition that ${R_A}^2$ of Eq. (7.41) is small compared with $\omega^2{M_A}^2$. This reference volume velocity is consistent with the efficiency defined in Sec. 6.9.

The reference sound pressure at low frequencies, where it can be assumed that there is unity directivity factor, is found from Eqs. (7.33) and (7.51):

$$p_{\text{rms}} = \frac{e_{g(\text{rms})}BlS_D\rho_0}{(R_g + R_E)M_M 4\pi r} \tag{7.52}$$

It is emphasized that the reference sound pressure will not be the actual sound pressure in the region above the resonance frequency unless the motion of the diaphragm is mass-controlled and unless the directivity factor is nearly unity. The reference pressure is, however, a convenient way of locating "zero" decibels on a relative sound-pressure-level response curve, and this is the reason for defining it here.

Radiated sound pressure for $\mathbf{ka} < 1$***.*** The radiated sound pressure in the frequency region where the circumference of the diaphragm ($2\pi a$) is less than a wavelength (i.e., where there is negligible

directivity) is found by inserting the volume velocity from Eqs. (7.49) and (7.50) into Eq. (7.33) so that

$$\tilde{p}(r) = -\frac{\tilde{e}_g BlS_D\rho_0}{(R_g+R_E)M_M}\cdot\frac{e^{-jkr}}{4\pi r}\,\alpha_C(f), \qquad kR << 1 \tag{7.53}$$

where $\alpha_C(f)$ is a frequency-response function in the form of a 2nd-order high-pass filter which is proportional to the acceleration of the cone. It is defined by

$$\alpha_C(f) = \frac{-\dfrac{f^2}{f_C^2}}{1-\dfrac{f^2}{f_C^2}+j\dfrac{1}{Q_{TC}}\cdot\dfrac{f}{f_C}} \tag{7.54}$$

Notice that Eq. (7.53) is very similar to Eq. (6.32) for the sound pressure radiated from a loudspeaker in an infinite baffle, the only difference being the factor of 4 in the denominator instead of 2. The reason for this is that the sound pressure is doubled when radiating into half space instead of whole space. Otherwise, there are very little difference in the reference sensitivity apart from that due to the change in mass loading when the loudspeaker is mounted in the enclosure. However, this will be negligible in most cases. Similarly, the sensitivity is the same as that given in Eq. (6.33) but with a factor of 4 in the denominator:

$$\text{Sensitivity} = 20\log_{10}\left(\frac{\sqrt{Z_{\text{nom}}W_E}\,BlS_D\rho_0}{4\pi r(R_g+R_E)M_M\times 20\times 10^{-6}}\right)\text{ dB SPL/W/m} \tag{7.55}$$

Alignments for pre-determined frequency-response shapes. The normalized sound pressure level (SPL) is plotted Fig. 7.16 using $20\log_{10}|\alpha_C|$ from Eq. (7.54). Note that at the resonance frequency f_C, the SPL is simply $20\log_{10}Q_{TC}$ so that it is 6 dB for $Q_{TC}=2$, 3 dB for $Q_{TC}=\sqrt{2}$, 0 dB for $Q_{TC}=1$, and so forth.

We should observe that, even in the frequency range where the diaphragm diameter is less than one-third wavelength, the value of Q_{TC} is not strictly constant because $\boldsymbol{R}_{AR}$ increases with the square of the frequency. In using Eq. (7.54) and Fig. 7.16, therefore, R_A in Q_{TC} probably ought to be calculated as a function of ω/ω_C. Usually, however, the value of R_A at ω_C is the only case for which calculation is necessary.

The curve for $Q_{TC}=1/\sqrt{2}$, also known as critical damping, has a Butterworth high-pass frequency-response shape. It gives the flattest possible response down to f_C where it is 3 dB below the pass-band level. Hence we see that we can choose a frequency-response shape and engineer the loudspeaker accordingly. Instead of defining the shape by the Q_{TC} factor, which only tells us the magnitude at the resonance frequency f_C, it is more convenient to define the largest amount of deviation from the flat level that we wish to allow, or ripple factor, in dB. Chebyshev alignments are defined in this way, and the Q_{TC} values needed for various ripple factors are given in Table 7.2. These are calculated from the formulae given in Appendix I. Small loudspeakers are often deliberately designed with a peak in the bass response in order to make them sound more impressive on first hearing and thus compensate for the lack of deep bass. On the other hand, if this is overdone, the effect of the poor transient response (see Sec. 6.17), with the resulting "one

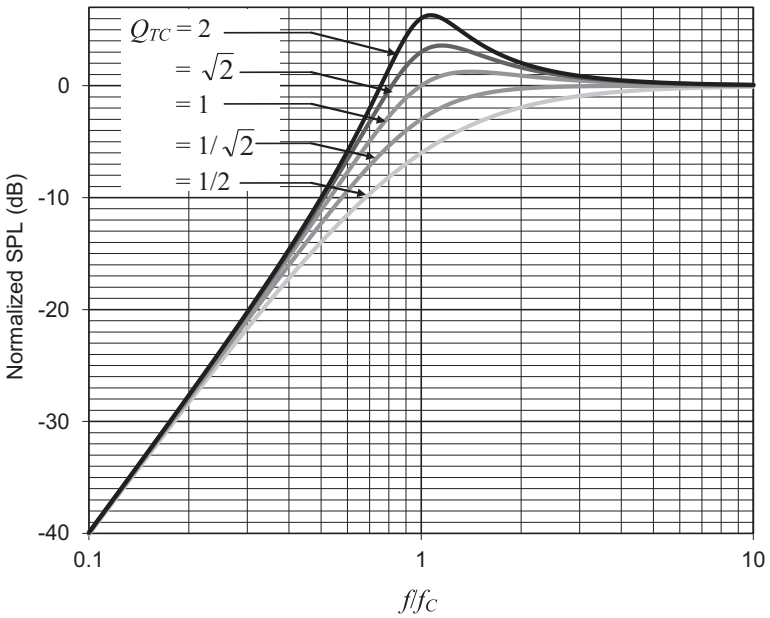

FIG. 7.16 Normalized sound-pressure-level (SPL) response of a loudspeaker in a closed box at low frequencies using $20\log_{10}|\alpha_C|$ from Eq. (7.54).

An infinite baffle or a closed-box enclosure is assumed. Q_{TC} is the same as Q_{TC} of Eq. (7.48) and ω_C is found from Eq. (7.45). The graph applies only to the frequency range where the wavelengths are greater than about three times the advertised diameter of the diaphragm.

Table 7.2 Resonance frequencies and Q values for various 2nd-order frequency-response shapes

Frequency-response shape	f_{3dB}/f_C	Q_{TC}
Synchronous	1.5538	0.5000
Bessel	1.2720	0.5774
Butterworth	1.0000	0.7071
Chebyshev with 0.1 dB ripple	0.93682	0.76736
Chebyshev with 0.5 dB ripple	0.88602	0.86372
Chebyshev with 1.0 dB ripple	0.86234	0.9565
Chebyshev with 2.0 dB ripple	0.84461	1.1287
Chebyshev with 3.0 dB ripple	0.84090	1.3047
Chebyshev with 4.0 dB ripple	0.84312	1.4934
Chebyshev with 5.0 dB ripple	0.84842	1.6996
Chebyshev with 6.0 dB ripple	0.85544	1.9269

note" bass, can be fatiguing. For larger loudspeakers with more extended bass, the Bessel frequency-response shape, which has a maximally linear phase response, offers a useful compromise between bass extension and good transient response. If the loudspeaker is to be situated in a relatively small listening room where the low frequencies are likely to be augmented by room modes, then a gentle roll-off is desirable, as provided by the synchronous shape, which has two real coincident poles. In this case, a relatively small room is one in which the largest dimension is less than 6 m.

Referring back to Eq. (6.115), we find that we suggested for satisfactory transient response that $\omega_S/(2Q_{TS}) > 92\ \text{s}^{-1}$. Let us see what this means in terms of Q_{TC}.

In terms of Q_{TC} the suggested criterion for satisfactory transient response is

$$Q_{TC} < \frac{\omega_C}{184} \tag{7.56}$$

As an example, if $\omega_C = 2\pi f_C = 2\pi 40 = 251$ rad/s, then Q_{TC} should be less than 1.37. This would mean that the peak in the response curve must be less than 2.7 dB. Methods for achieving desired Q_{TC} values will be discussed as part of the example below.

Setting the value of Q_{TC} and determination of the total box volume V_T. The Q_{TC} of a loudspeaker in a closed box is never the same as its free-space Q_{TS} unless the box is extremely large and empty. However, it is the closed-box Q_{TC} which determines the final frequency-response shape. Its value obviously depends upon the inherent mechanical resistance [see Q_{MC} from Eq. (7.47)] and electrical damping [see Q_{EC} from Eq. (7.46)] of the drive unit, which we cannot change very easily in the case of a passive loudspeaker design except through the choice of drive unit. However, we can control the box volume and filling material. If we ignore the acoustic mass loading effect so that $M_A = S_D^2 M_{MS}$, the ratio of Q_{TC} to Q_{TS} is found from Eqs. (7.48) and (6.9):

$$\frac{Q_{TC}}{Q_{TS}} = \frac{\dfrac{B^2 l^2}{R_g + R_E} + R_{MS}}{\dfrac{B^2 l^2}{R_g + R_E} + R_{MS} + R_{MB}} \sqrt{1 + \frac{C_{AS}}{C_{AB}}} \tag{7.57}$$

Let us define Q_{MB} for the box:

$$Q_{MB} = \frac{1}{R_{MB}} \sqrt{\frac{M_{MS}}{C_{MS}}} = \frac{\rho_0 c^2}{R_{AB} \omega_S V_{AS}} \tag{7.58}$$

where R_{AB} is calculated from Eq. (7.7). Hence

$$\frac{Q_{TC}}{Q_{TS}} = \frac{\dfrac{1}{Q_{ES}} + \dfrac{1}{Q_{MS}}}{\dfrac{1}{Q_{ES}} + \dfrac{1}{Q_{MS}} + \dfrac{1}{Q_{MB}}} \sqrt{1 + \frac{V_{AS}}{V_{AB}}} \tag{7.59}$$

where $V_{AB} = V_A + \gamma V_M$, which is solved for V_A to yield

$$V_A = V_{AB} - \gamma V_M = \frac{V_{AS}}{Q_{TC}^2 \left(\dfrac{1}{Q_{TS}} + \dfrac{1}{Q_{MB}} \right)^2 - 1} - \gamma V_M \tag{7.60}$$

where V_M is the volume of the lining material and V_A the remaining free space. Although a value of V_A is required to calculate R_{AB} from Eq. (7.7), a first approximation is given by letting $Q_{MB} = \infty$ so that

$$V_A \approx \frac{V_{AS}}{(Q_{TC}/Q_{TS})^2 - 1} - \gamma V_M \tag{7.61}$$

The total internal volume of the box is then $V_B = V_A + V_M$.

Cone displacement. The first time integral of the velocity from Eqs. (7.49) and (7.50) gives the displacement:

$$\tilde{\eta}_C = \frac{\tilde{u}_C}{j\omega} = \frac{\tilde{U}_C}{j\omega S_D} = \frac{\tilde{e}_g}{\omega_C B l Q_{EC}} \gamma_C(f) \tag{7.62}$$

where $\gamma_C(f)$ is a dimensionless frequency response function given by

$$\gamma_C(f) = \frac{1}{1 - \dfrac{f^2}{f_C^2} + j\dfrac{1}{Q_{TC}} \cdot \dfrac{f}{f_C}} \tag{7.63}$$

This is plotted in Fig. 7.17. At very low frequencies we have

$$\tilde{\eta}_0 = \frac{\tilde{e}_g}{\omega_C B l Q_{EC}} = \frac{\tilde{e}_g}{\omega_S B l Q_{ES}(1 + V_{AS}/V_{AB})} \tag{7.64}$$

Hence, reducing the size of the box reduces the amount of displacement at low frequencies below ω_C and thus enables greater sound pressure to be obtained at higher frequencies above ω_C with less risk of displacement limiting due to the low frequencies present. On the other hand, reducing the box volume raises ω_C and therefore reduces the sound pressure at low frequencies, so a compromise has to be reached somewhere.

7.7 MEASUREMENT OF BAFFLE CONSTANTS

The constants of the baffle may be measured after the loudspeaker constants are known. Refer to Fig. 7.6. The quantities $\boldsymbol{R}_{AR}$ and X_{AR} are determined from Eqs. (7.31) and (7.32). The electrical and mechanical quantities are measured directly.

Measurement of C_{AB}. Using the same procedure as for measuring f_S and Q_{EC} in Sec. 6.10, determine a new f_C and Q_{EC}, and solve for C_{AB} from Eq. (6.71) so that

$$C_{AB} = \frac{V_{AS}}{\rho_0 c^2 \left(\dfrac{f_C Q_{EC}}{f_S Q_{ES}} - 1 \right)} \tag{7.65}$$

Measurement of R_{AB}. Using the same procedure as for measuring Q_{ES} and Q_{MS} in Sec. 6.10, determine a new Q_{EC} and Q_{MC} and solve for R_{AB} from

$$R_{AB} = \frac{\omega_C(M_{AD} + M_{A1} + M_{AB})}{Q_{MC}} - (R_{AS} + \boldsymbol{R}_{AR})$$

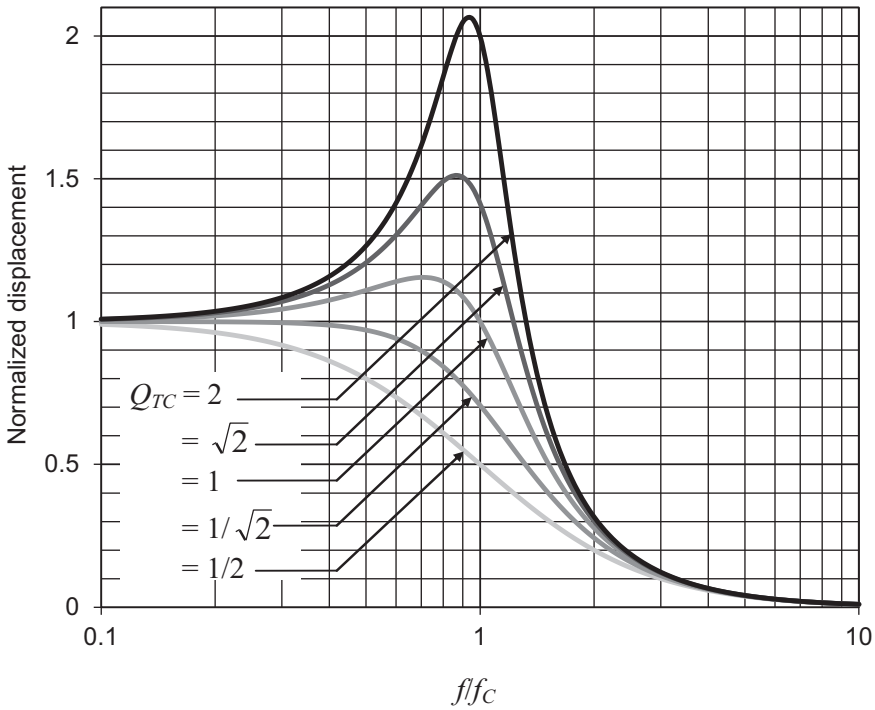

FIG. 7.17 Normalized cone displacement of a loudspeaker in a closed box at low frequencies using $|\gamma_C(f)|$ from Eq. (7.63). Q_{TC} is the same as Q_{TC} of Eq. (7.48) and ω_C is found from Eq. (7.45).

where $M_{AD} = M_{MD}/S_D^2$; M_{A1} is given by Eq. (7.32*b*), and

$$R_{AS} + \boldsymbol{R}_{AR} = \frac{R_{MS} + \boldsymbol{R}_{MR}}{S_D^2}$$

Example 7.1. Miniature loudspeaker. A miniature loudspeaker intended for use in mobile products has the Thiele–Small parameters given below:

$R_E = 7.2\ \Omega$
$Q_{ES} = 2.05$
$Q_{MS} = 3.48$
$f_S = 476$ Hz
$S_D = 1.40\ \text{cm}^2$
$V_{AS} = 4.81\ \text{cm}^3$

It is assumed that the loudspeaker will be used mainly near a large flat surface such as a table.

Determine the reference sound pressure at a distance of 0.1 m for 0.5 W input.
Determine the percentage shift in the first resonance frequency of the loudspeaker from the value for an infinite baffle if an unlined box having a volume of 1 cm^3 is used.

Determine the sound pressure at the closed box resonance frequency, assuming $R_{AB} = 0$.
Determine the volume of a box that will cause a shift in infinite-baffle resonance frequency of only 25%.
Determine the sound pressure at the closed box resonance frequency for the box of (*c*).

Solution, *1*. In order to calculate the maximum SPL, we first obtain C_{MS}, M_{MS}, and Bl from Eqs. (6.27), (6.28), and (6.30) respectively:

$$C_{MS} = \frac{4.81 \times 10^{-6}}{(1.40 \times 10^{-4})^2 \times 1.18 \times 345^2} = 1.75 \text{ mm/N}$$

$$M_{MS} = \frac{1}{(2 \times 3.14 \times 476)^2 \times 0.00175} = 64 \text{ mg}$$

$$Bl = \sqrt{\frac{7.2}{2 \times 3.14 \times 476 \times 2.05 \times 0.00175}} = 0.82 \text{ T·m}$$

From Eq. (6.33) we obtain the reference sound pressure:

$$20 \log_{10}\left(\frac{\sqrt{8 \times 0.5} \times 0.82 \times 1.401 \times 10^{-4} \times 1.18}{2 \times 3.14 \times 0.1 \times 7.2 \times 64 \times 10^{-6} \times 20 \times 10^{-6}}\right) = 93.4 \text{ dB SPL}$$

Solution, 2. From Eq. (7.28) we obtain the closed-box resonance frequency:

$$f_C = f_S\sqrt{1 + \frac{V_{AS}}{V_B}} = 476 \times \sqrt{1 + \frac{4.81}{1}} = 1147 \text{ Hz}$$

Solution, 3. The sound pressure at resonance is simply increased by a factor of Q_{TC} compared to the reference level. From Eq. (6.10), $Q_{TS} = 2.05 \times 3.48/(2.05 + 3.48) = 1.29$. At resonance,

$$Q_{TC} = \frac{f_C}{f_S} Q_{TS} = \frac{1147}{476} \times 1.29 = 3.11$$

Then the sound pressure is simply $93.4 + 20\log_{10}3.11 = 103.3$ dB SPL.

Solution, 4. We rearrange the equation of part 2 of the solution to obtain

$$V_B = \frac{V_{AS}}{(f_C/f_S)^2 - 1}$$

so that for a 25% shift in resonance frequency, where $f_C/f_S = 1.25$ or $f_C = 595$ Hz, we have

$$V_B = \frac{4.81}{1.25^2 - 1} = 8.55 \text{ cm}^2$$

which is too large a volume for most mobile products and, in any case, the diaphragm displacement becomes unacceptably large because of the greater compliance of air in the larger box.

Solution, 5. Using the same procedure as in part 3 of the solution, we obtain the sound pressure at the new resonance frequency of 595 Hz:

$$93.4 + 20\log_{10}\left(\frac{595}{476}\times 1.29\right) = 97.6 \text{ dB SPL}$$

Example 7.2. Low-frequency loudspeaker (woofer). Design a loudspeaker to be used with a 600 Hz crossover network and which is intended for use in a small to medium sized room where the bass response will be augmented by room modes. A maximum sound pressure of 99 dB SPL will be sufficient. Let us choose the Bandor type 100DW/8A drive unit which has a 6-inch diameter aluminum cone that is free from resonances until well above the cross-over frequency. The Thiele–Small parameters are:

$R_E = 6.27\ \Omega$
$Q_{ES} = 0.55$
$Q_{MS} = 2.2$
$f_S = 39$ Hz
$S_D = 120\ \text{cm}^2$
$V_{AS} = 21.6$ L

which gives a Q_{TS} value of

$$Q_{TS} = \frac{Q_{ES}Q_{MS}}{Q_{ES}+Q_{MS}} = 0.44$$

For a small listening room we desire a smooth low-frequency roll-off, so we choose the Butterworth alignment from Table 7.2, which returns a Q_{TC} value of $1/\sqrt{2}$ and gives a good transient response without ringing. The frequency response shape for this value is shown in Fig. 7.16. However, in order to reuse this design with a bass-reflex port in a future example, we set $Q_{TC} = 0.7$, which is close enough. Also, we will not fill the box completely with lining material because this would kill the bass-reflex resonance when the port is added. Therefore we set the volume of the lining material to be one third of that of the remaining free space or one quarter of the total volume. That is, $V_M = V_A/3 = V_B/4$ because $V_B = V_A + V_M$. We estimate V_A from Eq. (7.61):

$$V_A \approx \frac{V_{AS}}{(1+\gamma/3)(Q_{TC}^2/Q_{TS}^2-1)} = \frac{21.6}{(1+1.4/3)(0.7^2/0.44^2-1)} = 9.6\text{ L}$$

and $V_M = 9.6/3 = 3.2$ L, which we use to compute R_{AB} from Eq. (7.7), where $C_{AA} = V_A/(\gamma P_0)$. First though, we have to calculate $R_{AM} = R_f d/(3S_M)$, where R_f is the flow resistance of the lining material chosen such that $R_f d/3 = \rho_0 c = 412$ rayl, which is the impedance of free space and thus provides optimum sound absorption at higher frequencies. Also, S_M is the area of the lining material, which in this case is the area of the back panel given by $S_M = lxly = 0.15 \times 0.3175 = 0.04763\ \text{m}^2$, so that $R_{AM} = 412/0.047625 = 8651\ \text{N}\cdot\text{s/m}^5$. We just need to find the internal depth lz from the volume after computing the following from Eq. (7.7)

$$R_{AB} \approx \frac{8651}{\left(1+\frac{3}{1.4}\right)^2+\left(2\times 3.14\times\frac{0.7}{0.44}\times 39\right)^2\times 8651^2\times\left(\frac{0.0096}{1.4\times 10^5}\right)^2} = 871\ \text{N}\cdot\text{s/m}^5$$

Then from Eq. (7.58) the box Q is determined:

$$Q_{MB} = \frac{1.18 \times 345^2}{871 \times 2 \times 3.14 \times 39 \times 0.0216} = 30.5$$

so that after inserting this into Eq. (7.60) we obtain the air volume:

$$V_A = \frac{V_{AS}}{\left(1+\frac{\gamma}{3}\right)\left\{Q_{TC}^2\left(\frac{1}{Q_{TS}}+\frac{1}{Q_{MB}}\right)^2-1\right\}} = \frac{21.6}{\left(1+\frac{1.4}{3}\right)\left\{0.7^2\left(\frac{1}{0.44}+\frac{1}{30.5}\right)^2-1\right\}} = 9.15 \text{ L}$$

from which $V_M = 9.15/3 = 3.05$ L, $V_B = 9.15 + 3.05 = 12.2$ L, and $V_{AB} = 9.15 + (1.4 \times 3.05) = 13.42$ L. The internal depth is then $lz = V_A/S_M = 0.00915/0.04763 = 0.192$ m. The box is shown in Fig. 7.18. The internal width lx is 15 cm, which is the smallest width that will accommodate the drive unit. The acoustic center of the drive unit is about one third of the internal height from the bottom so as not to coincide with the anti-nodes of the first or second vertical modes. The box contains one 31.8 by 15 by 6.4 cm piece of lining material. From Eq. (7.28) we obtain the closed-box resonance frequency:

$$f_C = \sqrt{1+\frac{21.6}{13.42}} \times 39 = 63 \text{ Hz}$$

From Table 7.2 we see that the cut-off frequency is $f_{3\text{dB}} = 1 \times 63 = 63$ Hz. From Eq. (6.48) we can calculate the reference efficiency, noting that a loudspeaker in a box is half as efficient as one radiating from both sides in an infinite baffle:

$$E_{ff} = 100\frac{8 \times 3.14^2 \times 0.0216 \times 39^3}{2 \times 0.55 \times 345^3} = 0.224\%$$

In order to calculate the maximum SPL, we first obtain C_{MS}, M_{MS}, and Bl from Eqs. (6.27), (6.28), and (6.30) respectively:

$$C_{MS} = \frac{0.0216}{0.012^2 \times 1.18 \times 345^2} = 1.07 \text{ mm/N}$$

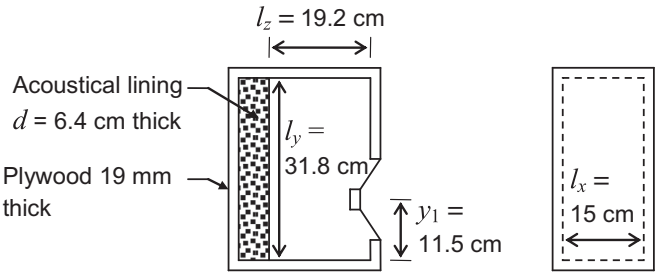

FIG. 7.18 Example of closed-box enclosure design.

$$M_{MS} = \frac{1}{(2 \times 3.14 \times 39)^2 \times 0.00107} = 0.0156 \text{ kg}$$

$$Bl = \sqrt{\frac{6.27}{2 \times 3.14 \times 39 \times 0.55 \times 0.00107}} = 6.59 \text{ T·m}$$

Knowing that the power rating $W_{\max}$ is 100W, we obtain from Eq. (6.33)

$$\text{SPL}_{\max} = 20 \log_{10}\left(\frac{\sqrt{6.27 \times 100} \times 6.59 \times 0.012 \times 1.18}{4 \times 3.14 \times 6.27 \times 0.0156 \times 20 \times 10^{-6}}\right) = 99.6 \text{ dB SPL @ 1 m}$$

where a drive unit in a box produces the half the pressure of one in an infinite baffle. Next use Eq. (7.64) to check the peak displacement at low frequencies at full power:

$$\eta_{\max} = \frac{\sqrt{2 \times 6.27 \times 100}}{2 \times 3.14 \times 39 \times 6.59 \times 0.55 \times (1 + 21.6/13.42)} = 15.3 \text{ mm}$$

but at the resonance frequency $f_C = 63$ Hz, the maximum displacement is $Q_{TC}\eta_{\max} = 0.7 \times 15.3 = 10.7$ mm. It turns out that the $x_{\max}$ value of the drive unit is 14 mm, so there should be no problems with this design as most program material is above this frequency.

Let us now create a semi-analytical simulation model of the design of Fig. 7.18 using 2-port networks and transmission matrices, as introduced in Sec. 3.10 and Fig. 4.43. The schematic is shown in Fig. 7.19. Although it is based on the circuit of Fig. 7.6, a gyrator has been inserted between the electrical elements and the mechanical ones, which enables us to calculate more easily the generator current $\tilde{i}_g$ from which we obtain the electrical impedance. We are ignoring the generator impedance R_g since in the experimental setup this is negligible compared to R_E. The dashed boxes are lumped-element 2-port networks and the solid boxes are analytical ones. From the schematic we create the transmission matrices required to represent each 2-port network as follows.

1. Coil.

$$\begin{bmatrix} \tilde{e}_g \\ \tilde{i}_g \end{bmatrix} = \begin{bmatrix} 1 & Z_E \\ 0 & 1 \end{bmatrix} \cdot \begin{bmatrix} \tilde{e}_1 \\ \tilde{i}_1 \end{bmatrix} = \mathbf{C} \cdot \begin{bmatrix} \tilde{e}_1 \\ \tilde{i}_1 \end{bmatrix}$$

where $Z_E = R_E + j\omega L_E$

2. Electro-mechanical transduction.

$$\begin{bmatrix} \tilde{e}_1 \\ \tilde{i}_1 \end{bmatrix} = \begin{bmatrix} 0 & Bl \\ (Bl)^{-1} & 0 \end{bmatrix} \cdot \begin{bmatrix} \tilde{f}_2 \\ \tilde{u}_2 \end{bmatrix} = \mathbf{E} \cdot \begin{bmatrix} \tilde{f}_2 \\ \tilde{u}_2 \end{bmatrix}$$

3. Diaphragm.

$$\begin{bmatrix} \tilde{f}_2 \\ \tilde{u}_2 \end{bmatrix} = \begin{bmatrix} 1 & Z_{MD} \\ 0 & 1 \end{bmatrix} \cdot \begin{bmatrix} \tilde{f}_3 \\ \tilde{u}_3 \end{bmatrix} = \mathbf{D} \cdot \begin{bmatrix} \tilde{f}_3 \\ \tilde{u}_3 \end{bmatrix}$$

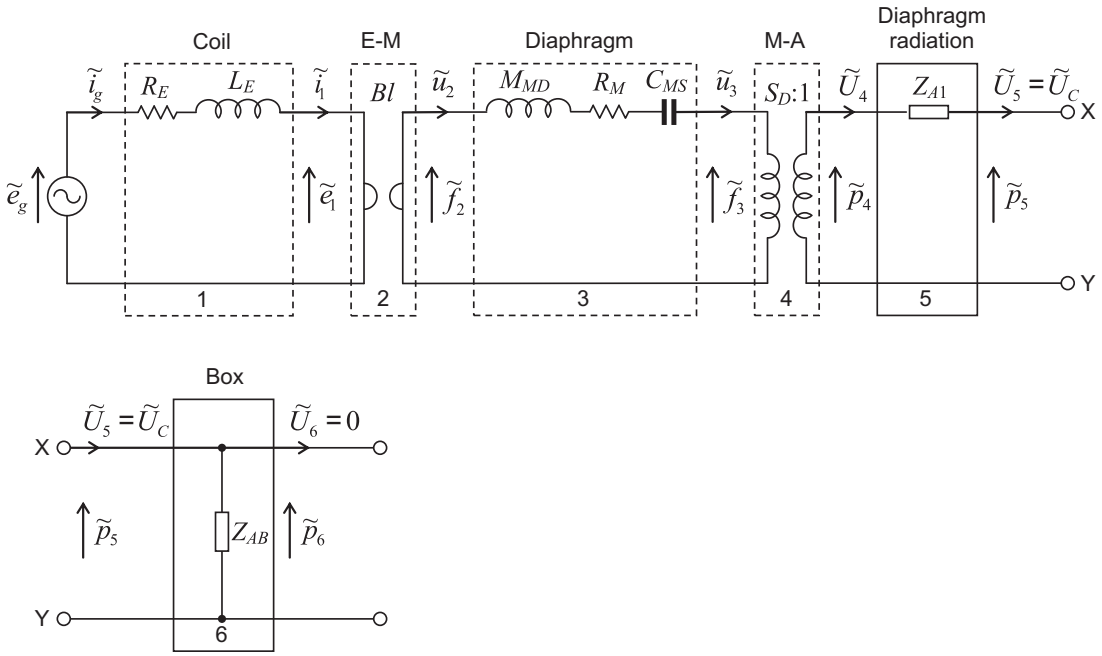

FIG. 7.19 Semi-analytical model of example closed-box enclosure design shown in Fig. 7.18, using transmission matrices.

The dashed boxes are lumped-element 2-port networks and the solid boxes are analytical ones.

where $Z_{MD} = j\omega M_{MD} + R_{MS} + 1/(j\omega C_{MS})$. We must exclude the radiation mass from the diaphragm so that $M_{MD} = M_{MS} - 16\rho_0 a^3/3$, where $a = \sqrt{S_D/\pi}$.

4. Mechano-acoustical transduction.

$$\begin{bmatrix} \tilde{f}_3 \\ \tilde{u}_3 \end{bmatrix} = \begin{bmatrix} S_D & 0 \\ 0 & S_D^{-1} \end{bmatrix} \cdot \begin{bmatrix} \tilde{p}_4 \\ \tilde{U}_4 \end{bmatrix} = \mathbf{M} \cdot \begin{bmatrix} \tilde{p}_4 \\ \tilde{U}_4 \end{bmatrix}$$

5. Diaphragm Radiation.

$$\begin{bmatrix} \tilde{p}_4 \\ \tilde{U}_4 \end{bmatrix} = \begin{bmatrix} 1 & Z_{A1} \\ 0 & 1 \end{bmatrix} \cdot \begin{bmatrix} \tilde{p}_5 \\ \tilde{U}_5 \end{bmatrix} = \mathbf{F} \cdot \begin{bmatrix} \tilde{p}_5 \\ \tilde{U}_5 \end{bmatrix}$$

where Z_{A1} is the acoustic radiation impedance of the diaphragm given by Eqs. (13.116), (13.117), and (13.118) with $a = \sqrt{S_D/\pi}$.

6. Box.

$$\begin{bmatrix} \tilde{p}_5 \\ \tilde{U}_5 \end{bmatrix} = \begin{bmatrix} 1 & 0 \\ Z_{AB}^{-1} & 1 \end{bmatrix} \cdot \begin{bmatrix} \tilde{p}_6 \\ \tilde{U}_6 \end{bmatrix} = \mathbf{B} \cdot \begin{bmatrix} \tilde{p}_6 \\ \tilde{U}_6 \end{bmatrix}$$

where Z_{AB} is given by Eq. (7.12) and

$$Z_s = \frac{R_f d}{3} + \frac{P_0}{j\omega d},$$

where the value of the lining flow resistance R_f is chosen such that $R_f d/3 = \rho_0 c = 412$ rayl, which is the impedance of free space and thus provides optimum sound absorption at higher frequencies. The dimensions are given in Fig. 7.18 except for $a_1 = b_1 = \sqrt{S_D}$.

First we evaluate $\tilde{p}_6$ at the end of the chain:

$$\begin{bmatrix} \tilde{e}_g \\ \tilde{i}_g \end{bmatrix} = \mathbf{A} \cdot \begin{bmatrix} \tilde{p}_6 \\ 0 \end{bmatrix}$$

where

$$\mathbf{A} = \mathbf{C} \cdot \mathbf{E} \cdot \mathbf{D} \cdot \mathbf{M} \cdot \mathbf{F} \cdot \mathbf{B} = \begin{bmatrix} a_{11} & a_{12} \\ a_{21} & a_{22} \end{bmatrix}$$

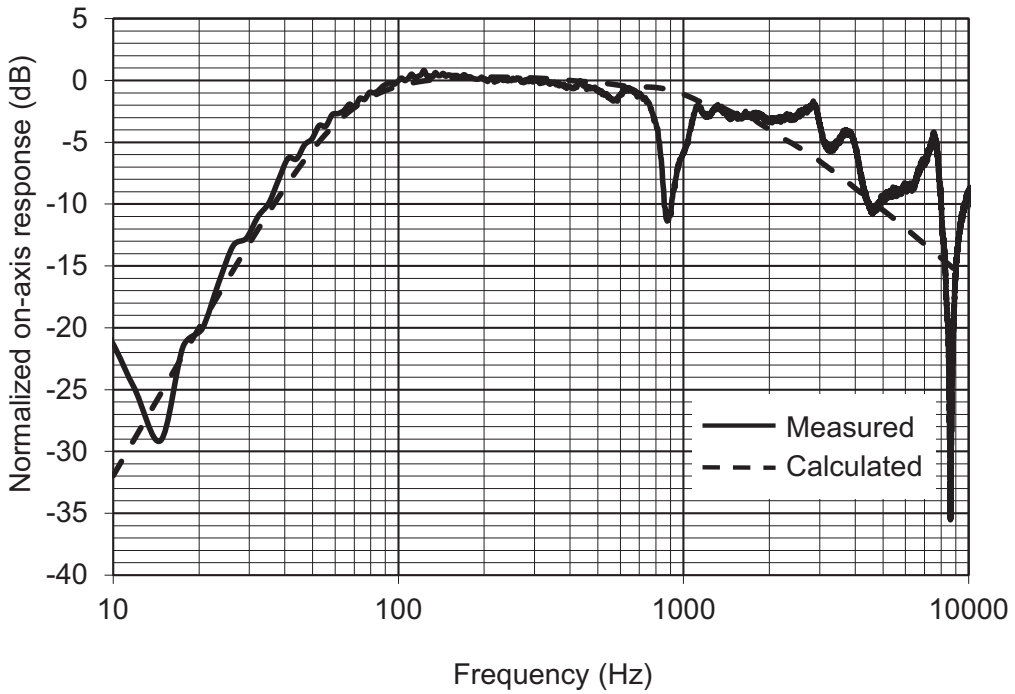

FIG. 7.20 Graphs of the on-axis sound pressure level produced by the closed-box enclosure design shown in Fig. 7.18. The dashed curves are calculated from 20 $\log_{10}|\tilde{U}_c/\tilde{U}_{ref}|$. Solid curves are measured.

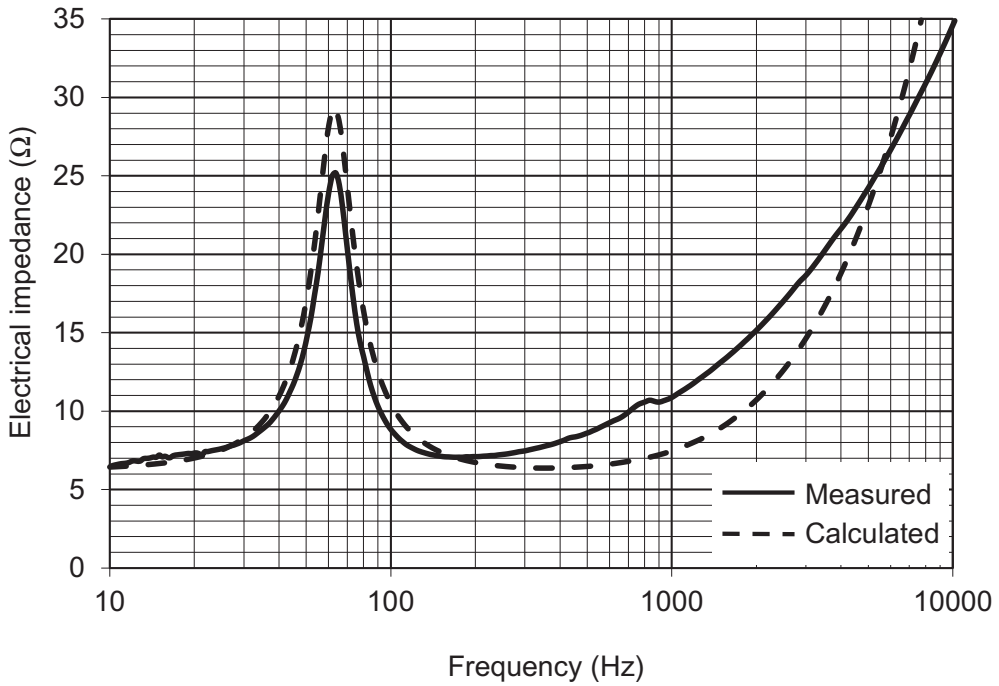

FIG. 7.21 Graphs of the electrical input impedance of the closed-box enclosure design shown in Fig. 7.18.

The dashed curves are calculated from $Z_E = |\tilde{e}_g/\tilde{i}_g| = a_{11}/a_{21}$. Solid curves are measured.

Hence $\tilde{p}_6 = \tilde{e}_g/a_{11}$. Then we work backwards to obtain the volume velocities we wish to evaluate. In particular, we are interested in the far-field pressure which, according to Eq. (7.33), is a function of $\tilde{U}_c = \tilde{U}_5$. This procedure is fairly straightforward and does not involve any matrix inversion. From the box matrix (6), we obtain the diaphragm volume velocity:

$$\tilde{U}_c = \tilde{U}_5 = \tilde{p}_6/Z_{AB}$$

In order to plot the normalized far-field on-axis pressure, we simply divide $\tilde{U}_c$ by a reference volume velocity

$$\tilde{U}_{ref} = \frac{\tilde{e}_g BlS_D}{\omega M_{MS} R_E}$$

and plot $20\log_{10}|\tilde{U}_c/\tilde{U}_{ref}|$ as shown in Fig. 7.20. The output from the diaphragm is fairly smooth apart from one small feature at 430 Hz, which is due to the fundamental vertical mode of the box. Finally, we can obtain the input impedance from $\tilde{e}_g/\tilde{i}_g$ where $\tilde{i}_g = a_{21}\tilde{p}_6$ and from above $\tilde{p}_6 = \tilde{e}_g/a_{11}$. Therefore the input impedance is simply $Z_E = a_{11}/a_{21}$, as plotted in Fig. 7.21.

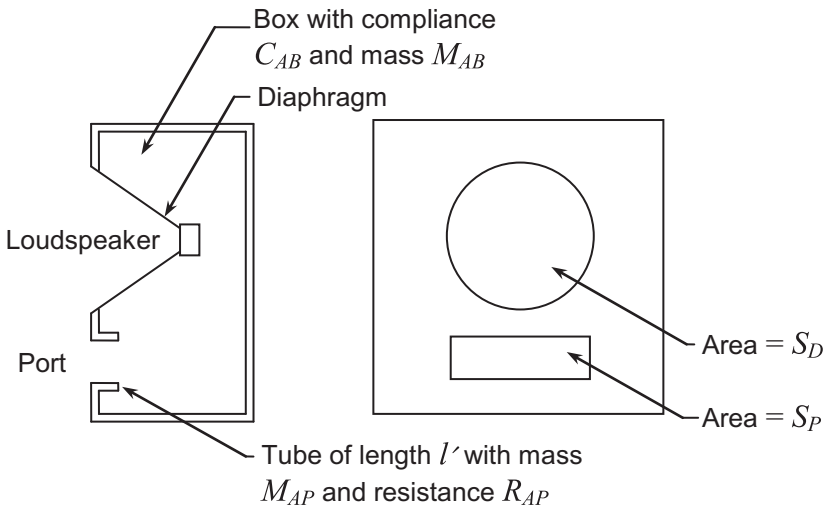

FIG. 7.22 Bass-reflex baffle.

The port has an area S_p, and the diaphragm has an area S_D. The inner end correction for the tube is included in the magnitude of M_{AP}.

PART XXII: BASS-REFLEX ENCLOSURES

7.8 GENERAL DESCRIPTION

The bass-reflex enclosure is a closed box in which an opening, usually called the *port*, has been made [13–22]. The area of the port is commonly made equal to or smaller than the effective area of the diaphragm of the drive unit. A common construction of this type of loudspeaker is shown in Fig. 7.22. When the diaphragm vibrates, part of its displacement compresses the air inside the box and the remainder of its displacement moves air outward through the port. Thus the port is a second "diaphragm," driven by the back side of the loudspeaker diaphragm. The port is, at low frequencies, equivalent to a short length of tube with an acoustic mass reactance and a series acoustic resistance. This tube has an end correction on the inner end and a radiation impedance on the outer, or radiating, end.

We shall assume for the remainder of this analysis that $ka < 0.5$. In other words, we are restricting ourselves to the very low frequency region where the radiation from both the port and the loudspeaker is nondirectional.

7.9 ACOUSTICAL CIRCUIT

The acoustical circuit for the box and the port is given in Fig. 7.23. The series radiation mass and resistance on the front side of the diaphragm are, respectively, M_{A1} and $\boldsymbol{R}_{AR1}$. The mass loading

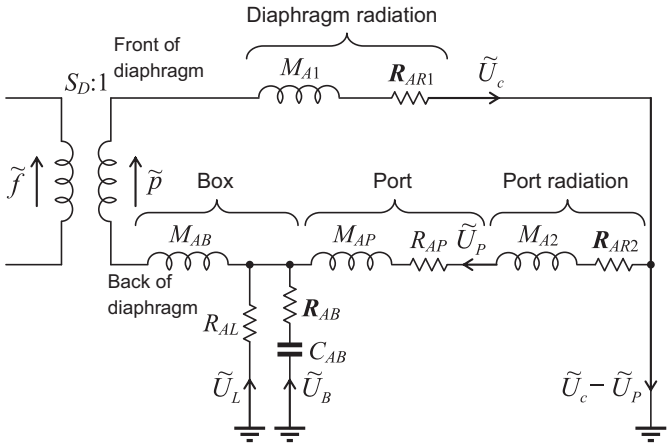

FIG. 7.23 Analogous acoustical circuit for a loudspeaker box with a port.

The volume velocity of the diaphragm is $\tilde{U}_c$, that of the port is $\tilde{U}_P$, that of the box is $\tilde{U}_B$, and that due to leakage is $\tilde{U}_L$.

on the back side of the diaphragm is M_{AB}. The resistance due to leakage through the walls of the box, or even through a woven dust cap or gasket, is R_{AL}. The compliance and resistance of the lined box are C_{AB} and R_{AB}. The mass and resistance of the air in the port that penetrates the side of the box, including the inner end correction, are M_{AP} and R_{AP}, respectively. Finally, the series radiation mass and resistance from the front side of the port are, respectively, M_{A2} and $\boldsymbol{R}_{AR2}$. The values of these quantities are M_{AB} as in Eq. (7.5); R_{AB} as in Eq. (7.7); C_{AB} as in Eq. (7.20); M_{A2} as in Eq. (7.32), but with a_2 instead of a, that is, $M_{A2} = 0.64a_2\rho_0/(\pi a_2^2)$; $\boldsymbol{R}_{AR2}$ as in Eq. (7.31); and

M_{A1} is acoustic-radiation mass for the front side of the loudspeaker diaphragm $= 0.2026\rho_0/a$ kg/m^4. Note that we assume the loudspeaker unit is equivalent to a piston radiating from one side only in free space.
$\boldsymbol{R}_{AR1} = 0.01075f^2$ is acoustic-radiation resistance for the front side of the loudspeaker diaphragm in N·s/m^5 (see Fig. 4.39 for $ka > 1.0$).
$M_{AP} = (t + 0.64a_2)\rho_0/(\pi a_2^2)$ is acoustic mass of the air in the port in kg/m^4. This quantity includes the inner end correction.
R_{AP} is acoustic resistance of the air in the port in N·s/m^5. [See Eq. (4.23). Use the number (1) in the parentheses.]
ρ_0 is density of air in kg/m^3 (normally about 1.18 kg/m^3).
a_2 is effective radius in m of the port in the vented enclosure. If the port is not circular, then let $a_2 = \sqrt{S_p/\pi}$, where S_p is the effective area of the opening in m^2.
$S_p = \pi a_2^2$ is effective area of the port in m^2.
t is length of the tube or the thickness of the wall of the enclosure in which the port is cut in m.

In case the port is composed of a number of identical small openings or tubes, the following procedure is followed.

Let N equal the number of such openings in the enclosure. For each opening the acoustic mass and resistance including M_{A2} and $\boldsymbol{R}_{AR2}$ are:

$M_A = (t + 1.7a_3)\rho_0/(\pi a_3^2)$ kg/m^4 [see Eq. (4.26)]
R_A is acoustic resistance of each opening in N·s/m^5 [see Eq. (4.25)]
a_3 is effective radius of each opening in m.

The total acoustic mass and resistance for the N identical openings are:

$M_{A2} + M_{AP} = M_A/N$ kg/m^4
$\boldsymbol{R}_{AR2} + R_{AP} = R_A/N$ N·s/m^5.

The directivity factor for a group of holes is about equal to that for a piston with an area equal to the area within a line circumscribing the entire group of holes.

7.10 ELECTRO-MECHANO-ACOUSTICAL CIRCUIT

The complete circuit for a loudspeaker in a bass-reflex enclosure is obtained by combining Fig. 6.4(b) and Fig. 7.23. To do this, the acoustical radiation element of the circuit labeled "$2M_{M1}$" in Fig. 6.4(b) is removed, and the circuit of Fig. 7.23 is substituted in its place. The resulting circuit with the transformer removed and everything referred to the acoustical side is shown in Fig. 7.24.

If the port is closed off so that $\tilde{U}_P$, the volume velocity of the air in the port, equals zero, then Fig. 7.24 essentially reduces to Fig. 7.6. At very low frequencies the mass of air moving *out* of the lower opening is nearly equal to that moving into the upper opening at all instants. In other words, at very low frequencies, the volume velocities at the two openings are nearly equal in magnitude and opposite in phase.

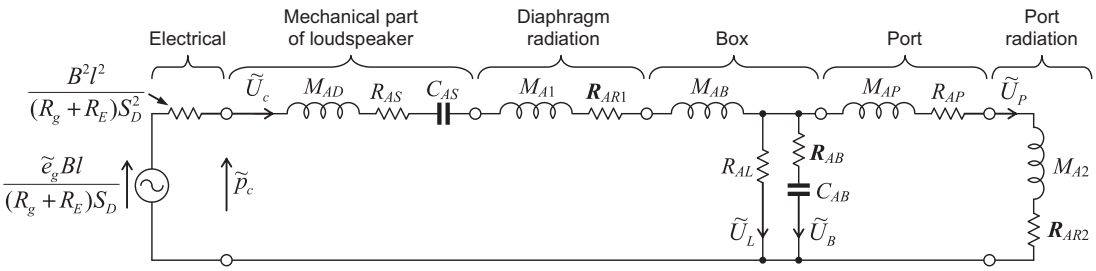

FIG. 7.24 Complete electro-mechano-acoustical circuit for a bass-reflex loudspeaker.

The total force produced at the voice coil by the electric current is $\tilde{p}_c S_D$, where S_D is the area of the diaphragm. The volume velocity of the diaphragm is $\tilde{U}_c$, that of the port is $\tilde{U}_P$, that of the box is $\tilde{U}_B$, and that due to leakage is $\tilde{U}_L$. Note that M_{AP} includes the inner mass loading for the port.

Summary of bass-reflex design

To determine the cut-off frequency, frequency response and the volume of the box:

If the Thiele–Small parameters (R_E, Q_{ES}, Q_{MS}, f_S, S_D, and V_{AS}) of the chosen drive unit are not supplied by the manufacturer, they may be measured according to Sec. 6.10. Then $Q_{TS} = Q_{ES}Q_{MS}/(Q_{ES} + Q_{MS})$.

From Table 7.4, select the frequency-response shape for which the Q_{TS} value is closest to that of the chosen drive unit (or choose a drive unit whose Q_{TS} value is closest to that of the desired frequency-response shape).

From the values of f_{3dB}/f_S, f_B/f_S, and V_{AB}/V_{AS} given in the table, compute the cut-off frequency f_{3dB}, box resonance frequency f_B, and apparent box volume V_{AB} respectively from the Thiele-Small parameters f_S and V_{AS}.

The frequency-response shape below the first diaphragm break-up mode is shown in Fig. 7.26.

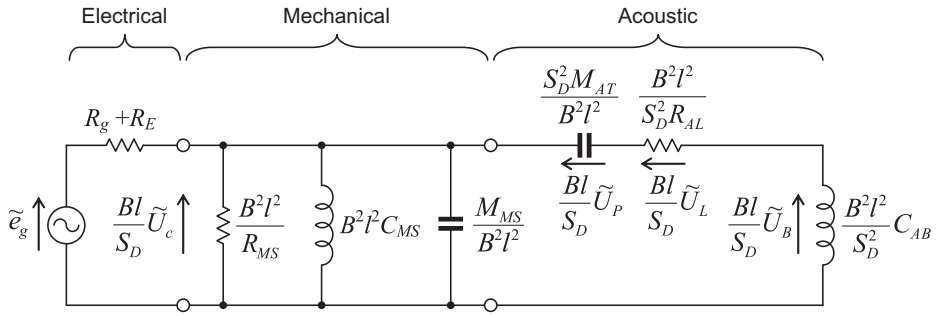

FIG. 7.25 Simplification of the circuit of Fig. 7.24, where the mechanical and acoustical quantities are referred to the electrical side using the admittance type analogy.

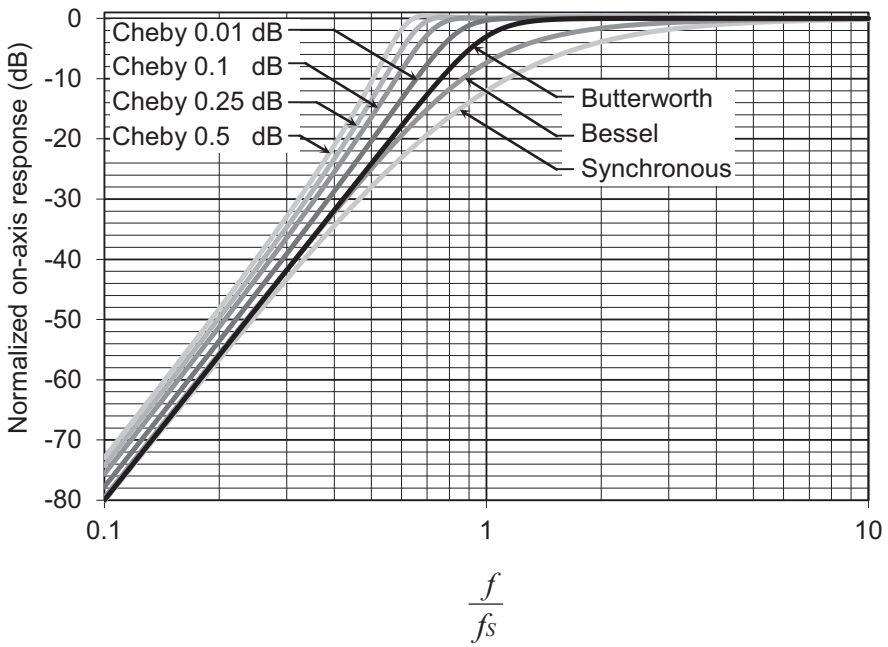

FIG. 7.26 On-axis frequency responses of 4th-order bass-reflex alignments generated from Table 7.4 by taking 20 times the logarithm of Eq. (7.73).

To determine the maximum sound pressure level (SPL):

If the loudspeaker is to be used near a wall or a rigid planar surface, which is large compared to the longest wavelength to be reproduced, then the maximum sound pressure SPL_{max} at a distance r is obtained from Eq. (6.34) to give

$$\text{SPL}_{\text{max}} = 20\log_{10}\left(\frac{1}{rc\times 20\times 10^{-6}}\sqrt{\frac{Z_{\text{nom}}W_{\text{max}}2\pi f_S^3 V_{AS}\rho_0}{R_E Q_{ES}}}\right)\ \text{dB SPL @ 1 m}$$

where W_{max} is the maximum rated input power. Otherwise, if it is to be used in the free field, subtract 6 dB from SPL_{max}.

To determine the excursion limit:

The maximum peak diaphragm displacement at frequencies well below the box resonance is obtained from Eq. (7.101) to give

$$\eta_{\text{max}} = \frac{1}{S_D c}\sqrt{\frac{Z_{\text{nom}}W_{\text{max}}V_{AS}}{R_E Q_{ES}\pi f_s \rho_0}}$$

However, we see from Fig. 7.27 that at frequencies above the box resonance, the displacement peaks at a smaller value. For example, the displacement peaks at $0.5\eta_{\text{max}}$ in the case of the 0.25 dB Chebyshev alignment or $0.25\eta_{\text{max}}$ in the case of the Butterworth alignment. If this peak value is greater than the rated

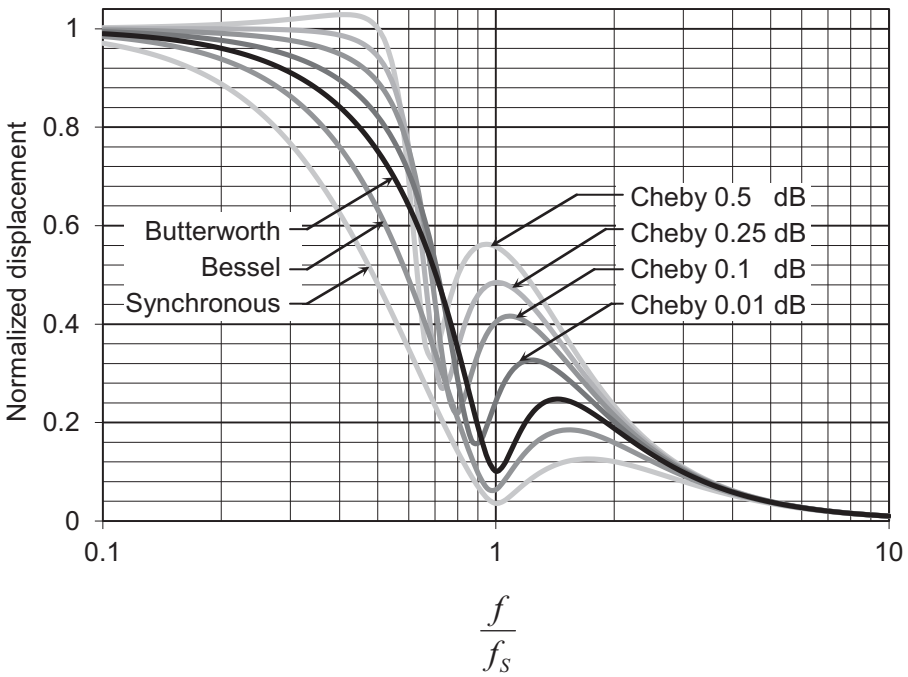

FIG. 7.27 Plots of normalized displacement $\tilde{\eta}/\tilde{\eta}_0$ for the 4th-order bass-reflex alignments of Table 7.4.

For simplicity, we assume that $Q_{MS} >> Q_{ES}$ so that $Q_{ES} \approx Q_{TS}$.

x_{max} limit of the drive unit, then an alternate drive unit with a greater x_{max} limit should be considered. If however the sub-resonance η_{max} value is greater than the rated x_{max} limit of the drive unit, it should be arranged for the box resonance frequency to be placed at the lower limit of the frequency range of the program material to be reproduced. If this is not possible, a high-pass filter should be employed to remove all content below the box resonance frequency. Best results are obtained when the filter is designed as part of the overall system.[16],[21],[22] If this is not possible either, then an alternate drive unit with a greater x_{max} limit should be considered.

To determine the port dimensions:

The maximum peak pressure p_{max} in Pa is obtained from SPL_{max} using

$$p_{max} = 2\sqrt{2} \times 10^{\left(\frac{SPL_{max}}{20} - 5\right)} \text{ Pa}$$

Determine the peak volume displacement V_{max} required to produce p_{max} at the box resonance frequency f_B, which is obtained from Eq. (13.104) to yield

$$V_{max} = \frac{r p_{max}}{2\pi f_B{}^2 \rho_0} \text{ m}^3$$

Choose the volume of the port V_P to be several times larger than V_{max} but within a reasonable limit. Then calculate the approximate length t of the port using Eq. (7.97) and the approximate cross-sectional area $S_P = V_P/t$. Either choose a convenient area S_P and calculate the exact length t using Eq. (7.98) or choose a convenient length t and calculate the exact area S_P using Eq. (7.99).

Study Secs. 7.16 and 7.17 (pages 342–343) for construction, adjustment, and performance.

The quantities not listed in the previous paragraph are

$\tilde{e}_g$ is open-circuit voltage in V of the audio amplifier.
B is flux density in the air gap in T (1 T = 10^4 gauss).
l is length in m of voice-coil wire.
R_g is output electrical resistance in Ω of the audio amplifier.
R_E is electrical resistance in Ω of the voice coil.
a is effective radius of the diaphragm in m.
$M_{AD} = M_{MD}/S_D{}^2$ is acoustic mass of the diaphragm and the voice coil in kg/m^4.
$C_{AS} = C_{MS}S_D^2$ is acoustic compliance of the diaphragm suspension in m^5/N.
$R_{AS} = R_{MS}/S_D^2$ is acoustic resistance of the diaphragm suspension in N·s/m^5.

7.11 RADIATED SOUND

The port in the box of a bass-reflex baffle is generally effective only at fairly low frequencies. At those frequencies its dimensions are generally so small it can be treated as though it were a simple source. The loudspeaker diaphragm can also be treated as a simple source because its area is often nearly the same as that of the opening.

Referring to Eq. (4.71), we find that the sound pressure a distance r away from the bass-reflex loudspeaker is

$$\tilde{p} = \tilde{p}_1 + \tilde{p}_2 + \tilde{p}_3 \approx \frac{j\omega\rho_0}{4\pi r}\left(\tilde{U}_c e^{-jkr_1} - \tilde{U}_P e^{-jkr_2} - \tilde{U}_L e^{-jkr_3}\right) \tag{7.66}$$

where

$\tilde{p}_1$, $\tilde{p}_2$, and $\tilde{p}_3$ are complex sound pressures, respectively, from the diaphragm, port, and leakage outlet at distance r.
r is average distance of the point of observation from the diaphragm and the port. Note that r is large compared with the diaphragm and port radii.
r_1, r_2, and r_3 are actual distances, respectively, of the point of observation from the diaphragm, port, and leakage outlet.
$\tilde{U}_c$ is complex volume velocity of the diaphragm.
$\tilde{U}_P$ is complex volume velocity of the port. Note that the negative sign is used for $\tilde{U}_P$ because, except for phase shift introduced by C_{AB} and M_{AP}, the air from the port moves outward when the air from the diaphragm moves inward.
$\tilde{U}_L$ is complex volume velocity of the leakage path.

Also, the complex volume velocity necessary to compress and expand the air in the box is

$$\tilde{U}_B = \tilde{U}_c - \tilde{U}_P - \tilde{U}_L \tag{7.67}$$

If we now let $r_1 = r_2 = r_3 = r$ by confining our attention to a particular point in space in front of the loudspeaker where this is true, we get

$$\tilde{p} \approx \frac{j\omega\rho_0}{4\pi r}(\tilde{U}_c - \tilde{U}_P - \tilde{U}_L)e^{-jkr} \tag{7.68}$$

Since $\tilde{U}_c - \tilde{U}_P - \tilde{U}_L = \tilde{U}_B$, we have simply that

$$\left|\tilde{p}\right| \approx \frac{f\rho_0\left|\tilde{U}_B\right|}{2r} \tag{7.69}$$

Amazing as it seems, the sound pressure produced at faraway points equidistant from cone and port of a bass-reflex loudspeaker is directly proportional to the volume velocity necessary to compress and expand the air inside the box!

At very low frequencies, where the reactance of C_{AB} is very high, $\tilde{U}_c$ becomes nearly equal to $\tilde{U}_P$, and $\tilde{U}_L$ becomes insignificant so that the pressure, measured at points $r = r_1 = r_2 = r_3$ approaches zero. In fact, the two sources $\tilde{U}_c$ and $\tilde{U}_P$ behave like a dipole so that the radiated sound pressure decreases by a factor of 4 for each halving of frequency. In addition, if we are below the lowest resonance frequency of the circuit of Fig. 7.24, the diaphragm velocity $\tilde{U}_c$ halves for each halving of frequency. Hence, in this very low frequency region, the sound pressure decreases by a factor of 16, which is 24 dB, for each halving of frequency. In other words, the slope is 4th order. Note that this decrease is greater than that for a loudspeaker in a closed box or in an infinite baffle.

7.12 ALIGNMENTS FOR PREDETERMINED FREQUENCY-RESPONSE SHAPES

As with the loudspeaker in a closed-box enclosure, we can choose a predetermined frequency-response shape and engineer the loudspeaker accordingly using an alignment table, which we shall generate in this section. In the interest of simplifying our analysis, let us redraw Fig. 7.24 to be as shown in

Fig. 7.25, referring the mechanical and acoustical quantities to the electrical side. Furthermore, we have assumed that at low frequencies we can ignore $\boldsymbol{R}_{AR1}$ and $\boldsymbol{R}_{AR2}$ and that the effects of the box and port resistances, $\boldsymbol{R}_{AB}$ and R_{AP} respectively, can be accounted for by adjusting the value of R_{AL}. It has been found in practice that R_{AL} is the dominant source of damping of the box resonance.[17] The new quantities shown on that circuit are defined as follows:

$$M_{MS} = M_{MD} + S_D^2(M_{A1} + M_{AB}) \tag{7.70}$$

$$M_{AT} = M_{A2} + M_{AP} \tag{7.71}$$

This circuit is exactly that which appears across the generator, which makes it easier to evaluate the electrical input impedance. Also, it looks more like an electrical filter network. The electrical and mechanical sections form a 1st-order band-pass filter, which in conjunction with the 1st-order time derivative in Eq. (7.69) given by the frequency term f, produces a net 2nd-order high-pass filter. The acoustical section forms a second 2nd-order high-pass filter so that the overall response is 4th-order. However, these two 2nd-order filters do not operate in isolation but are coupled to a degree which depends upon their relative resonance frequencies and the size of the box. Hence we shall introduce a coupling factor V_{AS}/V_{AB} during the following analysis, commonly known as the *compliance ratio*. As the volume of the box V_{AB} is increased relative to the suspension equivalent volume V_{AS}, the amount of coupling is weakened. Deriving the transfer function for such a complicated circuit as that shown in Fig. 7.25 can be very laborious, but in Chapter 14, a computer method is presented which can be applied using a mathematical software tool with symbolic computation, such as Maple or Mathematica. The circuit of Fig. 7.25 is used as the first worked example and it is shown in Eq. (14.79) that

$$\tilde{p}(r) = \frac{\tilde{e}_g Bl S_D \rho_0}{(R_g + R_E)M_{MS}} \cdot \frac{e^{-jkr}}{4\pi r} G(s) \tag{7.72}$$

where the frequency-response function $G(s)$ is given by

$$G(s) = \frac{s^4}{s^4 + P_3 s^3 + P_2 s^2 + P_1 s + P_0} \tag{7.73}$$

and the coefficients of the denominator polynomial in $s = j\omega$ are given by

$$P_3 = \frac{\omega_S}{Q_{TS}} + \frac{\omega_B}{Q_L} \tag{7.74}$$

$$P_2 = \left(1 + \frac{V_{AS}}{V_{AB}}\right)\omega_S^2 + \omega_B^2 + \frac{\omega_S \omega_B}{Q_{TS} Q_L} \tag{7.75}$$

$$P_1 = \frac{\omega_S \omega_B^2}{Q_{TS}} + \frac{\omega_S^2 \omega_B}{Q_L} \tag{7.76}$$

$$P_0 = \omega_S^2 \omega_B^2 \tag{7.77}$$

where ω_S is the angular suspension resonant-frequency in an infinite baffle given by

$$\omega_S = \frac{1}{\sqrt{M_{MS}C_{MS}}} \tag{7.78}$$

Q_{ES} is the electrical Q factor

$$Q_{ES} = \omega_S \frac{R_g + R_E}{(Bl)^2} M_{MS} \tag{7.79}$$

Q_{MS} is the mechanical Q factor

$$Q_{MS} = \omega_S \frac{1}{R_{MS}} M_{MS} \tag{7.80}$$

Q_{TS} is the total Q factor

$$Q_{TS} = \frac{Q_{ES}Q_{MS}}{Q_{ES} + Q_{MS}} \tag{7.81}$$

ω_B is the angular resonant-frequency of the box and port (including end corrections) given by

$$\omega_B = \frac{1}{\sqrt{M_{AT}C_{AB}}} \tag{7.82}$$

Q_L is the acoustical Q factor due to box and port losses

$$Q_L = \omega_B R_{AL} C_{AB} \tag{7.83}$$

V_{AB} is the apparent box volume, including the lining, which is related to the acoustic compliance by

$$V_{AB} = \rho_0 c^2 C_{AB} \tag{7.84}$$

and V_{AS} is the suspension equivalent volume

$$V_{AS} = S_D^2 \rho_0 c^2 C_{MS} \tag{7.85}$$

In order to solve Eqs. (7.74) to (7.77) for ω_S, ω_B, Q_{TS}, and V_{AS}/V_{AB}, we first eliminate Q_{TS} from Eqs. (7.74) and (7.76) and insert $\omega_S^2 = P_4/\omega_B^2$ from Eq. (7.77), which gives

$$\frac{\omega_B^4}{Q_L} - P_3\omega_B^3 + P_1\omega_B - \frac{P_0}{Q_L} = 0 \tag{7.86}$$

which is a quartic equation that has to be solved for ω_B. Although there are four roots to the polynomial, only one produces a full set of parameters (ω_B, ω_S, Q_{TS}, and V_{AS}/V_{AB}) which are positive and real. Then from Eqs. (7.77), (7.74), and (7.75) respectively we obtain the other three quantities:

$$\omega_S = \frac{\sqrt{P_0}}{\omega_B} \tag{7.87}$$

$$Q_{TS} = \frac{Q_L\omega_S}{P_3Q_L - \omega_B} \tag{7.88}$$

$$\frac{V_{AS}}{V_{AB}} = \frac{P_2 - \omega_B^2}{\omega_S^2} - \frac{\omega_B}{Q_{TS}Q_L\omega_S} - 1 \tag{7.89}$$

Let a pre-defined 4th-order frequency-response function be given by

$$G(s) = \frac{s^4}{\left(s^2 + \frac{\omega_1}{Q_1}s + \omega_1^2\right)\left(s^2 + \frac{\omega_2}{Q_2}s + \omega_2^2\right)} \tag{7.90}$$

which has a value of $1/\sqrt{2}$ or -3 dB when $\omega = 1$. The values of ω_1, ω_2, Q_1, and Q_2 for a number of frequency response shapes are given in Table 7.3, which are calculated from the formulas given in Appendix I. Because the suspension and box resonance frequencies are the same in the Butterworth alignment, the two complex-conjugate pole pairs lie on a semicircle in the complex plane with angles of $\pi/4$ between them. We shall see in Sec. 7.15 that these coincident resonance frequencies are useful when it comes to evaluating Q_L. We may create a range of sub-Butterworth alignments with such coincident resonance frequencies by multiplying the angles between the poles and the negative real axis by a scaling factor B, which has values between 0 and 1. When $B = 0$, we have the synchronous alignment in which all four poles are coincident and real. These sub-Butterworth alignments are generated by solving the quartic equation $\Omega^4 + 2(a+b)\Omega^3 + 2(1+2ab)\Omega^2 + 2(a+b)\Omega - 1 = 0$ for Ω, where $a = \cos B\pi/4$ and $b = \cos 3B\pi/4$. Although there are four solutions for Ω, only one is real and positive. Then $\omega_1 = \omega_2 = \sqrt{\Omega}$, $Q_1 = 0.5\sec B\pi/8$, and $Q_2 = 0.5\sec 3B\pi/8$.

Equating the denominator of Eq. (7.90) with that of Eq. (7.73) gives

$$P_3 = \frac{\omega_1}{Q_1} + \frac{\omega_2}{Q_2} \tag{7.91}$$

$$P_2 = \omega_1^2 + \omega_2^2 + \frac{\omega_1\omega_2}{Q_1Q_2} \tag{7.92}$$

$$P_1 = \frac{\omega_1\omega_2^2}{Q_1} + \frac{\omega_1^2\omega_2}{Q_2} \tag{7.93}$$

$$P_0 = \omega_1^2\omega_2^2 \tag{7.94}$$

Table 7.3 Resonance frequencies and Q values for various 4th-order frequency-response shapes

Frequency-response shape	ω_1	Q_1	ω_2	Q_2
Synchronous (B = 0)	0.4350	0.5000	0.4350	0.5000
Sub-Butterworth (B = 0.6)	0.5634	0.5142	0.5634	0.6575
Bessel (close to B = 0.77)	0.6992	0.5219	0.6237	0.8055
Sub-Butterworth (B = 0.9)	0.8482	0.5329	0.8482	1.0233
Butterworth (B = 1)	1.0000	0.5412	1.0000	1.3066
Chebyshev with 0.01 dB ripple	1.2870	0.5746	1.0356	1.7237
Chebyshev with 0.1 dB ripple	1.5370	0.6188	1.0519	2.1829
Chebyshev with 0.25 dB ripple	1.6900	0.6573	1.0574	2.5361
Chebyshev with 0.5 dB ripple	1.8310	0.7051	1.0600	2.9406

Table 7.4 4th-order alignments for bass-reflex enclosures for $Q_L = 7$

Frequency-response shape	f_{3dB}/f_S	V_{AB}/V_{AS}	Q_{TS}	f_B/f_S
Synchronous (B = 0)	2.2990	0.2899	0.2593	1.0000
Sub-Butterworth (B = 0.6)	1.7748	0.4028	0.3010	1.0000
Bessel (close to B = 0.77)	1.4941	0.5242	0.3312	0.9735
Sub-Butterworth (B = 0.9)	1.1790	0.6914	0.3689	1.0000
Butterworth (B = 1)	1.0000	0.9422	0.4048	1.0000
Chebyshev with 0.01 dB ripple	0.8143	1.5511	0.4572	0.8838
Chebyshev with 0.1 dB ripple	0.6963	2.3308	0.5120	0.7839
Chebyshev with 0.25 dB ripple	0.6374	2.9747	0.5553	0.7259
Chebyshev with 0.5 dB ripple	0.5894	3.7464	0.6073	0.6742

Then after inserting these values for P_0 to P_3 into Eqs. (7.86) to (7.89), we can generate the alignments given in Table 7.4.

Shown in Fig. 7.26 are frequency responses generated from Table 7.4 using Eq. (7.73). The frequency scale is normalized using f_S as the reference point because this is a fixed parameter of the loudspeaker drive unit. We see that the Chebyshev alignments give greater low-frequency extension at the cost of increased box size.

7.13 PORT DIMENSIONS

Knowing the Thiele–Small parameters of the drive unit (R_E, Q_{ES}, Q_{MS}, f_S, S_D, and V_{AS}) we choose a suitable alignment from Table 7.4, which gives us the required box volume V_{AB} and resonance frequency f_B. The total acoustic mass of the port including end corrections and assuming that it behaves as a flanged tube at one end only is given by

$$M_{AT} = \frac{\rho_0}{S_P}\left(t + 0.84\sqrt{S_P}\right) \tag{7.95}$$

Otherwise, if it is flanged at both ends, the correction factor is changed from 0.84 to 0.96, or to 0.72 if unflanged at both ends. The volume of air in the port V_P, which is simply the product of its cross-sectional area S_P and its length t, should be chosen to be several times greater than the amount of air it has to displace in order to produce the maximum sound pressure at full power. Hence

$$S_P = V_P/t \tag{7.96}$$

Inserting Eqs. (7.84), (7.95), and (7.96) into Eq. (7.82) but ignoring the end-correction factor yields the following approximate equation for the port length t:

$$t \approx \frac{c}{\omega_B}\sqrt{\frac{V_P}{V_{AB}}} \tag{7.97}$$

in which case the approximate cross-sectional area S_P is given by Eq. (7.96). However, we may wish to choose a more convenient area S_P and readjust the length t accordingly using the following exact formula:

$$t = \frac{S_P c^2}{V_{AB}\omega_B^2} - 0.84\sqrt{S_P} \tag{7.98}$$

or we may wish to choose a length t and calculate the exact area S_P using

$$S_P = \frac{0.84^2 V_{AB}^2 \omega_B^4}{4c^4}\left(1 + \sqrt{1 + \frac{4c^2 t}{0.84^2 V_{AB}\omega_B^2}}\right)^2 \tag{7.99}$$

7.14 DIAPHRAGM DISPLACEMENT

From the circuit of Fig. 7.25 we can derive the diaphragm volume velocity $\tilde{U}_c$ from which we obtain the diaphragm displacement:

$$\begin{aligned}\tilde{\eta} &= \tilde{U}_c/(j\omega S_D) \\ &= \frac{\omega_S \tilde{e}_g}{BlQ_{ES}}\left(\frac{s^2 + (\omega_B/Q_L)s + \omega_B^2}{s^4 + P_3 s^3 + P_2 s^2 + P_1 s + P_0}\right)\end{aligned} \tag{7.100}$$

At very low frequencies, the loudspeaker is virtually open at the back because the acoustic impedances of the box and port present very little opposition. Hence the low-frequency displacement $\tilde{\eta}_0$ is determined purely by the mechanical compliance C_{MS} of the suspension:

$$\tilde{\eta}\big|_{\omega\to 0} = \tilde{\eta}_0 = \frac{\tilde{e}_g}{BlQ_{ES}\omega_S} = C_{MS}Bl\frac{\tilde{e}_g}{R_E} \ (i.e.\ \text{Hooke's law where } Bl\frac{\tilde{e}_g}{R_E} = \tilde{f}) \tag{7.101}$$

This makes a useful reference point with which to normalize the displacement curves which are shown in Fig. 7.27 for the alignments of Table 7.4. We see that the Chebyshev alignments, which give greater low-frequency extension, not only require a larger box size, but also require a loudspeaker drive unit with a greater excursion limit $x_{\max}$.

7.15 ELECTRICAL INPUT IMPEDANCE AND EVALUATION OF Q_L

Also from the circuit of Fig. 7.25 we can derive the electrical input impedance Z_E as seen across the loudspeaker terminals:

$$Z_E = \frac{\tilde{e}_g R_E}{\tilde{e}_g - Bl\tilde{U}_c/S_D} = R_E\left\{1 + \frac{\omega_S s}{Q_{ES}}\left(\frac{s^2 + (\omega_B/Q_L)s + \omega_B^2}{s^4 + E_3 s^3 + E_2 s^2 + E_1 s + E_0}\right)\right\} \tag{7.102}$$

where the denominator polynomial coefficients are given by

$$E_3 = \frac{\omega_S}{Q_{MS}} + \frac{\omega_B}{Q_L} \tag{7.103}$$

$$E_2 = \left(1 + \frac{V_{AS}}{V_{AB}}\right)\omega_S^2 + \omega_B^2 + \frac{\omega_S \omega_B}{Q_{MS} Q_L} \tag{7.104}$$

$$E_1 = \frac{\omega_S \omega_B^2}{Q_{MS}} + \frac{\omega_S^2 \omega_B}{Q_L} \tag{7.105}$$

$$E_0 = \omega_S^2 \omega_B^2 \tag{7.106}$$

The coefficients E_0 to E_3 differ from the coefficients P_0 to P_3 of Eqs. (7.74) to (7.77) respectively in that Q_{TS} is replaced by Q_{MS}. Normalized impedance curves are plotted in Fig. 7.28 for the alignments of Table 7.4. When comparing these curves with the impedance of a loudspeaker in an infinite baffle, as shown in Fig. 6.8, we see that the peak at f_S due to the parallel resonance of M_{MS} with C_{MS} has been split into two peaks with a minima in between at f_B due to the series resonance of M_{AT} with C_{AB}. For the Synchronous, Bessel, and Butterworth alignments where $f_B = f_S$, the two peaks are symmetrical either side of f_B. However, in the case of the Chebyshev alignments the peaks are asymmetrical with the smaller peak occurring below f_B which indicates that the low-frequency response is extended at the cost of extra power.

The minima at f_B is particularly useful for checking the tuning of the port. Furthermore, in the case of alignments where $f_B = f_S$, (e.g. Synchronous, Bessel, and Butterworth) we can simplify Eq. (7.102) at $f = f_B$ to give the impedance at the box resonance dip:

$$Z_E\Big|_{\omega=\omega_s=\omega_B} = Z_{EB} = R_E\left(1 + \frac{\dfrac{1}{Q_{ES}Q_L}}{\dfrac{V_{AS}}{V_{AB}} + \dfrac{1}{Q_{MS}Q_L}}\right) \tag{7.107}$$

from which we obtain

$$Q_L = \frac{V_{AB}}{V_{AS}}\left(\frac{1}{Q_{ES}((Z_{EB}/R_E) - 1)} - \frac{1}{Q_{MS}}\right) \tag{7.108}$$

which enables us to measure the Q_L value for the box and port resonance. See Sec. 7.17.

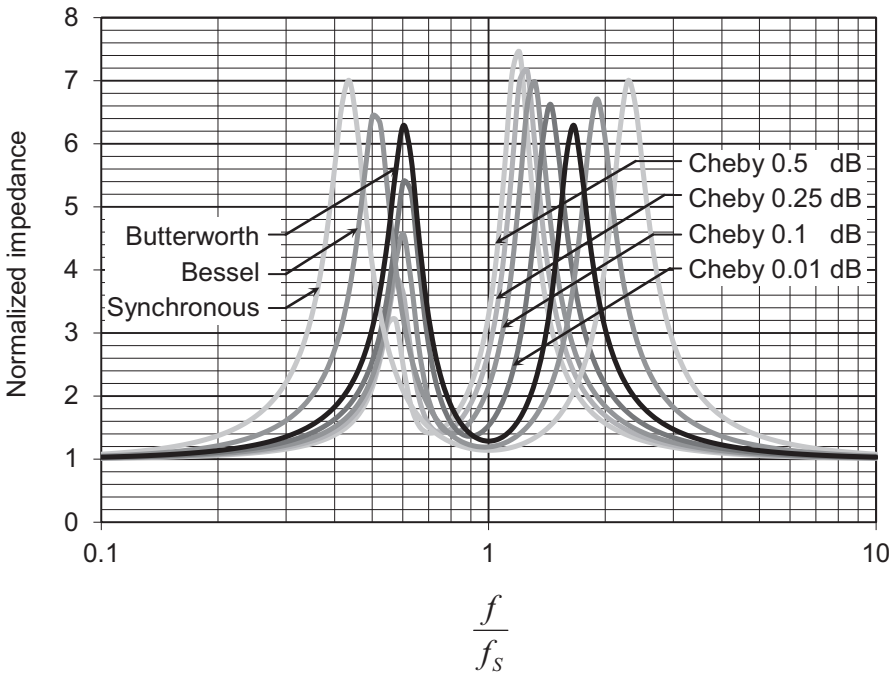

FIG. 7.28 Plots of normalized electrical impedance magnitude $|Z_E/R_E|$ for the 4th-order bass-reflex alignments of Table 7.4.

We let $Q_{MS} = 9Q_{TS}$ so that $Q_{ES} = 1.125Q_{TS}$.

7.16 PERFORMANCE

With the formulas and charts just given, it is possible to calculate the response of the loudspeaker in a bass-reflex enclosure. A complete example is given after Sec. 7.17.

From Fig. 7.25, we see that for frequencies below ω_B, radiation from the port (proportional to $-\tilde{U}_P$) is out of phase with the radiation from the diaphragm (proportional to $\tilde{U}_c$). As a result, the response at very low frequencies is usually not enhanced by the addition of the port. Above the resonance frequency ω_B, radiation from the port is in phase with that from the diaphragm, with a resulting enhancement over the closed-baffle response. The amount of the increase in response generally averages about 3 dB over a frequency range of one to two octaves.

An important reason for using a bass-reflex enclosure is that the loudspeaker produces less distortion at frequencies of around ω_B for a given acoustic power radiated than would be the case if the box were closed. The assumption on which this statement is made is that the motion of the air in the port is distortionless even though the amplitude of vibration is large. This is true generally because there is no suspension or magnetic circuit in the port in which nonlinear effects can occur. However, in order to avoid turbulence, the port should be as smooth as possible with filleted edges at each end. A large loudspeaker diaphragm usually is superior to a small one because the amplitude of its motion is less, thereby reducing nonlinear distortion.

One disadvantage of a bass-reflex enclosure is that the port can produce pipe modes at higher frequencies and these cannot be damped using absorbent material without negating the benefit of the port. However, their effect can be mitigated by locating the mouth of the port on the rear of the box so that they are less audible at the front. At the box resonance, the wavelength is usually very large compared to the box dimensions, so the small resulting phase difference between the outputs of the port and diaphragm will have little effect on the performance. [39]

An advantage of a bass-reflex enclosed loudspeaker is that, where room space is a factor, a properly tuned bass-reflex system helps to offset the effect of the small box volume.

7.17 CONSTRUCTION AND ADJUSTMENT NOTES

Bear in mind that many drive units nowadays are designed for use in "air-suspension" closed-box enclosures and can be identified by their very low resonance frequencies. In a bass-reflex design the high compliance of their suspensions could lead to excessive diaphragm excursion below the box resonance frequency.

The box should be very rigid in order to resist vibration. The joints should be tight-glued and the larger panels should be braced by gluing reinforcing strips to them. The access side should be screwed on securely with strips of sealing material such as neoprene. Most drive units are now supplied with sealing gaskets.

When the cabinet has been completed and the loudspeaker has been installed, the correctness of the tuning may be determined by connecting an audio oscillator with an output impedance about 100 times that of the loudspeaker to the electrical terminals. Next, connect a voltmeter across the loudspeaker terminals. Then vary the frequency of the oscillator in order to find the minimum reading between the two peaks (see Fig. 7.28). This should occur at the calculated frequency ω_B if the design is correct. The ratio of the voltage reading at this frequency to that at some very low frequency, where it reaches an absolute minimum, gives the ratio Z_{EB}/R_E from which we can calculate Q_L using Eq. (7.108).

The resonance frequency ω_B of the enclosure can be adjusted by varying the length of the port. A typical value of Q_L is around 7. If it is much lower than this, there is probably a problem with leakage caused by a poor seal. In order to find the source of leakage, block the port and drive the loudspeaker (with minimum source impedance) at a very low frequency and listen around the box for any turbulent "hissing" sounds.

Example 7.3. Bass-reflex enclosure design. In the previous part we discussed in detail the design of a closed-box baffle for a low-frequency (woofer) loudspeaker. We presented methods for the determination of its physical constants, and we showed a comparison between measurements and calculations.

In this part we shall use the same loudspeaker drive unit as part of a pair with double the box volume, so that each unit "sees" the same volume as before. If a pair of 8 Ω drive units is used, this provides a choice of 4 Ω or 16 Ω loads for parallel or series combinations respectively. A port will be introduced into the box that resonates with the box compliance to the same frequency as the mechanical or driver part of the circuit of Fig. 7.25, that is,

$$\omega_S = 1/\sqrt{M_{MS}C_{MS}}.$$

Your brief is to design a compact floor-standing loudspeaker that can produce 105 dB SPL @ 1 m so that it will be suitable for a medium to large listening area. In other words, the low frequencies will not be augmented by room modes. Therefore the frequency response should be a flat as possible down to 41 Hz, the lowest note on a bass guitar. In order to give the widest possible dispersion and for cosmetic reasons, the drive unit should not be too large. A suitable drive unit is the Bandor type 100DW/8A used in the previous closed-box example. In order to reach the required SPL we will need to use two of these, one above the other, which doubles the radiating area without increasing the width and therefore maintains the horizontal directivity pattern. From actual measurements (see Sec 6.10) the Thiele-Small parameters are:

$R_E = 6.27\ \Omega$
$Q_{ES} = 0.522$
$Q_{MS} = 1.9$
$f_S = 37$ Hz
$S_D = 120\ \text{cm}^2$
$V_{AS} = 24$ L

If we re-use the same volume per drive unit as the closed-box design, then V_{AB} = 13.42 L. Hence V_{AB}/V_{AS} = 13.42/24 = 0.56, which from Table 7.4 would suggest the use of a Bessel alignment where V_{AB}/V_{AS} = 0.52 and the frequency response is plotted in Fig. 7.26. At f_S = 37 Hz, the response is - 7.4 dB with the - 3 dB point at $1.49f_S$ = 55 Hz. However, The Q_{TS} value of

$$Q_{TS} = \frac{Q_{ES}Q_{MS}}{Q_{ES} + Q_{MS}} = 0.41$$

is somewhat higher than the optimum value of 0.33 given by Table 7.4 for a Bessel alignment. This may be corrected by using an amplifier with a negative output impedance of R_g = -1.45 Ω (due to positive current feedback [42]). However, for the purpose of this analysis, we shall proceed with an "underdamped" Bessel alignment by setting R_g = 0.

$$V_{AB} = 2 \times 0.5242 \times 24 = 25.2\ \text{L}$$

From Eq. (6.48) we can calculate the reference efficiency, noting that on one hand a loudspeaker in a box is half as efficient as one radiating from both sides in an infinite baffle, but on the other, this is compensated for by having two of them:

$$E_{ff} = 100\frac{8 \times 3.14^2 \times 0.024 \times 37^3}{0.522 \times 345^3} = 0.448\%$$

In order to calculate the maximum SPL, we first obtain C_{MS}, M_{MS}, and Bl from Eqs. (6.27), (6.28), and (6.30) respectively

$$C_{MS} = \frac{0.024}{0.012^2 \times 1.18 \times 345^2} = 1.19\ \text{mm/N}$$

$$M_{MS} = \frac{1}{(2 \times 3.14 \times 37)^2 \times 0.00119} = 0.0156\ \text{kg}$$

$$Bl = \sqrt{\frac{6.27}{2 \times 3.14 \times 37 \times 0.522 \times 0.00119}} = 6.59 \text{ T·m}$$

Knowing that the power rating $W_{\max}$ is 100W, we obtain from Eq. (6.33)

$$\text{SPL}_{\max} = 20 \log_{10}\left(\frac{\sqrt{6.27 \times 100} \times 6.59 \times 0.012 \times 1.18}{2 \times 3.14 \times 6.27 \times 0.0156 \times 20 \times 10^{-6}}\right) = 105.6 \text{ dB SPL @ 1 m}$$

where two drive units in a box produce the same pressure as a single one in an infinite baffle. Next use Eq. (7.101) to check the peak displacement at low frequencies at full power:

$$\eta_{\max} = \frac{\sqrt{2 \times 6.27 \times 100}}{6.59 \times 0.522 \times 2 \times 3.14 \times 37} = 44.3 \text{ mm}$$

but from Fig. 7.27 we see that for the Bessel alignment the maximum above f_S frequency is 0.126 times this value, or 5.6 mm. It turns out that the $x_{\max}$ value of the drive unit is 14 mm, with a linear limit of 4.5 mm, so there should be no problems with this design. Now we turn to the port dimensions, but first we must calculate the volume displacement $V_{\max}$ required from the maximum pressure $p_{\max}$ (See "Summary of Bass-reflex Design", p. 334).

$$p_{\max} = 2 \times 1.414 \times 10^{\frac{105.6-7.4}{20}-5} = 2.3 \text{ Pa}$$

so that from Eq. (6.35)

$$V_{\max} = \frac{1 \times 2.3}{2 \times 3.14 \times 37^2 \times 1.18} = 0.23 \text{ L}$$

Let the volume of the port be ten times the maximum volume displacement, or $V_P = 10V_{\max} = 2.3$ L. From Table 7.4, the box resonance frequency is $f_B = 0.9735 f_S = 36$ Hz. The approximate length of the port excluding end effects is obtained from Eq. (7.97):

$$t \approx \frac{345}{2 \times 3.14 \times 36}\sqrt{\frac{2.3}{25.2}} = 46.1 \text{ cm}$$

so that the approximate cross-sectional area is

$$S_P = V_P/t = 0.0023/0.461 = 50 \text{ cm}^2, \text{say } 15 \text{ cm} \times 3.4 \text{ cm} = 51 \text{ cm}^2$$

Then the actual length is calculated from Eq. (7.98):

$$t = \frac{0.0051 \times 345^2}{0.0252 \times (2 \times 3.14 \times 36)^2} - 0.84 \times \sqrt{0.0051} = 41.1 \text{ cm}$$

We let the lining material occupy one quarter of the total box volume so that $V_M = V_B/4 = V_A/3$ because $V_B = V_A + V_M$. We already know that $V_{AB} = V_A + \gamma V_M = 25.2$ L where $\gamma = 1.4$. Hence

$$V_A = \frac{25.2}{1 + 1.4/3} = 17.2 \text{ L}$$

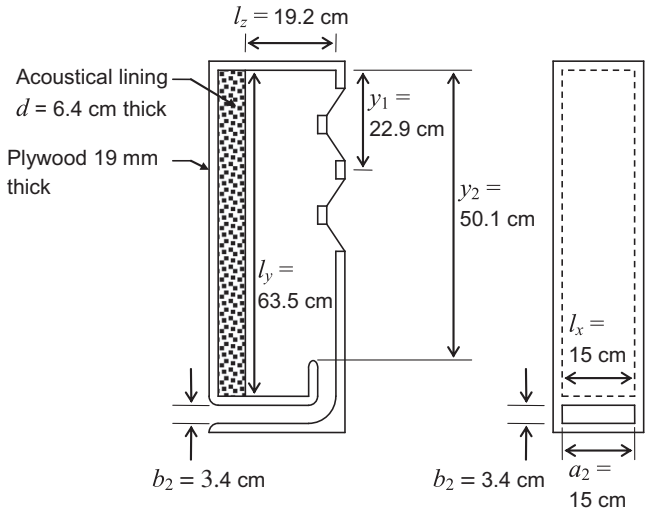

FIG. 7.29 Example of bass-reflex enclosure design.

and $V_M = 17.2/3 = 5.7$ L so that $V_B = 17.2 + 5.7 = 22.9$ L. Hence the compliance of the air in the box is $C_{AA} = V_A/(\gamma P_0) = 0.0172/(1.4 \times 10^5) = 1.23 \times 10^{-7}$ and the lining material $C_{AM} = V_M/P_0 = 0.0061/10^5 = 6.1 \times 10^{-8}$ so that the apparent compliance is $C_{AB} = C_{AA} + \gamma C_{AM} = 1.23 \times 10^{-7} + 6.1 \times 10^{-8} = 1.84 \times 10^{-7}$. The box and port dimensions are shown in Fig. 7.29. The internal width W is 15 cm, which is the smallest width that will accommodate the drive units. The acoustic center of the two drive units is about one third of the internal height from the top so as not to coincide with the anti-nodes of the first or second vertical modes. The box contains one 63.5 by 15 by 6.4 cm piece of lining material. Let us now calculate the box and port losses. If the flow resistance is $R_f = 200$ rayl/cm, then acoustic resistance of the lining material with a depth of 6.4 cm becomes

$$R_{AM} = \frac{6.4 \times 200}{3 \times 0.635 \times 0.15} = 4480 \text{ N}\cdot\text{s/m}^5$$

so that the box resistance from Eq. (7.7) is

$$R_{AB} = \frac{4480}{\left(1 + \dfrac{17.2}{1.4 \times 6.1}\right)^2 + (2 \times 3.14 \times 36 \times 4480 \times 1.23 \times 10^{-7})^2} = 492 \text{ N}\cdot\text{s/m}^5$$

from which we obtain Q_A due to absorption within the box:

$$Q_A = \frac{1}{\omega_B R_{AB} C_{AB}} = \frac{1}{2 \times 3.14 \times 36 \times 492 \times 1.84 \times 10^{-7}} = 49$$

The resistance of the port is given by Eq. (4.23):

$$R_{AP} = \frac{\sqrt{4 \times 3.14 \times 36 \times 1.18 \times 1.86 \times 10^{-5}}}{0.15 \times 0.034}\left(\frac{0.411}{\sqrt{0.15 \times 0.034/3.14}} + 2\right) = 238\ \mathrm{N \cdot s/m^5}$$

from which we obtain Q_p of the port:

$$Q_p = \frac{1}{\omega_B R_{AP} C_{AB}} = \frac{1}{2 \times 3.14 \times 36 \times 238 \times 1.84 \times 10^{-7}} = 101$$

These Q values are very high, which supports the commonly held view that leakage losses dominate. Unfortunately, the effect of leakage cannot be determined until the loudspeaker and its enclosure are assembled and measured. A common value of Q_L due to all losses is around 7.

Let us now create a semi-analytical simulation model of the design of Fig. 7.29 using 2-port networks and transmission matrices, as introduced in Sec. 3.10 and Fig. 4.43. The schematic is shown in Fig. 7.30. Although it is based on the circuit of Fig. 7.24, a gyrator has been inserted between the electrical elements and the mechanical ones, which enables us to calculate more easily the generator current $\tilde{i}_g$ from which we obtain the electrical impedance. We are ignoring the generator impedance R_g

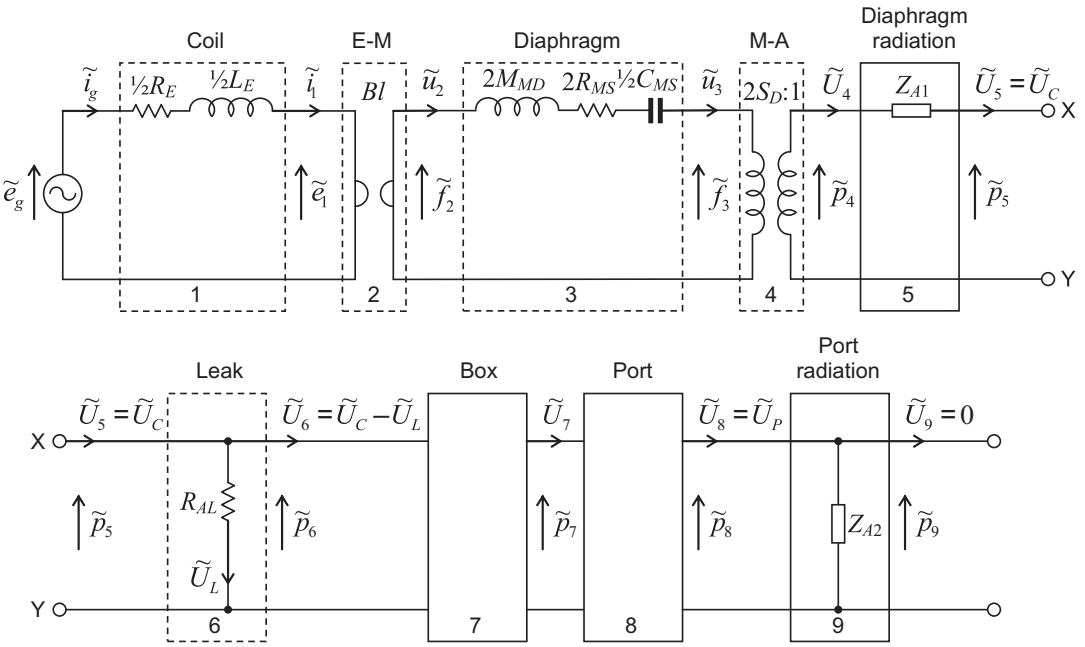

FIG. 7.30 Semi-analytical model of example bass-reflex enclosure design shown in Fig. 7.29 using transmission matrices.

The dashed boxes are lumped-element 2-port networks and the solid boxes are analytical ones. Here the two drive units are connected in parallel so that the net coil resistance R_E is halved. If the drive units are connected in series, replace $\frac{1}{2}R_E$, $\frac{1}{2}L_E$, and Bl with $2R_E$, $2L_E$, and $2Bl$.

since in the experimental setup this is negligible compared to R_E. The dashed boxes are lumped-element 2-port networks and the solid boxes are analytical ones. Here the two drive units are connected in parallel so that the net coil resistance R_E is halved. If the drive units are connected in series, replace $\frac{1}{2}R_E$, $\frac{1}{2}L_E$, and Bl with $2R_E$, $2L_E$, and $2Bl$. From the schematic we create the transmission matrices required to represent each 2-port network as follows.

1. Coil.

$$\begin{bmatrix} \tilde{e}_g \\ \tilde{i}_g \end{bmatrix} = \begin{bmatrix} 1 & \frac{1}{2}Z_E \\ 0 & 1 \end{bmatrix} \cdot \begin{bmatrix} \tilde{e}_1 \\ \tilde{i}_1 \end{bmatrix} = \mathbf{C} \cdot \begin{bmatrix} \tilde{e}_1 \\ \tilde{i}_1 \end{bmatrix}$$

where $Z_E = R_E + j\omega L_E$.

2. Electro-mechanical transduction.

$$\begin{bmatrix} \tilde{e}_1 \\ \tilde{i}_1 \end{bmatrix} = \begin{bmatrix} 0 & Bl \\ (Bl)^{-1} & 0 \end{bmatrix} \cdot \begin{bmatrix} \tilde{f}_2 \\ \tilde{u}_2 \end{bmatrix} = \mathbf{E} \cdot \begin{bmatrix} \tilde{f}_2 \\ \tilde{u}_2 \end{bmatrix}$$

3. Diaphragm.

$$\begin{bmatrix} \tilde{f}_2 \\ \tilde{u}_2 \end{bmatrix} = \begin{bmatrix} 1 & 2Z_{MD} \\ 0 & 1 \end{bmatrix} \cdot \begin{bmatrix} \tilde{f}_3 \\ \tilde{u}_3 \end{bmatrix} = \mathbf{D} \cdot \begin{bmatrix} \tilde{f}_3 \\ \tilde{u}_3 \end{bmatrix}$$

where $Z_{MD} = j\omega M_{MD} + R_{MS} + 1/(j\omega C_{MS})$. We must exclude the radiation mass from the diaphragm so that $M_{MD} = M_{MS} - 16\rho_0 a^3/3$, where $a = \sqrt{S_D/\pi}$.

4. Mechano-acoustical transduction.

$$\begin{bmatrix} \tilde{f}_3 \\ \tilde{u}_3 \end{bmatrix} = \begin{bmatrix} 2S_D & 0 \\ 0 & (2S_D)^{-1} \end{bmatrix} \cdot \begin{bmatrix} \tilde{p}_4 \\ \tilde{U}_4 \end{bmatrix} = \mathbf{M} \cdot \begin{bmatrix} \tilde{p}_4 \\ \tilde{U}_4 \end{bmatrix}$$

5. Diaphragm radiation.

$$\begin{bmatrix} \tilde{p}_4 \\ \tilde{U}_4 \end{bmatrix} = \begin{bmatrix} 1 & Z_{A1} \\ 0 & 1 \end{bmatrix} \cdot \begin{bmatrix} \tilde{p}_5 \\ \tilde{U}_5 \end{bmatrix} = \mathbf{F} \cdot \begin{bmatrix} \tilde{p}_5 \\ \tilde{U}_5 \end{bmatrix}$$

where Z_{A1} is the acoustic radiation impedance of the diaphragm, taking into account the mutual radiation impedance, given by Eqs. (13.334) and (13.339) where $Z_{A1} = (Z_{11} + Z_{12})/S_D$ and $a = \sqrt{S_D/\pi}$.

6. Leak.

$$\begin{bmatrix} \tilde{p}_5 \\ \tilde{U}_5 \end{bmatrix} = \begin{bmatrix} 1 & 0 \\ R_{AL}^{-1} & 1 \end{bmatrix} \cdot \begin{bmatrix} \tilde{p}_6 \\ \tilde{U}_6 \end{bmatrix} = \mathbf{L} \cdot \begin{bmatrix} \tilde{p}_6 \\ \tilde{U}_6 \end{bmatrix}$$

where the leakage resistance is given by

$$R_{AL} = Q_L/(2\pi f_B C_{AB}) = 7/(2 \times 3.14 \times 36 \times 1.84 \times 10^{-7}) = 168,200\ \mathrm{N \cdot s/m^5}.$$

7. Box.

$$\begin{bmatrix} \tilde{p}_6 \\ \tilde{U}_6 \end{bmatrix} = \begin{bmatrix} b_{11} & b_{12} \\ b_{21} & b_{22} \end{bmatrix} \cdot \begin{bmatrix} \tilde{p}_7 \\ \tilde{U}_7 \end{bmatrix} = \mathbf{B} \cdot \begin{bmatrix} \tilde{p}_7 \\ \tilde{U}_7 \end{bmatrix}$$

The mechanical z-parameters of the 2-port network for the bass-reflex enclosure are given by Eq. (7.131) in Sec. 7.18. We obtain the acoustical z-parameters by dividing through by $a_p a_q b_p b_a$ to yield

$$Z_{pq} = \rho_0 c \left\{ \frac{1}{l_x l_y} \frac{\frac{Z_s}{\rho_0 c} + j \tan k l_z}{1 + j \frac{Z_s}{\rho_0 c} \tan k l_z} + \frac{8 l_y}{\pi^2 b_p b_q l_x} \right.$$

$$\times \sum_{n=1}^{\infty} \frac{k}{n^2 k_{0n}} \cos\left(\frac{n\pi y_p}{l_y}\right) \cos\left(\frac{n\pi y_q}{l_y}\right) \sin\left(\frac{n\pi b_p}{2l_y}\right) \sin\left(\frac{n\pi b_q}{2l_y}\right) \frac{\frac{k_{0n} Z_s}{k\rho_0 c} + j \tan k_{0n} l_s}{1 + j \frac{k_{0n} Z_s}{k\rho_0 c} \tan k_{0n} l_s}$$

$$+ \frac{2 l_x}{\pi^2 a_p a_q l_y} \sum_{m=1}^{\infty} \frac{k}{m^2 k_{m0}} \sin\left(\frac{m\pi a_p}{l_x}\right) \sin\left(\frac{m\pi a_q}{l_x}\right) \frac{\frac{k_{m0} Z_s}{k\rho_0 c} + j \tan k_{m0} l_z}{1 + j \frac{k_{m0} Z_s}{k\rho_0 c} \tan k_{m0} l_z}$$

$$+ \frac{16 l_x l_y}{\pi^4 a_p a_q b_p b_q} \sum_{m=1}^{\infty} \sum_{n=1}^{\infty} \frac{k}{m^2 n^2 k_{mn}} \sin\left(\frac{m\pi a_p}{l_x}\right) \sin\left(\frac{m\pi a_q}{l_x}\right) \cos\left(\frac{m\pi y_p}{l_y}\right)$$

$$\left. \times \cos\left(\frac{n\pi y_q}{l_y}\right) \sin\left(\frac{n\pi b_p}{2l_y}\right) \sin\left(\frac{n\pi b_q}{2l_y}\right) \frac{\frac{k_{mn} Z_s}{k\rho_0 c} + j \tan k_{mn} l_z}{1 + j \frac{k_{mn} Z_s}{k\rho_0 c} \tan k_{mn} l_z} \right\}$$

where

$$k_{mn} = \sqrt{k^2 - \left(\frac{2m\,\pi}{l_x}\right)^2 - \left(\frac{n\,\pi}{l_y}\right)^2}$$

and

$$Z_s = \frac{R_f d}{3} + \frac{P_0}{j\omega d}$$

where the value of the lining flow resistance R_f is chosen such that $R_f d/3 = \rho_0 c = 412$ rayl, which is the impedance of free space and thus provides optimum sound absorption at higher frequencies. Then the transmission-matrix parameters for the box are given by $b_{11} = z_{11}/z_{21}$, $b_{12} = (z_{11}z_{22} - z_{12}z_{21})/z_{21}$, $b_{21} = 1/z_{21}$, and $b_{22} = z_{22}/z_{21}$. The dimensions are given in Fig. 7.29 except for $a_1 = b_1 = \sqrt{S_D}$.

8. Port.

$$\begin{bmatrix} \tilde{p}_7 \\ \tilde{U}_7 \end{bmatrix} = \begin{bmatrix} \cos k_p t & jZ_p \sin k_p t \\ jZ_p^{-1} \sin k_p t & \cos k_p t \end{bmatrix} \cdot \begin{bmatrix} \tilde{p}_9 \\ \tilde{U}_9 \end{bmatrix} = \mathbf{P} \cdot \begin{bmatrix} \tilde{p}_8 \\ \tilde{U}_8 \end{bmatrix}$$

where the port wave number k_P and characteristic impedance Z_P are obtained from Eqs. (4.215) and (4.217) respectively. The port is assumed to be large enough to ignore boundary slip and thermal conduction so that we only consider the viscous flow losses to obtain $k_P = \omega\xi/c = 2\pi f\xi/c$, $Z_P = \rho_0 c\xi/S_P$, and $S_P = a_2 b_2$ where

$$\xi = \sqrt{1 - \frac{2J_1(k_V a_P)}{k_V a_P J_0(k_V a_P)}},\ a_p = \sqrt{a_2 b_2/\pi},\ \text{and}\ k_V = \sqrt{-j\pi 2 f \rho_0/\mu}$$

where $\mu = 1.86 \times 10^{-5}$ m^2/s is the viscosity coefficient for air at 20°C.

9. Port radiation.

$$\begin{bmatrix} \tilde{p}_8 \\ \tilde{U}_8 \end{bmatrix} = \begin{bmatrix} 1 & 0 \\ Z_{A2}^{-1} & 1 \end{bmatrix} \cdot \begin{bmatrix} \tilde{p}_9 \\ \tilde{U}_9 \end{bmatrix} = \mathbf{R} \cdot \begin{bmatrix} \tilde{p}_9 \\ \tilde{U}_9 \end{bmatrix}$$

In this case, the port outlet is rectangular and close to the floor so that Z_{A2} may be given by the impedance of a rectangular piston in an infinite baffle using Eqs. (13.326) and (13.327), where $Z_{A2} = (\boldsymbol{R}_s + jX_s)/(a_2 b_2)$.

First we evaluate $\tilde{p}_9$ at the end of the chain:

$$\begin{bmatrix} \tilde{e}_g \\ \tilde{i}_g \end{bmatrix} = \mathbf{A} \cdot \begin{bmatrix} \tilde{p}_9 \\ 0 \end{bmatrix}$$

where

$$\mathbf{A} = \mathbf{C} \cdot \mathbf{E} \cdot \mathbf{D} \cdot \mathbf{M} \cdot \mathbf{F} \cdot \mathbf{L} \cdot \mathbf{B} \cdot \mathbf{P} \cdot \mathbf{R} = \begin{bmatrix} a_{11} & a_{12} \\ a_{21} & a_{22} \end{bmatrix}$$

Hence $\tilde{p}_9 = \tilde{e}_g/a_{11}$. Then we work backwards to obtain the volume velocities we wish to evaluate. In particular, we are interested in the far-field pressure, which according to Eq. (7.69) is a function of

$$\tilde{U}_B = \tilde{U}_c - \tilde{U}_L - \tilde{U}_p = \tilde{U}_6 - \tilde{U}_8.$$

This procedure is fairly straightforward and does not involve any matrix inversion. From the port radiation matrix (9), we obtain

$$\tilde{U}_P = \tilde{U}_8 = \tilde{p}_9/Z_{A2}$$

and working back further to the box matrix (7) we obtain

$$\begin{bmatrix} \tilde{p}_6 \\ \tilde{U}_6 \end{bmatrix} = \mathbf{N} \cdot \begin{bmatrix} \tilde{p}_9 \\ 0 \end{bmatrix}$$

where

$$\mathbf{N} = \mathbf{B} \cdot \mathbf{P} \cdot \mathbf{R} = \begin{bmatrix} n_{11} & n_{12} \\ n_{21} & n_{22} \end{bmatrix}$$

so that

$$\tilde{U}_c - \tilde{U}_L = \tilde{U}_6 = n_{21}\tilde{p}_9$$

and therefore

$$\tilde{U}_B = \tilde{U}_c - \tilde{U}_L - \tilde{U}_P = \tilde{U}_6 - \tilde{U}_8 = (n_{21} - 1/Z_{A2})\tilde{e}_g/a_{11}$$

The port volume velocity is given by

$$\tilde{U}_P = \tilde{U}_8 = \tilde{e}_g/(a_{11}Z_{A2})$$

and the diaphragm volume velocity by

$$\tilde{U}_c - \tilde{U}_L = \tilde{U}_6 = n_{21}\tilde{e}_g/a_{11}$$

In order to plot the normalized far-field on-axis pressure, we simply divide $\tilde{U}_B$ by a reference volume velocity

$$\tilde{U}_{ref} = \frac{2\tilde{e}_g BIS_D}{\omega M_{MS} R_E}$$

and plot $20\log_{10}|\tilde{U}_B/\tilde{U}_{ref}|$ as shown in Fig. 7.31. The port and diaphragm volume velocities,

$$20\log_{10}\left|\tilde{U}_P/\tilde{U}_{ref}\right| \quad \text{and} \quad 20\log_{10}\left|\left(\tilde{U}_c - \tilde{U}_L\right)/\tilde{U}_{ref}\right|,$$

respectively, are plotted separately in Fig. 7.32. Although the effects of box and port modes are clearly seen in the calculated response of Fig. 7.31, most of the irregularities are emanating from the mouth of the port as is seen from Fig. 7.32. By contrast, the output from the diaphragm is fairly smooth apart from one small feature at 220 Hz, which is due to the fundamental vertical mode of the box. At 375, 750, and 1125 Hz we see the 1st, 2nd, and 3rd port modes respectively. The effect of these will be mitigated somewhat by mounting the port on the rear of the enclosure as is seen from the measured response of Fig. 7.31. Finally, we can obtain the input impedance from $\tilde{e}_g/\tilde{i}_g$ where $\tilde{i}_g = a_{21}\tilde{p}_9$ and from above $\tilde{p}_9 = \tilde{e}_g/a_{11}$. Therefore the input impedance is simply $Z_E = a_{11}/a_{21}$, as plotted in Fig. 7.33.

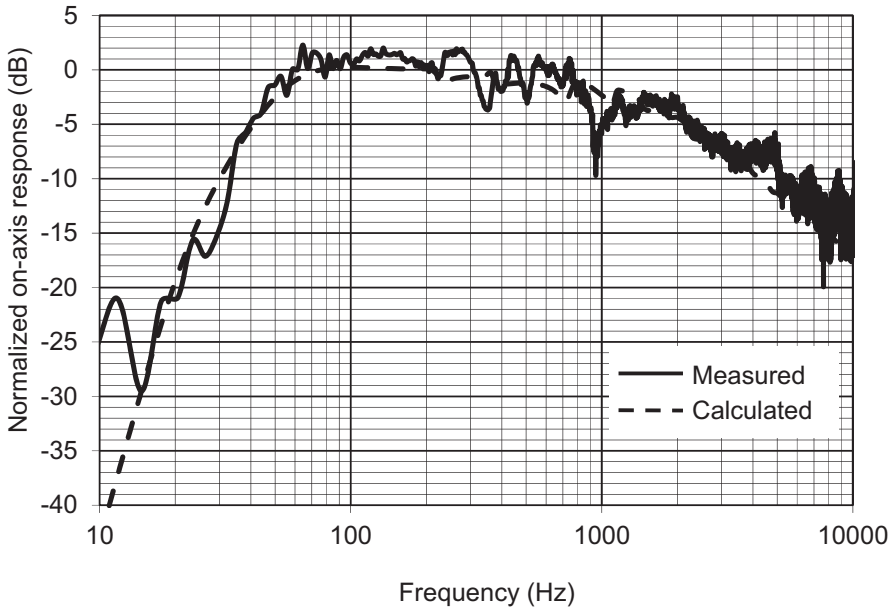

FIG. 7.31 Graphs of the on-axis sound pressure level produced by the bass-reflex enclosure design shown in Fig. 7.29.

The dashed curves are calculated from $20 \log_{10}|\tilde{U}_B/\tilde{U}_{ref}|$. Solid curves are measured.

PART XXIII: 2-PORT NETWORK FOR SMALL ENCLOSURES

In this part we shall use the 2-port network theory, introduced in Sec. 3.10 and Fig. 4.43, to create a z-parameter matrix that describes a bass-reflex enclosure in which the rear of the loudspeaker diaphragm connects to one port and the bass-reflex port connects to the other. Absorbent lining material is located on the internal wall opposite the diaphragm and bass-reflex port. This matrix is valid for all wavelengths since it is based on eigenfunction expansions of the internal modes.

For a closed-box enclosure, we simply set the velocity at the bass-reflex port to zero so that we are left with 1-port network or impedance at the rear of the diaphragm, which is given by the first element of the matrix z_{11}.

7.18 2-PORT NETWORK FOR A BASS-REFLEX ENCLOSURE

A sketch of the bass-reflex enclosure is shown in Fig. 7.34. In order to make the problem solvable, we assume that the loudspeaker and port apertures, represented by piston 1 and piston 2, are rectangular and planar, which should give a reasonable approximation when they are circular, in which case their radii are given by

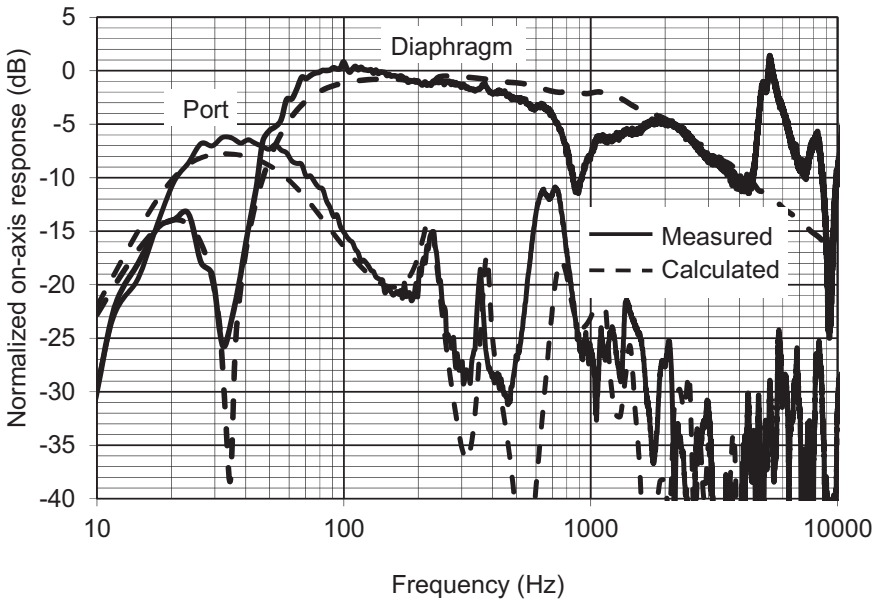

FIG. 7.32 Graphs of the on-axis sound pressure level produced by port and diaphragm of the bass-reflex enclosure design shown in Fig. 7.29.

The dashed curves are calculated from $20\log_{10}|\tilde{U}_P/\tilde{U}_{ref}|$ and $20\log_{10}|(\tilde{U}_c - \tilde{U}_L)/\tilde{U}_{ref}|$ for the port and diaphragm respectively. Solid curves are measured.

$$r_1 = \sqrt{a_1 b_1/\pi} \quad \text{and} \quad r_2 = \sqrt{a_2 b_2/\pi}.$$

To further simplify the problem, we have acoustic lining only on the rear surface of the enclosure. For a bass-reflex enclosure it is not desirable to have too much lining because that will produce excessive losses as the air passes through it and thus negate the advantage of having a port. If the force and velocity at piston 1 are given by $\tilde{F}_1$ and $\tilde{u}_1$ respectively and the force and velocity at piston 2 by $\tilde{F}_2$ and $\tilde{u}_2$, then

$$\begin{bmatrix} \tilde{F}_1 \\ \tilde{F}_2 \end{bmatrix} = \begin{bmatrix} z_{11} & z_{12} \\ z_{21} & z_{22} \end{bmatrix} \begin{bmatrix} \tilde{u}_1 \\ \tilde{u}_2 \end{bmatrix} \tag{7.109}$$

where the mechanical self impedance z_{11} of piston 1 is the ratio of the force to velocity at piston 1 with piston 2 blocked:

$$z_{11} = \frac{\tilde{F}_1}{\tilde{u}_1}\bigg|_{\tilde{u}_2=0} \tag{7.110}$$

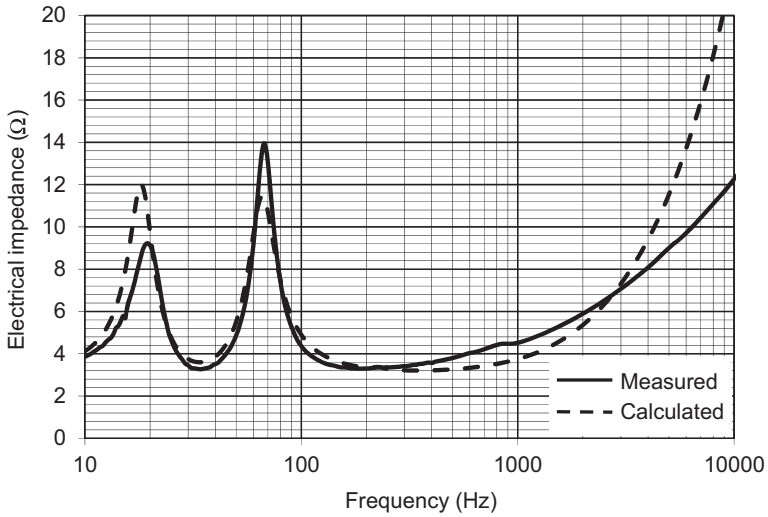

FIG. 7.33 Graphs of the electrical input impedance of the bass-reflex enclosure design shown in Fig. 7.29, where the two drive units are connected in parallel.

The dashed curves are calculated from $Z_E = |\tilde{e}_g/\tilde{i}_g| = a_{11}/a_{21}$. Solid curves are measured.

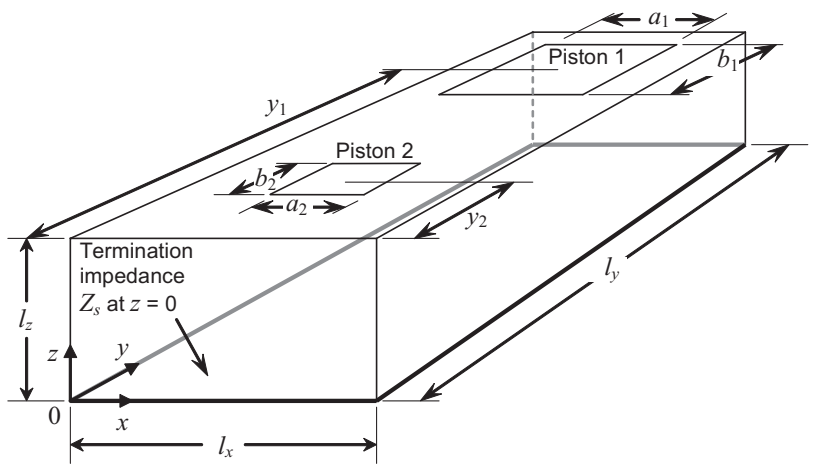

FIG. 7.34 Sketch of the bass-reflex enclosure as a 2-port network.

Similarly the mechanical self impedance z_{22} of piston 2 is the ratio of the force to velocity at piston 2 with piston 1 blocked:

$$z_{22} = \frac{\tilde{F}_2}{\tilde{u}_2}\Big|_{\tilde{u}_1=0} \tag{7.111}$$

which is obtained by interchanging "1" and "2" in the expression for z_{11}. In a passive network such as this, the mutual impedances z_{12} and z_{21} are equal and given by

$$z_{12} = \frac{\tilde{F}_1}{\tilde{u}_2}\Big|_{\tilde{u}_1=0} = z_{21} = \frac{\tilde{F}_2}{\tilde{u}_1}\Big|_{\tilde{u}_2=0} \tag{7.112}$$

If for simplicity we let $\tilde{u}_1 = \tilde{u}_2 = \tilde{u}_0$, the pressure field inside the enclosure due to an applied velocity $\tilde{u}_0$ at either piston is given by

$$\tilde{p}(x,y,z) = \rho_0 c\tilde{u}_0 \sum_{m=0}^{\infty}\sum_{n=0}^{\infty}(A_{mn}e^{-jk_{mn}z} + B_{mn}e^{jk_{mn}z})\cos(m\pi x/l_x)\cos(n\pi y/l_y) \tag{7.113}$$

where

$$k_{mn} = \sqrt{k^2 - \left(\frac{m\pi}{l_x}\right)^2 - \left(\frac{n\pi}{l_y}\right)^2} \tag{7.114}$$

The boundary condition of zero pressure gradient at the perfectly rigid side walls ($x=0$, $x=l_x$, $y=0$, $y=l_y$) is accounted for by the cosine expansions in m and n. In other words, only standing waves whose wavelengths are integer or half-integer divisions of l_x and l_y can exist in the x and y directions respectively. The term with the coefficient B_{mn} represents plane waves traveling from the pistons in the negative z direction, and the term with the coefficient A_{mn} represents reflected plane waves traveling in the positive z direction. The strengths of the reflections depend on the value of the specific impedance Z_s in the plane $z=0$. The unknown expansion coefficients A_{mn} and B_{mn} are found by applying the boundary conditions at the pistons in the front baffle ($z=l_z$) and at the rear wall ($z=0$), which is terminated in a specific impedance Z_s. The velocity in the z direction is given by

$$\begin{aligned}\tilde{u}_z(x,y,z) &= \frac{1}{-jk\rho_0 c}\,\frac{\partial}{\partial z}\,\tilde{p}(x,y,z) \\ &= \frac{1}{k}\,\tilde{u}_0\sum_{m=0}^{\infty}\sum_{n=0}^{\infty}k_{mn}\left(A_{mn}e^{-jk_{mn}z} - B_{mn}e^{jk_{mn}z}\right)\cos(m\pi x/l_x)\cos\left(n\pi y/l_y\right)\end{aligned} \tag{7.115}$$

At $z=0$,

$$\tilde{p}(x,y,0) = -Z_s\tilde{u}_z(x,y,0) \tag{7.116}$$

so that

$$B_{mn} = \frac{k_{mn}Z_s + k\rho_0 c}{k_{mn}Z_s - k\rho_0 c}A_{mn} \tag{7.117}$$

In order to evaluate the pressure field due to a velocity $\tilde{u}_0$ at piston 1, we set the following boundary conditions at $z = l_z$:

$$\tilde{u}_z(x,y,l_z) = \begin{cases} \tilde{u}_0, & \frac{l_x}{2} - \frac{a_1}{2} \le x \le \frac{l_x}{2} + \frac{a_1}{2}, \quad y_1 - \frac{b_1}{2} \le y \le y_1 + \frac{b_1}{2} \\ 0, & 0 \le x < \frac{l_x}{2} - \frac{a_1}{2}, \quad \frac{l_x}{2} + \frac{a_1}{2} < x \le l_x \\ 0, & 0 \le y < y_1 - \frac{b_1}{2}, \quad y_1 + \frac{b_1}{2} y \le l_y \end{cases} \tag{7.118}$$

After inserting Eq. (7.117) into Eq. (7.115), we then multiply through by $\cos(p\pi x/l_x)$ and $\cos(q\pi y/l_y)$ and integrate over x and y as follows:

$$\begin{aligned} \tilde{u}_z(x,y,l_z) &= \frac{2}{k}\,\tilde{u}_0 \sum_{m=0}^{\infty}\sum_{n=0}^{\infty} k_{mn}A_{mn}\frac{k\rho_0 c\cos k_{mn}l_z + jk_{mn}Z_s \sin k_{mn}l_z}{k\rho_0 c - k_{mn}Z_s} \\ &\times \int_0^{l_x} \cos(m\pi x/l_x)\cos(p\pi x/l_x)dx \int_0^{l_y} \cos(n\pi y/l_y)\cos(q\pi y/l_y)dy \\ &= \tilde{u}_0 \int_{(l_x-a_1)/2}^{(l_x+a_1)/2} \cos(p\pi x/l_x)dx \int_{(y_1-b_1)/2}^{y_1+b_1/2} \cos(q\pi y/l_y)dy \end{aligned} \tag{7.119}$$

Using the property of *orthogonality* such that only terms with $p = m$ and $q = n$ are non-zero, together with the integral solutions

$$\int_0^{l_x} \cos^2(m\pi x/l_x)dx = \begin{cases} l_x, & m = 0 \\ l_x/2, & m = 1,2,\cdots \end{cases} \tag{7.120}$$

$$\int_0^{l_y} \cos^2(n\pi y/l_y)dy = \begin{cases} l_y, & n = 0 \\ l_y/2, & n = 1,2,\cdots \end{cases} \tag{7.121}$$

$$\int_{(l_x-a_1)/2}^{(l_x+a_1)/2} \cos(m\pi x/l_x)dx = \begin{cases} a_1, & m = 0 \\ \frac{2l_x}{m\pi}\cos\left(\frac{m\pi}{2}\right)\sin\left(\frac{m\pi a_1}{2l_x}\right), & m = 1,2,\cdots \end{cases} \tag{7.122}$$

$$\int_{(y_1-b_1)/2}^{(y_1+b_1)/2} \cos\left(n\pi x/l_y\right)dy = \begin{cases} b_1, & n = 0 \\ \dfrac{2l_y}{n\pi}\cos\left(\dfrac{n\pi y_1}{l_y}\right)\sin\left(\dfrac{n\pi b_1}{2l_y}\right), & n = 1,2,\cdots \end{cases} \tag{7.123}$$

we obtain

$$A_{00} = \frac{a_1 b_1}{2l_x l_y}\,\frac{\rho_0 c - Z_s}{\rho_0 c\cos kl_z + jZ_s \sin kl_s} \tag{7.124}$$

$$A_{0n} = \frac{2a_1 k}{n\pi l_x k_{0n}}\cos\left(\frac{n\pi y_1}{l_y}\right)\sin\left(\frac{n\pi b_1}{2l_y}\right)\frac{k\rho_0 c - k_{0n}Z_s}{k\rho_0 c\cos k_{0n}l_z + jk_{0n}Z_s\sin k_{0n}l_z} \tag{7.125}$$

$$A_{m0} = \frac{2b_1 k}{m\pi l_y k_{m0}}\cos\left(\frac{m\pi}{2}\right)\sin\left(\frac{m\pi a_1}{2l_x}\right)\frac{k\rho_0 c - k_{m0}Z_s}{k\rho_0 c\cos k_{m0}l_z + jk_{m0}Z_s\sin k_{m0}l_z} \tag{7.126}$$

$$A_{mn} = \frac{8k}{\pi^2 mnk_{mn}}\cos\left(\frac{m\pi}{2}\right)\sin\left(\frac{m\pi a_1}{2l_x}\right)\cos\left(\frac{n\pi y_1}{l_y}\right)\sin\left(\frac{n\pi b_1}{2l_y}\right) \times\frac{k\rho_0 c - k_{mn}Z_s}{k\rho_0 c\cos k_{mn}l_z + jk_{mn}Z_s\sin k_{mn}l_z} \tag{7.127}$$

The mechanical self impedances are given by

$$Z_{11} = \frac{1}{-\tilde{u}_0}\int_{(l_x-a_1)/2}^{(l_x+a_1)/2}\int_{y_1-b_1/2}^{y_2+b_1/2}\tilde{p}(x,y,l_z)dydx \tag{7.128}$$

$$Z_{22} = \frac{1}{-\tilde{u}_0}\int_{(l_x-a_2)/2}^{(l_x+a_2)/2}\int_{y_2-b_2/2}^{y_2+b_2/2}\tilde{p}(x,y,l_z)dydx \tag{7.129}$$

and the mechanical mutual impedance by

$$Z_{12} = Z_{21} = \frac{1}{-\tilde{u}_0}\int_{(l_x-a_2)/2}^{(l_x+a_2)/2}\int_{y_2-b_2/2}^{y_2+b_2/2}\tilde{p}(x,y,l_z)dydx \tag{7.130}$$

Both of these are found using the integral solutions of Eqs. (7.122) and (7.123), where we note that $\cos(m\pi/2) = 0$ for odd values of m and therefore replace m with $2m$. Furthermore all of the impedances z_{11}, z_{12}, z_{21}, and z_{22} can be expressed by the single equation

$$Z_{pq} = \rho_0 c \left\{ \frac{a_p a_q b_p b_q}{l_x l_y} \frac{\frac{Z_s}{\rho_0 c} + j \tan kl_z}{1 + j \frac{Z_s}{\rho_0 c} \tan kl_z} + \frac{8 a_p a_q l_y}{\pi^2 l_x} \right.$$

$$\times \sum_{n=1}^{\infty} \frac{k}{n^2 k_{0n}} \cos\left(\frac{n\pi y_p}{l_y}\right) \cos\left(\frac{n\pi y_q}{l_y}\right) \sin\left(\frac{n\pi b_p}{2l_y}\right) \sin\left(\frac{n\pi b_q}{2l_y}\right) \frac{\frac{k_{0n} Z_s}{k\rho_0 c} + j \tan k_{0n} l_s}{1 + j \frac{k_{0n} Z_s}{k\rho_0 c} \tan k_{0n} l_s}$$

$$+ \frac{2 b_p b_q l_x}{\pi^2 l_y} \sum_{m=1}^{\infty} \frac{k}{m^2 k_{m0}} \sin\left(\frac{m\pi a_p}{l_x}\right) \sin\left(\frac{m\pi a_q}{l_x}\right) \frac{\frac{k_{m0} Z_s}{k\rho_0 c} + j \tan k_{m0} l_z}{1 + j \frac{k_{m0} Z_s}{k\rho_0 c} \tan k_{m0} l_z} \tag{7.131}$$

$$+ \frac{16 l_x l_y}{\pi^4} \sum_{m=1}^{\infty} \sum_{n=1}^{\infty} \frac{k}{m^2 n^2 k_{mn}} \sin\left(\frac{m\pi a_p}{l_x}\right) \sin\left(\frac{m\pi a_q}{l_x}\right) \cos\left(\frac{n\pi y_p}{l_y}\right)$$

$$\left. \times \cos\left(\frac{n\pi y_q}{l_y}\right) \sin\left(\frac{n\pi b_p}{2l_y}\right) \sin\left(\frac{n\pi b_q}{2l_y}\right) \frac{\frac{k_{mn} Z_s}{k\rho_0 c} + j \tan k_{mn} l_z}{1 + j \frac{k_{mn} Z_s}{k\rho_0 c} \tan k_{mn} l_z} \right\}$$

where

$$k_{mn} = \sqrt{k^2 - \left(\frac{2m\pi}{l_x}\right)^2 - \left(\frac{n\pi}{l_y}\right)^2} \tag{7.132}$$

PART XXIV: TRANSMISSION-LINE ENCLOSURES

7.19 TRANSMISSION-LINE ENCLOSURES

7.19.1 General Description

A transmission-line enclosure has a duct or tube between the back of the loudspeaker diaphragm and the outside world, which is usually folded in order to save space. There are two approaches as shown in Fig. 7.35a and Fig. 7.35b. In the first, the duct has a uniform cross-sectional area over much of its length and is usually designed to enhance the bass response around its fundamental resonance frequency rather like a bass-reflex enclosure. Unlike a bass-reflex enclosure where the dimensions of the enclosure and port are usually small compared to the wavelength, the transmission line is long enough for there to be significant phase shift between the diaphragm and outlet at low frequencies. Hence, when the wavelength is four times the length of the transmission line, there is a 90° phase shift within it which leads to maximum air displacement at the opening (resonance anti-node) but minimum displacement at the loudspeaker diaphragm (resonance node). This leads to a significant enhancement

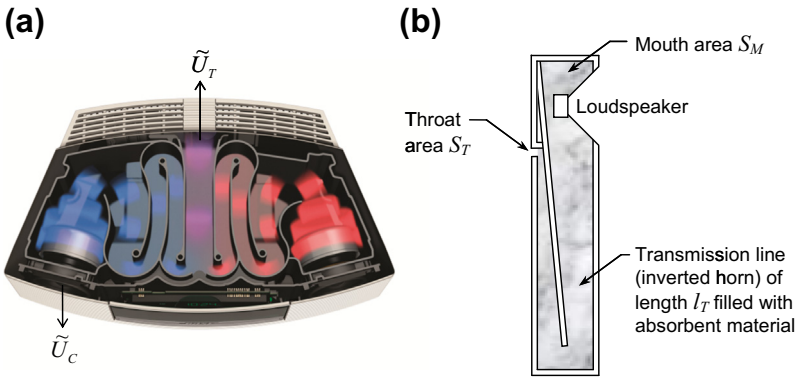

FIG. 7.35 Transmission-line enclosures: (a) Substantially "Straight" transmission line, except for some flaring near the drive unit, as used in the Bose Wave® music system. *Courtesy of Bose Corporation.* (b) "Tapered" transmission line.

As the name suggests, the Bowers & Wilkins Nautilus™ loudspeaker uses a tapered transmission line folded into a spiral. The diaphragm has an area S_D.

of the bass performance in the region of the quarter-wavelength resonance frequency. The problem, however, is how to attenuate the output of the transmission line at frequencies where it cancels the sound from the front of the loudspeaker diaphragm even if the standing waves within it are well damped using absorbent filling material. However, many products now contain a digital signal processor which can be used to equalize the resulting lumpy frequency response.

Summary of transmission-line design

To determine the cutoff frequency, frequency response, and the volume of the box:

If the Thiele–Small parameters (R_E, Q_{ES}, Q_{MS}, f_S, S_D, and V_{AS}) of the chosen drive unit are not supplied by the manufacturer, they may be measured according to Sec. 6.10. Then $Q_{TS} = Q_{ES}Q_{MS}/(Q_{ES} + Q_{MS})$.

If we assume that the drive unit will behave more or less as if it were mounted in an infinite baffle, we can select the frequency-response shape from Table 7.2 for which the Q_{TC} value is closest to the Q_{TS} value of the chosen drive unit (or choose a drive unit whose Q_{TS} value is closest to that of the desired frequency-response shape). From the value of f_{3dB}/f_C in the table, compute the cutoff frequency f_{3dB} assuming that $f_C \approx f_S$.

The frequency-response shape below the first diaphragm break-up mode but above the transmission-line cut-off frequency f_T is shown in Fig. 7.16. Below f_T, the roll-of increases from 2nd-order (12 dB/octave) to 3rd-order (18 dB/octave).

To determine the maximum sound pressure level (SPL):

If the loudspeaker is to be used near a wall or a rigid planar surface, which is large compared to the longest wavelength to be reproduced, then the maximum sound pressure SPL_{max} at a distance r is obtained from Eq. (6.34) to give

$$\text{SPL}_{\text{max}} = 20 \log_{10} \left(\frac{1}{rc \times 20 \times 10^{-6}} \sqrt{\frac{Z_{nom} W_{\text{max}} 2\pi f_s^3 V_{AS} \rho_0}{R_E Q_{ES}}} \right) \text{dB SPL @ 1m}$$

where W_{max} is the maximum rated input power. Otherwise, if it is to be used in the free field, subtract 6 dB from SPL_{max}.

To determine the excursion limit:

The maximum peak diaphragm displacement at frequencies well below the suspension resonance is obtained from Eq. (7.101) to give

$$\eta_{\max} = \frac{1}{S_D c}\sqrt{\frac{Z_{nom} W_{\max} V_{AS}}{R_E Q_{ES} \pi f_S \rho_0}}$$

If this value is greater than the rated $x_{\max}$ limit of the drive unit, then a high-pass filter should be employed to remove all content below the suspension resonance frequency. If this is not possible, then an alternate drive unit with a greater $x_{\max}$ limit should be considered

To determine the transmission-line dimensions and filling material:

Determine the flow velocity u from Eq. (7.137) and the flow resistance of the filling material from Eq. (7.8).

Calculate the length l_T of the transmission-line using Eq. (7.138). Choose a convenient mouth area S_M to fit around the back of the drive unit and choose a throat area S_T which is about 4-8 times smaller. The volume of the transmission line V_T is then given by Eq. (7.139).

Calculate the specific acoustic resistance R_{ST} of the filling material from Eq. (7.140) and the transmission-line cut-off frequency from Eq. (7.141).

The cut-off frequency should be less than one half of the suspension resonance frequency f_S. If it is not, then consider a different filling material with a higher flow resistance R_f. Alternatively, increase the length l_T of the transmission line or reduce the throat area S_T or both.

If we wish to design a stand-alone loudspeaker with a smooth frequency response, the tapered transmission line shown in Fig. 7.35b is preferable. Although a horn is commonly used as a high-pass filter because it increases the radiated volume velocity above its cut-off frequency, here we have an inverted parabolic horn which, as we shall see, acts as a high-pass filter because it attenuates the volume velocity radiated from its outlet or throat. In order to obtain the smoothest possible response, it is tuned to roll-off well below the fundamental resonance frequency of the drive unit, which in turn behaves as though it is mounted in large sealed enclosure except that the filling material may damp the fundamental resonance slightly. The low-frequency roll-off of a loudspeaker with a transmission-line enclosure has a 2nd-order slope initially, increasing to 3rd-order below the transmission-line cut-off frequency.

We shall assume for the remainder of this analysis that $ka < 0.5$. In other words, we are restricting ourselves to the very low frequency region where the radiation from both the port and the loudspeaker is nondirectional. Hence we can draw the simplified model of Fig. 7.36.

7.19.1.1 Acoustical circuit

The acoustical circuit for the transmission line and radiation is given in Fig. 7.36. The series radiation mass and resistance on the front side of the diaphragm are, respectively, M_{A1} and $\boldsymbol{R}_{AR1}$. Unlike with the bass-reflex enclosure, we omit leakage losses as we shall assume that the losses within the lining material will dominate over all others. Finally, the series radiation mass and resistance from the throat of the transmission line are, respectively, M_{A2} and $\boldsymbol{R}_{AR2}$. The values of these quantities are M_{A2} as in Eq. (7.32), but with a_T instead of a, that is,

$$M_{A2} = 0.2026\rho_0/a_{\mathrm{T}};$$

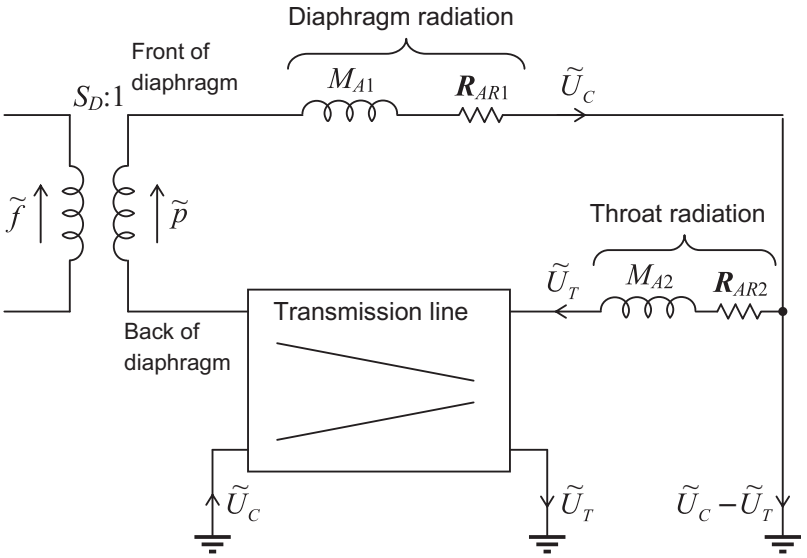

FIG. 7.36 Analogous acoustical circuit for a loudspeaker box with a transmission line, which is a reverse finite horn and may be modelled using the transmission-parameter matrices given in Section 9.13. In the case of Fig. 7.35 (b) it is parabolic.

The volume velocity of the diaphragm is $\tilde{U}_c$ and that of the transmission-line throat outlet is $\tilde{U}_T$.

$\boldsymbol{R}_{AR2}$ as in Eq. (7.31); and

M_{A1} is acoustic-radiation mass for the front side of the loudspeaker diaphragm $= 0.2026\rho_0/a$ kg/m^4. Note that we assume the loudspeaker unit is equivalent to a piston radiating from one side only in free space.
$\boldsymbol{R}_{AR1} = 0.01075f^2$ is acoustic-radiation resistance for the front side of the loudspeaker diaphragm in N·s/m^5 (see Fig. 4.39 for $ka > 1.0$).
ρ_0 is density of air in kg/m^3 (normally about 1.18 kg/m^3).
a_T is effective radius in m of the transmission-line throat. If it is not circular, then let $a_T = \sqrt{S_T/\pi}$, where S_T is the effective area of the throat opening in m^2.
$S_M = \pi a_M^2$ is effective cross-sectional area of the transmission-line mouth in m^2.
$S_T = \pi a_T^2$ is effective cross-sectional area of transmission-line throat outlet in m^2.
l_T is length of the transmission line in m.

7.19.1.2 Electro-mechano-acoustical circuit

The complete circuit for a loudspeaker with a transmission-line enclosure is obtained by combining Fig. 6.4(b) and Fig. 7.36. To do this, the acoustical radiation element of the circuit labeled "$2M_{M1}$" in Fig. 6.4(b) is removed, and the circuit of Fig. 7.36 is substituted in its place. The resulting circuit with the transformer removed and everything referred to the acoustical side is shown in Fig. 7.37.

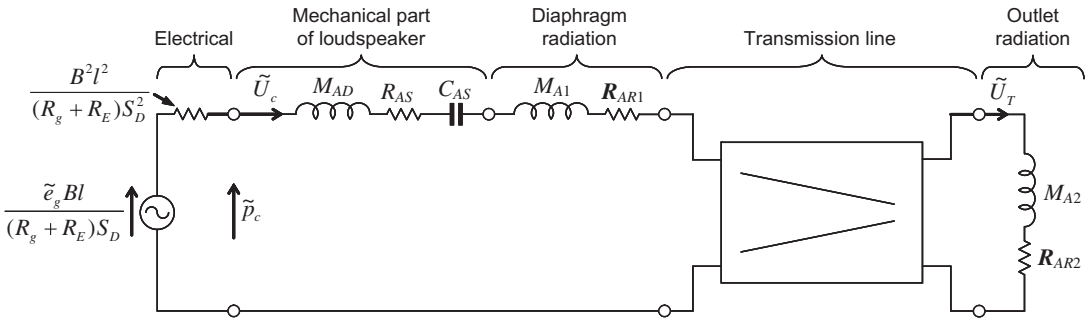

FIG. 7.37 Complete electro-mechano-acoustical circuit for a transmission-line loudspeaker.

The total force produced at the voice coil by the electric current is $\tilde{p}_c S_D$, where S_D is the area of the diaphragm. The volume velocity of the diaphragm is $\tilde{U}_c$ and that of the transmission-line throat outlet is $\tilde{U}_T$.

The quantities not listed in the previous paragraph are

$\tilde{e}_g$ is open-circuit voltage in V of the audio amplifier.
B is flux density in the air gap in T (1 T = 10^4 gauss).
l is length in m of voice-coil wire.
R_g is output electrical resistance in Ω of the audio amplifier.
R_E is electrical resistance in Ω of the voice coil.
a is effective radius of the diaphragm in m.
$M_{AD} = M_{MD}/S_D^2$ is acoustic mass of the diaphragm and the voice coil in kg/m^4.
$C_{AS} = C_{MS}S_D^2$ is acoustic compliance of the diaphragm suspension in m^5/N.
$R_{AS} = R_{MS}/S_D^2$ is acoustic resistance of the diaphragm suspension in N·s/m^5.

If the outlet of the transmission line is closed off so that $\tilde{U}_T$ equals zero, then Fig. 7.37 essentially reduces to Fig. 7.6. At very low frequencies the mass of air moving *out* of the lower opening is nearly equal to that moving into the upper opening at all instants. In other words, at very low frequencies, the volume velocities at the two openings are nearly equal in magnitude and opposite in phase.

7.19.1.3 Radiated sound

The outlet in the box of a transmission-line baffle is generally effective only at fairly low frequencies. At those frequencies its dimensions are generally so small it can be treated as though it were a simple source. The loudspeaker diaphragm can also be treated as a simple source because its area is often nearly the same as that of the opening.

Referring to Eq. (4.71), we find that the sound pressure a distance r away from the transmission-line loudspeaker is

$$\tilde{p} = \tilde{p}_1 + \tilde{p}_2 \approx \frac{j\omega\rho_0}{4\pi r}(\tilde{U}_c e^{-jkr_1} - \tilde{U}_T e^{-jkr_2}), \tag{7.133}$$

where

$\tilde{p}_1$ and $\tilde{p}_2$ are complex sound pressures, respectively from the diaphragm and transmission-line outlet at distance r.

r is average distance of the point of observation from the diaphragm and the transmission-line outlet. Note that r is large compared with the diaphragm and port radii.
r_1 and r_2 are actual distances, respectively of the point of observation from the diaphragm and transmission-line outlet.
$\tilde{U}_c$ is complex volume velocity of the diaphragm.
$\tilde{U}_T$ is complex volume velocity of the transmission-line outlet. Note that the negative sign is used for $\tilde{U}_T$ because, except for phase shift introduced by the transmission line, the air from its throat outlet moves outward when the air from the diaphragm moves inward.

Also, the complex volume velocity necessary to compress and expand the air inside the transmission-line is

$$\tilde{U}_B = \tilde{U}_c - \tilde{U}_T. \tag{7.134}$$

If we now let $r_1 = r_2 = r$ by confining our attention to a particular point in space in front of the loudspeaker where this is true, we get

$$\tilde{p} \approx \frac{j\omega\rho_0}{4\pi r}(\tilde{U}_c - \tilde{U}_T)e^{-jkr}. \tag{7.135}$$

Since $\tilde{U}_c - \tilde{U}_T = \tilde{U}_B$, we have simply that

$$\left|\tilde{p}\right| \approx \frac{f\rho_0\left|\tilde{U}_B\right|}{2r}. \tag{7.136}$$

As with the bass-reflex enclosure, the sound pressure produced at faraway points equidistant from cone and outlet of a transmission-line loudspeaker is directly proportional to the volume velocity necessary to compress and expand the air inside the transmission-line.

At very low frequencies, where the wavelength is much greater than the length l_T of the transmission line, $\tilde{U}_c$ becomes nearly equal to $\tilde{U}_T$, and the pressure, measured at points $r = r_1 = r_2$ approaches zero. In fact, the two sources behave like a dipole so that the radiated sound pressure decreases by a factor of 2 for each halving of frequency. In addition, if we are below the lowest resonance frequency of the circuit of Fig. 7.37, the diaphragm velocity $\tilde{U}_c$ halves for each halving of frequency. Hence, in this very low frequency region, the sound pressure decreases by a factor of 8, which is 18 dB, for each halving of frequency. In other words, the slope is 3rd order. Note that this decrease is greater than that for a loudspeaker in a closed box or in an infinite baffle (which is 2nd-order) but less than that for a loudspeaker in a vented box (which is 4th-order). The effect is somewhat similar to mounting the loudspeaker in a very large flat open-baffle (which is also 3rd-order).

The flow resistance R_f of the filling material, given by Eq. (7.8) is dependent upon the flow velocity u and is therefore nonlinear. The problem is that the flow velocity varies with frequency and with position along the tapered transmission line. This could lead to a very complicated analysis, but if we make sure that there is enough attenuation within the transmission line for the radiation from the throat outlet not to interfere too much with the direct radiation from the diaphragm, we need not worry too much about the accuracy of the model. The flow resistance will mainly affect the damping of the

fundamental resonance of the drive unit over a relatively small range of frequencies. Therefore we set the rms velocity value to that of the diaphragm at resonance at its maximum displacement:

$$u \approx \frac{\omega_s x_{\max}}{\sqrt{2}}. \tag{7.137}$$

We then obtain the flow resistance R_f from Eq. (7.8). Usually, we set the length l_T to be one quarter of the wavelength at the suspension resonance frequency f_S so that

$$l_T = \frac{c}{4f_s}. \tag{7.138}$$

This rather naïve formula assumes the free-space speed of sound c whereas in the lossy filling material it is somewhat slower [see Eqs. (2.80) and (2.82) for the speed of sound in a material with flow resistance R_f]. However, this is largely compensated for by the fact that the resonance in a tapered duct is not a true quarter-wavelength one, but rather occurs when $l_T = \alpha\lambda/(2\pi)$, where $J_0(\alpha) = 0$, or $l_T = \lambda/2.61274$ (assuming $S_T << S_M$). The volume occupied by the transmission line is

$$V_T = \frac{S_T + S_M}{2} l_T. \tag{7.139}$$

By examining the asymptotic low-frequency behavior of the tapered transmission line, we find that its specific resistance R_{ST}, as seen from the mouth, is

$$R_{ST} = \frac{S_M}{S_M - S_T} l_T R_f \ln \frac{S_M}{S_T}. \tag{7.140}$$

If the filling material has ample overall specific resistance (> 400 rayls) we can use the following empirical formula for the transmission-line cut-off frequency

$$f_T \approx \frac{2P_0}{3R_{ST} l_T}. \tag{7.141}$$

7.19.1.4 Performance

With the information just given, it is possible to calculate the response of the loudspeaker in a transmission-line enclosure. A complete example is given in the next section.

From Fig. 7.37, we see that, for frequencies below ω_T, radiation from the transmission-line outlet (proportional to $-\tilde{U}_0$) is out of phase with the radiation from the diaphragm (proportional to $\tilde{U}_c$). As a result, the response at very low frequencies is usually not enhanced by the transmission-line. Above the cut-off frequency ω_T, radiation from the throat is in phase with that from the diaphragm at some frequencies but out of phase at others. However, because the radiation from the throat is attenuated, it has relatively little influence on the overall response. Consequently, a transmission line enclosure behaves somewhat like a large open baffle, and the need for a reasonably stiff suspension is even greater than in the case of a bass-reflex enclosure. A large loudspeaker diaphragm usually is superior to a small one because the amplitude of its motion is less, thereby reducing nonlinear distortion.

At low-frequencies, the wavelength is usually very large compared to the box dimensions if the transmission line is folded, so the small resulting phase difference between the outputs of the transmission line and diaphragm will have little effect on the performance.

An advantage of a transmission-line loaded loudspeaker is that the build-up of pressure inside the enclosure is much less than inside a closed-box or even a bass-reflex enclosure above the box resonance. Therefore, pressure waves from the rear of the diaphragm are less likely to couple to the walls of the enclosure and cause unwanted vibrations.

Example 7.4. Transmission-line enclosure design. In the previous part we discussed in detail the design of a bass-reflex baffle for a low-frequency (woofer) loudspeaker. We presented methods for the determination of its physical constants, and we showed a comparison between measurements and calculations.

In this part we shall use a single full-range unit loaded at the rear with a transmission line. The brief here is to design a compact loudspeaker for domestic use with extended bass response at moderate listening levels in an enclosure no larger than 2½ liters. We aim to produce 86 dB SPL @ 1 m using just 2 W of input power, or 92 dB SPL from a stereo pair. We wish to extend the frequency response down to 140 Hz. We assume that the loudspeaker will be placed near a wall in order to support the low frequencies.

A suitable drive unit is the Peerless 2½-inch "Tymphany" type 830985. The Thiele–Small parameters are:

$R_E = 3.7\ \Omega$
$Q_{ES} = 0.83$
$Q_{MS} = 3.46$
$f_S = 140$ Hz
$S_D = 22\ \text{cm}^2$
$V_{AS} = 0.472$ L

Then

$$Q_{TS} = \frac{Q_{ES}Q_{MS}}{Q_{ES} + Q_{MS}} = 0.67.$$

From Eq. (6.48) we can calculate the reference efficiency

$$E_{ff} = 100\frac{8 \times 3.14^2 \times 472 \times 10^{-6} \times 140^3}{0.83 \times 344.8^3} = 0.3\%.$$

In order to calculate the maximum SPL, we first obtain C_{MS}, M_{MS}, and Bl from Eqs. (6.27), (6.28), and (6.30) respectively:

$$C_{MS} = \frac{472 \times 10^{-6}}{0.0022^2 \times 1.18 \times 344.8^2} = 0.695\ \text{mm/N},$$

$$M_{MS} = \frac{1}{(2 \times 3.14 \times 140)^2 \times 695 \times 10^{-6}} = 0.0019\ \text{kg},$$

$$Bl = \sqrt{\frac{3.7}{2 \times 3.14 \times 140 \times 0.83 \times 695 \times 10^{-6}}} = 2.7\ \text{T}\cdot\text{m}.$$

We obtain from Eq. (6.33)

$$\mathrm{SPL_{2W}} = 20\log_{10}\left(\frac{\sqrt{3.7\times 2}\times 2.7\times 0.0022\times 1.18}{2\times 3.14\times 3.7\times 0.0019\times 20\times 10^{-6}}\right) = 86.7\ \text{dB SPL @ 1 m.}$$

Next we use Eq. (6.35) to check the peak displacement at f_S for 86 dB SPL:

$$\eta_{\text{peak}} = \frac{\sqrt{2}\times 1\times 10^{\left(\frac{86}{20}-5\right)}}{\pi\times 140^2\times 1.18\times 0.0022} = 1.8\ \text{mm.}$$

However, $Q_{TS} = 0.66$ so that at resonance the actual displacement is $0.66\times 1.8 = 1.2$ mm and the sound pressure is $86 + 20\log_{10}0.66 = 82.4$ dB SPL. It turns out that the $x_{\max}$ value of the drive unit is 2 mm, so there should be no problems with this design provided that the input power is limited to just 2 W at low frequencies. For the purpose of evaluating the flow resistance of the filling material, we take the flow velocity u from Eq. (7.137) as follows:

$$u \approx \frac{2\pi 140\times 0.0012}{\sqrt{2}} = 0.75\ \text{m/s.}$$

Suppose that our filling material, which in this case is lamb's wool, has a porosity $\varphi = 0.98$ and an average fiber diameter of 50 μm. From Eq. (7.8) we obtain the flow resistance:

$$R_f = \frac{4\times 1.86\times 10^{-5}\times 0.02}{0.98\times 50^2\times 10^{-12}}\left(\frac{1-\frac{4}{\pi}\times 0.02}{2+\ln\frac{1.86\times 10^{-5}\times 0.98}{2\times 50\times 10^{-6}\times 1.18\times 0.75}}+\frac{6}{\pi}\times 0.02\right)$$
$$= 1433\ \text{rayls/m.}$$

Now we turn to the transmission-line dimensions. Let us make the length l_T equal to one quarter wavelength at f_S from Eq. (7.138), so that

$$l_T = \frac{344.8}{4\times 140} = 0.62\ \text{m.}$$

For convenience, we make the mouth area a square large enough to fit the diameter of the drive unit:

$$S_M = 7\ \text{cm}\times 7\ \text{cm} = 49\ \text{cm}^2$$

and

$$S_T = S_M/4 = = 12.25\ \text{cm}^2,$$

which from Eq. (7.139) makes the total volume

$$V_T = \frac{(12.25+49)\times 10^{-4}}{2}\times 0.62 = 1.9\times 10^{-3}\ \text{m}^3 \text{ or } 1.9\ \text{L.}$$

From Eq. (7.140) this gives a specific resistance value of

$$R_{ST} = \frac{49}{49 - 12.25} \times 0.62 \times 1433 \times \ln \frac{49}{12.25} = 1642 \text{ rayls}.$$

Now from Eq. (7.141) we can calculate the cut-off frequency

$$f_T \approx \frac{2 \times 10^5}{3 \times 1642 \times 0.62} = 65.5 \text{ Hz},$$

which is well below the suspension resonance frequency f_S of the drive unit.

Let us now create a semi-analytical simulation model of the design of Fig. 7.38 using 2-port networks and transmission matrices, as introduced in Sec. 3.10 and Fig. 4.43. The schematic is shown in Fig. 7.39. Although it is based on the circuit of Fig. 7.37, a gyrator has been inserted between the electrical elements and the mechanical ones, which enables us to calculate more easily the generator current $\tilde{i}_g$ from which we obtain the electrical impedance. We are ignoring the generator impedance R_g since in the experimental setup this is negligible compared to R_E. The dashed boxes are lumped-element 2-port networks and the solid boxes are analytical ones. From the schematic we create the transmission matrices required to represent each 2-port network as follows.

1. Coil.

$$\begin{bmatrix} \tilde{e}_g \\ \tilde{i}_g \end{bmatrix} = \begin{bmatrix} 1 & Z_E \\ 0 & 1 \end{bmatrix} \cdot \begin{bmatrix} \tilde{e}_1 \\ \tilde{i}_1 \end{bmatrix} = \mathbf{C} \cdot \begin{bmatrix} \tilde{e}_1 \\ \tilde{i}_1 \end{bmatrix}$$

where $Z_E = R_E + j\omega L_E$.

2. Electro-mechanical transduction.

$$\begin{bmatrix} \tilde{e}_1 \\ \tilde{i}_1 \end{bmatrix} = \begin{bmatrix} 0 & Bl \\ (Bl)^{-1} & 0 \end{bmatrix} \cdot \begin{bmatrix} \tilde{f}_2 \\ \tilde{u}_2 \end{bmatrix} = \mathbf{E} \cdot \begin{bmatrix} \tilde{f}_2 \\ \tilde{u}_2 \end{bmatrix}$$

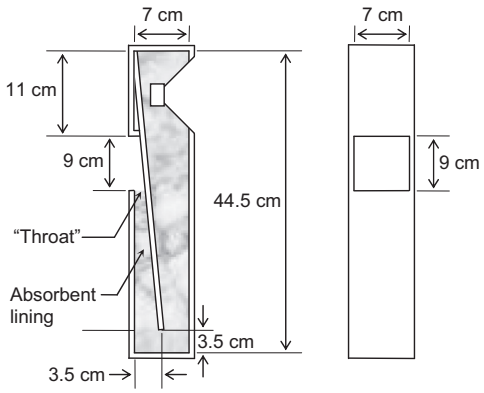

FIG. 7.38 Example of transmission-line enclosure design.

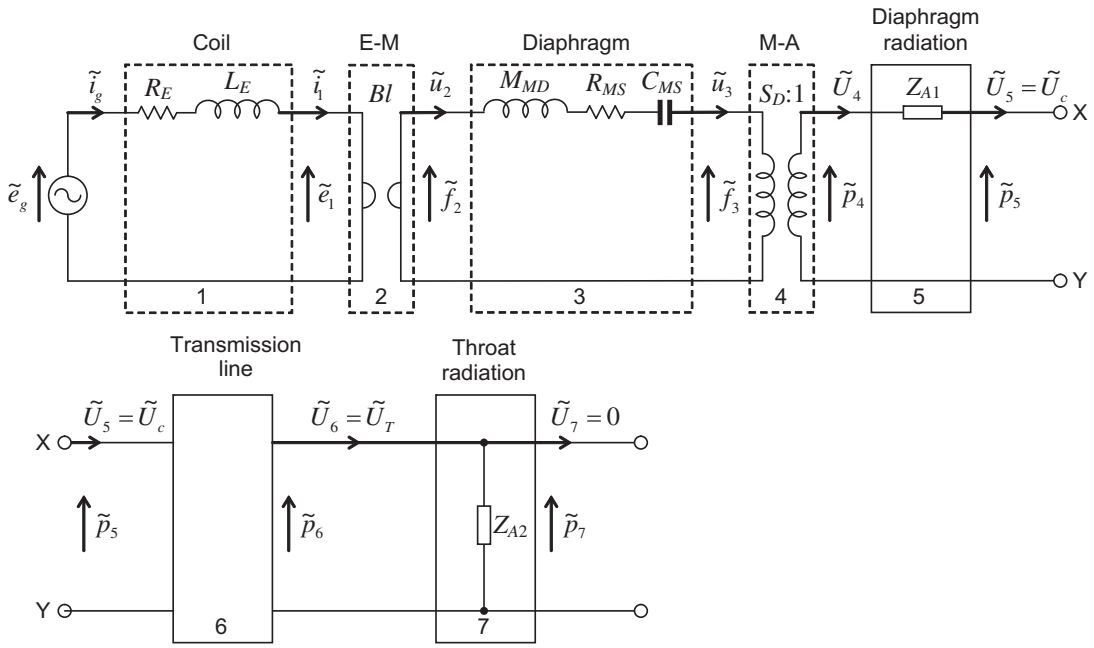

FIG. 7.39 Semi-analytical model of example transmission-line enclosure design shown in Fig. 7.38 using transmission matrices. The matrix for the transmission line is given in Eq. (9.65) for a reverse parabolic horn.

The dashed boxes are lumped-element 2-port networks and the solid boxes are analytical ones.

3. Diaphragm.

$$\begin{bmatrix} \tilde{f}_2 \\ \tilde{u}_2 \end{bmatrix} = \begin{bmatrix} 1 & Z_{MD} \\ 0 & 1 \end{bmatrix} \cdot \begin{bmatrix} \tilde{f}_3 \\ \tilde{u}_3 \end{bmatrix} = \mathbf{D} \cdot \begin{bmatrix} \tilde{f}_3 \\ \tilde{u}_3 \end{bmatrix}$$

where $Z_{MD} = j\omega M_{MD} + R_{MS} + 1/(j\omega C_{MS})$. We must exclude the radiation mass from the diaphragm so that $M_{MD} = M_{MS} - 16\rho_0 a^3/3$, where $a = \sqrt{S_D/\pi}$.

4. Mechano-acoustical transduction.

$$\begin{bmatrix} \tilde{f}_3 \\ \tilde{u}_3 \end{bmatrix} = \begin{bmatrix} S_D & 0 \\ 0 & S_D^{-1} \end{bmatrix} \cdot \begin{bmatrix} \tilde{p}_4 \\ \tilde{U}_4 \end{bmatrix} = \mathbf{M} \cdot \begin{bmatrix} \tilde{p}_4 \\ \tilde{U}_4 \end{bmatrix}$$

5. Diaphragm radiation.

$$\begin{bmatrix} \tilde{p}_4 \\ \tilde{U}_4 \end{bmatrix} = \begin{bmatrix} 1 & Z_{A1} \\ 0 & 1 \end{bmatrix} \cdot \begin{bmatrix} \tilde{p}_5 \\ \tilde{U}_5 \end{bmatrix} = \mathbf{D} \cdot \begin{bmatrix} \tilde{p}_5 \\ \tilde{U}_5 \end{bmatrix}$$

where Z_{A1} is the acoustic radiation impedance of the diaphragm given by Eqs. (13.116), (13.117), and (13.118) with $a = \sqrt{S_D/\pi}$.

6. Transmission line. Distributed parameter model:

$$\begin{bmatrix} \tilde{p}_5 \\ \tilde{U}_5 \end{bmatrix} = \frac{1}{a_{11}a_{22} - a_{12}a_{21}} \begin{bmatrix} a_{22} & a_{12} \\ a_{21} & a_{11} \end{bmatrix} \cdot \begin{bmatrix} \tilde{p}_6 \\ \tilde{U}_6 \end{bmatrix} = \mathbf{T} \cdot \begin{bmatrix} \tilde{p}_6 \\ \tilde{U}_6 \end{bmatrix}$$

where

$$a_{11} = -\frac{\pi}{2} \boldsymbol{k}x_M(J_0(\boldsymbol{k}x_T)Y_1(\boldsymbol{k}x_M) - J_1(\boldsymbol{k}x_M)Y_0(\boldsymbol{k}x_T))$$

$$a_{12} = j\frac{Z_{ST}}{S_M}\frac{\pi}{2} \boldsymbol{k}x_M(J_0(\boldsymbol{k}x_T)Y_0(\boldsymbol{k}x_M) - J_0(\boldsymbol{k}x_M)Y_0(\boldsymbol{k}x_T))$$

$$a_{21} = j\frac{S_T}{Z_{ST}}\frac{\pi}{2} \boldsymbol{k}x_M(J_1(\boldsymbol{k}x_T)Y_1(\boldsymbol{k}x_M) - J_1(\boldsymbol{k}x_M)Y_1(\boldsymbol{k}x_T))$$

$$a_{22} = \frac{S_T}{S_M}\frac{\pi}{2} \boldsymbol{k}x_M(J_1(\boldsymbol{k}x_T)Y_0(\boldsymbol{k}x_M) - J_0(\boldsymbol{k}x_M)Y_1(\boldsymbol{k}x_T))$$

where

$$x_T = S_T l_T/(S_M - S_T) \quad \text{and} \quad x_M = S_M l_T/(S_M - S_T).$$

For Z_{ST} and $\boldsymbol{k}$, we use Eqs. (7.10) and (7.11) respectively. The ratio of the throat volume velocity to the mouth volume velocity

$$\tilde{U}_T/\tilde{U}_c = \tilde{U}_6/\tilde{U}_5 = 1/a_{11}$$

is plotted in Fig. 7.40, assuming that the pressure at the throat is virtually zero. We see that the volume velocity rolls off smoothly above $f_T = 65.5$ Hz.

7. Throat radiation.

$$\begin{bmatrix} \tilde{p}_6 \\ \tilde{U}_6 \end{bmatrix} = \begin{bmatrix} 1 & 0 \\ Z_{A2}^{-1} & 1 \end{bmatrix} \cdot \begin{bmatrix} \tilde{p}_7 \\ \tilde{U}_7 \end{bmatrix} = \mathbf{R} \cdot \begin{bmatrix} \tilde{p}_7 \\ \tilde{U}_7 \end{bmatrix}$$

In this case, the throat outlet is rectangular and close to a large planar surface so that Z_{A2} may be given by the impedance of a rectangular piston in an infinite baffle using Eqs. (13.326) and (13.327), where

$$Z_{A2} = (\boldsymbol{R}_s + jX_s)/S_T.$$

First we evaluate $\tilde{p}_7$ at the end of the chain:

$$\begin{bmatrix} \tilde{e}_g \\ \tilde{i}_g \end{bmatrix} = \mathbf{A} \cdot \begin{bmatrix} \tilde{p}_7 \\ 0 \end{bmatrix}$$

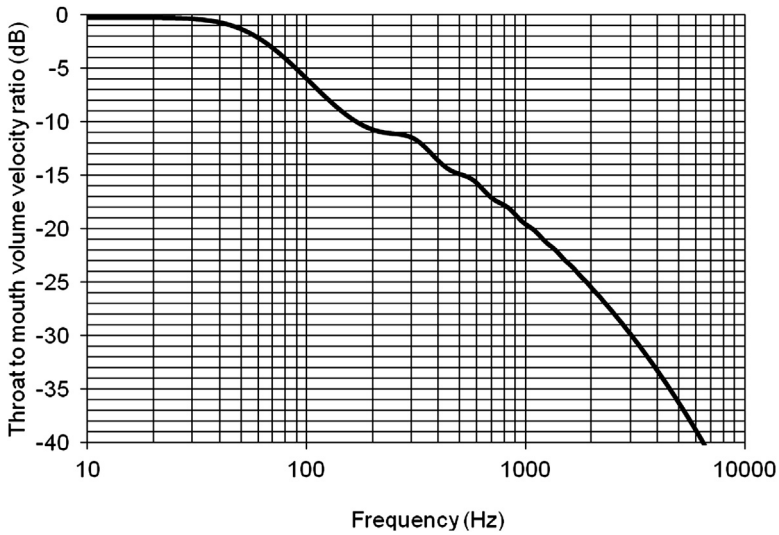

FIG. 7.40 Graph of the volume velocity attenuation produced by the transmission-line enclosure design shown in Fig. 7.38. Curve is calculated from 20 $\log_{10}|\tilde{U}_T/\tilde{U}_c|$.

where

$$\mathbf{A} = \mathbf{C}\cdot\mathbf{E}\cdot\mathbf{D}\cdot\mathbf{M}\cdot\mathbf{F}\cdot\mathbf{T}\cdot\mathbf{R} = \begin{bmatrix} a_{11} & a_{12} \\ a_{21} & a_{22} \end{bmatrix}$$

Hence $\tilde{p}_7 = \tilde{e}_g/a_{11}$. Then we work backwards to obtain the volume velocities we wish to evaluate. In particular, we are interested in the far-field pressure, which according to Eq. (7.136) is a function of

$$\tilde{U}_B = \tilde{U}_c - \tilde{U}_T = \tilde{U}_5 - \tilde{U}_6.$$

This procedure is fairly straightforward and does not involve any matrix inversion. From the outlet radiation matrix (7), we obtain

$$\tilde{U}_T = \tilde{U}_6 = \tilde{p}_7/Z_{A2}$$

and working back further to the transmission-line matrix (6) we obtain

$$\begin{bmatrix} \tilde{p}_5 \\ \tilde{U}_5 \end{bmatrix} = \mathbf{N}\cdot\begin{bmatrix} \tilde{p}_7 \\ 0 \end{bmatrix}$$

where

$$\mathbf{N} = \mathbf{T}\cdot\mathbf{R} = \begin{bmatrix} n_{11} & n_{12} \\ n_{21} & n_{22} \end{bmatrix}$$

so that

$$\tilde{U}_c = \tilde{U}_5 = n_{21}\tilde{p}_7$$

and therefore

$$\tilde{U}_B = \tilde{U}_c - \tilde{U}_T = \tilde{U}_5 - \tilde{U}_6 = (n_{21} - 1/Z_{A2})\tilde{e}_g/a_{11}$$

The throat volume velocity is given by

$$\tilde{U}_T = \tilde{U}_6 = \tilde{e}_g/(a_{11}Z_{A2})$$

and the diaphragm volume velocity by

$$\tilde{U}_c = \tilde{U}_5 = n_{21}\tilde{e}_g/a_{11}$$

In order to plot the normalized far-field on-axis pressure, we simply divide $\tilde{U}_B$ by a reference volume velocity

$$\tilde{U}_{ref} = \frac{\tilde{e}_g BIS_D}{\omega M_{MS} R_E}$$

and plot $20\log_{10}|\tilde{U}_B/\tilde{U}_{ref}|$ as shown in Fig. 7.41. The throat and diaphragm volume velocities,

$$20\log_{10}\left|\tilde{U}_T/\tilde{U}_{ref}\right| \text{ and } 20\log_{10}\left|\tilde{U}_c/\tilde{U}_{ref}\right|$$

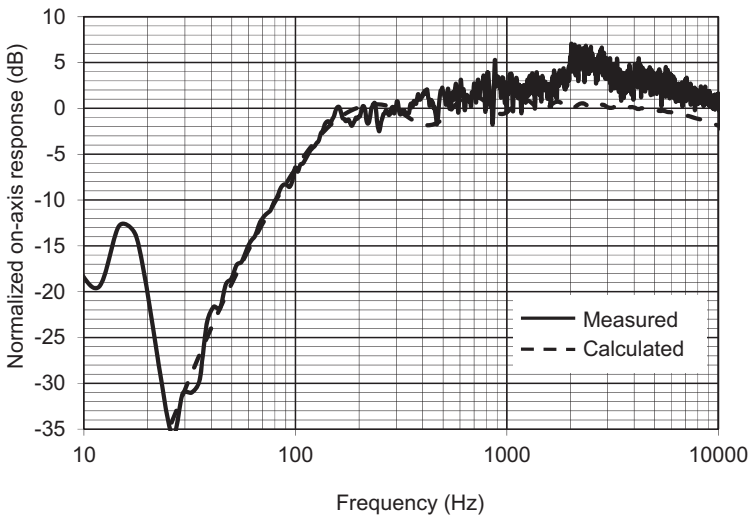

FIG. 7.41 Graphs of the on-axis sound pressure level produced by the transmission-line enclosure design shown in Fig. 7.38.

The dashed curves are calculated from $20\log_{10}|\tilde{U}_B/\tilde{U}_{ref}|$. Solid curves are measured.

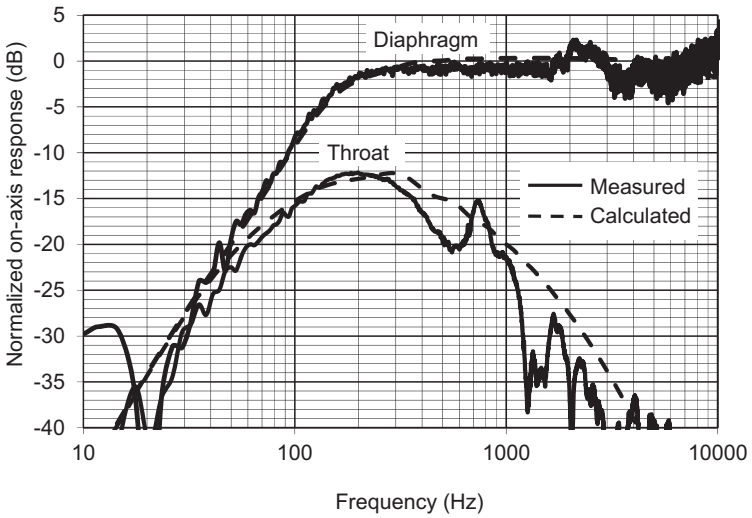

FIG. 7.42 Graphs of the on-axis sound pressure level produced by throat and diaphragm of the transmission-line enclosure design shown in Fig. 7.38.

The dashed curves are calculated from $20 \log_{10}|\tilde{U}_T/\tilde{U}_{ref}|$ and $20 \log_{10}|\tilde{U}_c/\tilde{U}_{ref}|$ for the transmission-line outlet and diaphragm respectively. Solid curves are measured.

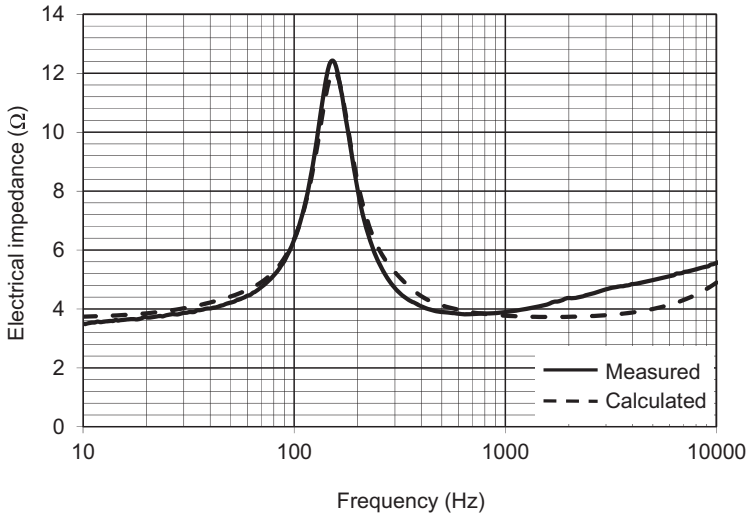

FIG. 7.43 Graphs of the electrical input impedance of the transmission-line enclosure design shown in Fig. 7.38.

The dashed curves are calculated from $Z_E = |\tilde{e}_g/\tilde{i}_g| = a_{11}/a_{21}$. Solid curves are measured.

respectively, are plotted separately in Fig. 7.42. Individually, the outputs from the diaphragm and throat are very smooth, but their combined output shown in Fig. 7.41 does exhibit some very small 1 dB ripples which will be hardly audible. Finally, we can obtain the input impedance from $\tilde{e}_g/\tilde{i}_g$ where $\tilde{i}_g = a_{21}\tilde{p}_7$ and from above $\tilde{p}_7 = \tilde{e}_g/a_{11}$. Therefore the input impedance is simply $Z_E = a_{11}/a_{21}$, as plotted in Fig. 7.43.

PART XXV: MULTIPLE DRIVE UNITS

7.20 CROSSOVER FILTERS

Many high-fidelity sound systems employ two or more loudspeaker drive units. One, called a *woofer* covers the low-frequency range while the other, called a *tweeter*, covers the high frequency range. Sometimes, a third unit or *squawker* is included to cover the midrange. An electrical network, called a *crossover* network, is used to divide the output energy from the amplifier into the different frequency regions covered by the multiple drive units. Here we shall concentrate on two-way crossovers as the same rules can be applied when designing loudspeakers with three or more drive units.

Classical crossover filters. Fig. 7.44 shows an outline schematic of a 2-way loudspeaker with a classical crossover network. The woofer is fed via a nth-order low-pass filter and the tweeter via a nth-order high-pass filter. The transfer functions of the low-pass and high-pass filters are $L_n(s)$ and $H_n(s)$ respectively where $s = j\omega$ is the complex frequency. These filters are designed such that when their outputs are summed, they form all-pass filters $F_n(s) = L_n(s) + H_n(s)$, that is $|F_n(s)| = 1$ at all frequencies, although the phase varies except in the case of $n = 1$. Furthermore, the input impedance is R at all frequencies, so that the power dissipation is uniform. Low-pass filter circuits of orders $n = 1$ to 6 are shown in Fig. 7.45 along with their transfer functions. The complementary high-pass filter circuits and transfer functions are shown in Fig. 7.46. The filters in these figures are labeled B1, $B1^2$, and so forth, where the B stands for Butterworth and the superscript denotes the number of cascaded sections. The even-order filters are commonly referred to as Linkwitz–Riley [23, 24] and are often favored because the woofer and tweeter are in phase at the crossover frequency, whereas in the case of odd-order filters they are 90° out of phase, as is seen from the Nyquist plots of Fig. 7.47. This is cited as reducing the chances of off-axis nulls occurring in the directivity pattern around the cross-over

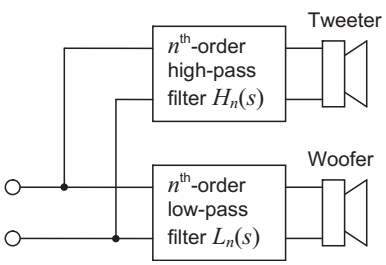

FIG. 7.44 Outline schematic of a 2-way loudspeaker with a classical crossover network.

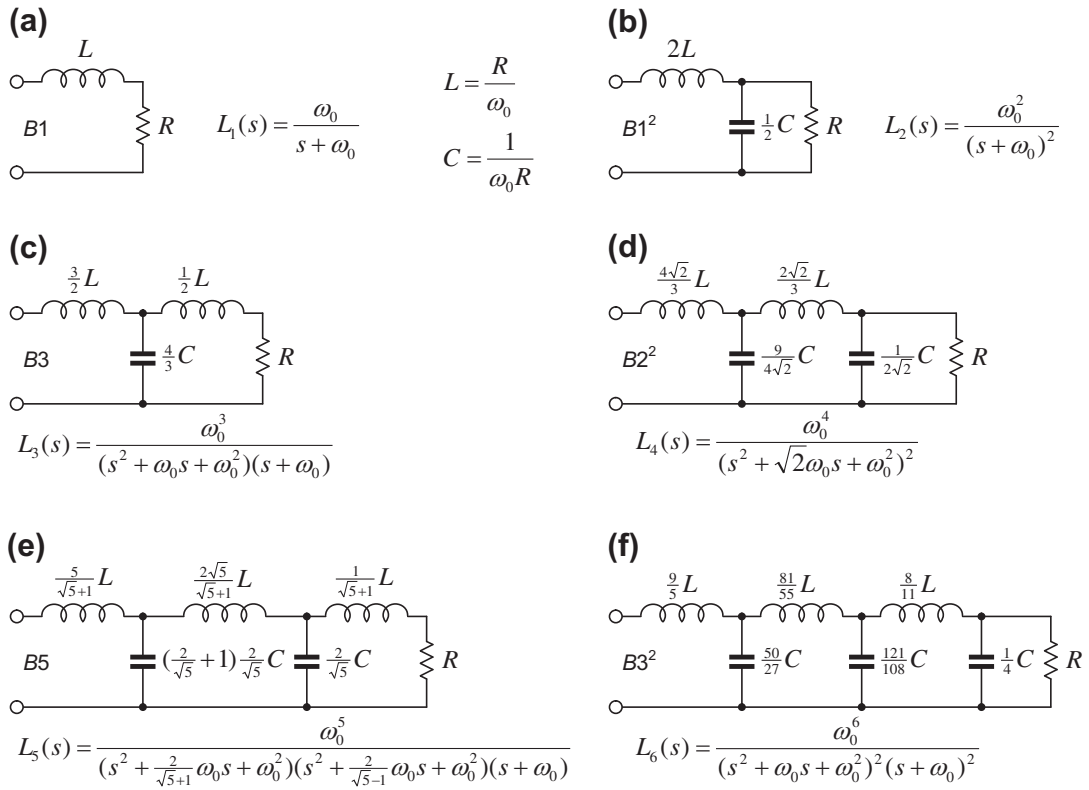

FIG. 7.45 Classical low-pass crossover filters: (a) 1st-order; (b) 2nd-order; (c) 3rd-order; (d) 4th-order; (e) 5th-order; (f) 6th-order.

In each case, the inductor and capacitor values are given by $L = R/\omega_0$ and $C = 1/(\omega_0 R)$ respectively, where $\omega_0 = 2\pi f_0$ is the crossover frequency and R is the coil resistance of the woofer. The labels $B1$, $B3^2$ and so forth are the names of the transfer functions where B stands for Butterworth and the number is the order of the function. Note that the square in $B3^2$ means that it is equivalent to two cascaded 3rd-order Butterworth filters, making a net 6th-order filter.

frequency [25], although this also largely depends upon the ratio of the wavelength to drive unit spacing. Obviously, the drive unit spacing should be as small as possible.

On the other hand, odd-order filters have a constant power response [26], regardless of drive unit spacing, and the coil inductance of the woofer can be included as part of the last inductor in the filter, thus eliminating the need for a Zobel network for correcting the load impedance as well as giving greater accuracy. All-pass filters need not be symmetrical [27–29]. If we include the low-frequency roll-off of the tweeter in its high-pass filter transfer function, the overall order of the filter is increased by 2. It would be making the low-pass filter to the woofer unnecessarily complicated to increase its order by the same amount.

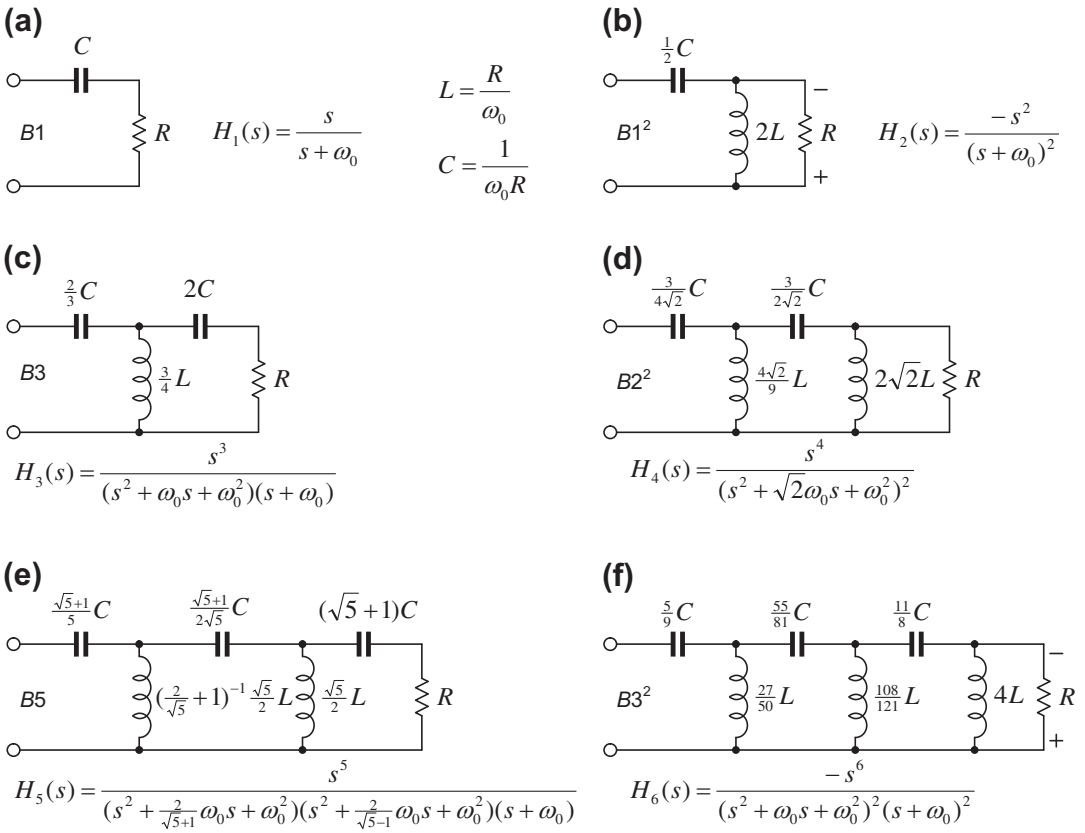

FIG. 7.46 Classical high-pass crossover filters: (a) 1st-order; (b) 2nd-order; (c) 3rd-order; (d) 4th-order; (e) 5th-order; (f) 6th-order.

In each case, the inductor and capacitor values are given by $L = R/\omega_0$ and $C = 1/(\omega_0 R)$ respectively, where $\omega_0 = 2\pi f_0$ is the crossover frequency and R is the coil resistance of the tweeter. Note that in the case of the 2nd- and 6th-order functions, the tweeter terminals must be reversed. The labels $B1$, $B3^2$ and so forth are the names of the transfer functions where B stands for Butterworth and the number is the order of the function. Note that the square in $B3^2$ means that it is equivalent to two cascaded 3rd-order Butterworth filters, making a net 6th-order filter.

High-pass crossover filters which take into account the native response of the tweeter. Classical crossover filters make two assumptions about the loudspeaker drive units. First, they assume that the load impedance is a constant resistance at all frequencies. Second, they assume that the frequency responses of the drive units are flat with zero phase shift in the crossover frequency range. If we were to select drive units and crossover frequencies such that these assumptions were approximately true, we would end up with more drive units than necessary in a complicated and expensive design, because each unit would be working over only part of its usable frequency range.

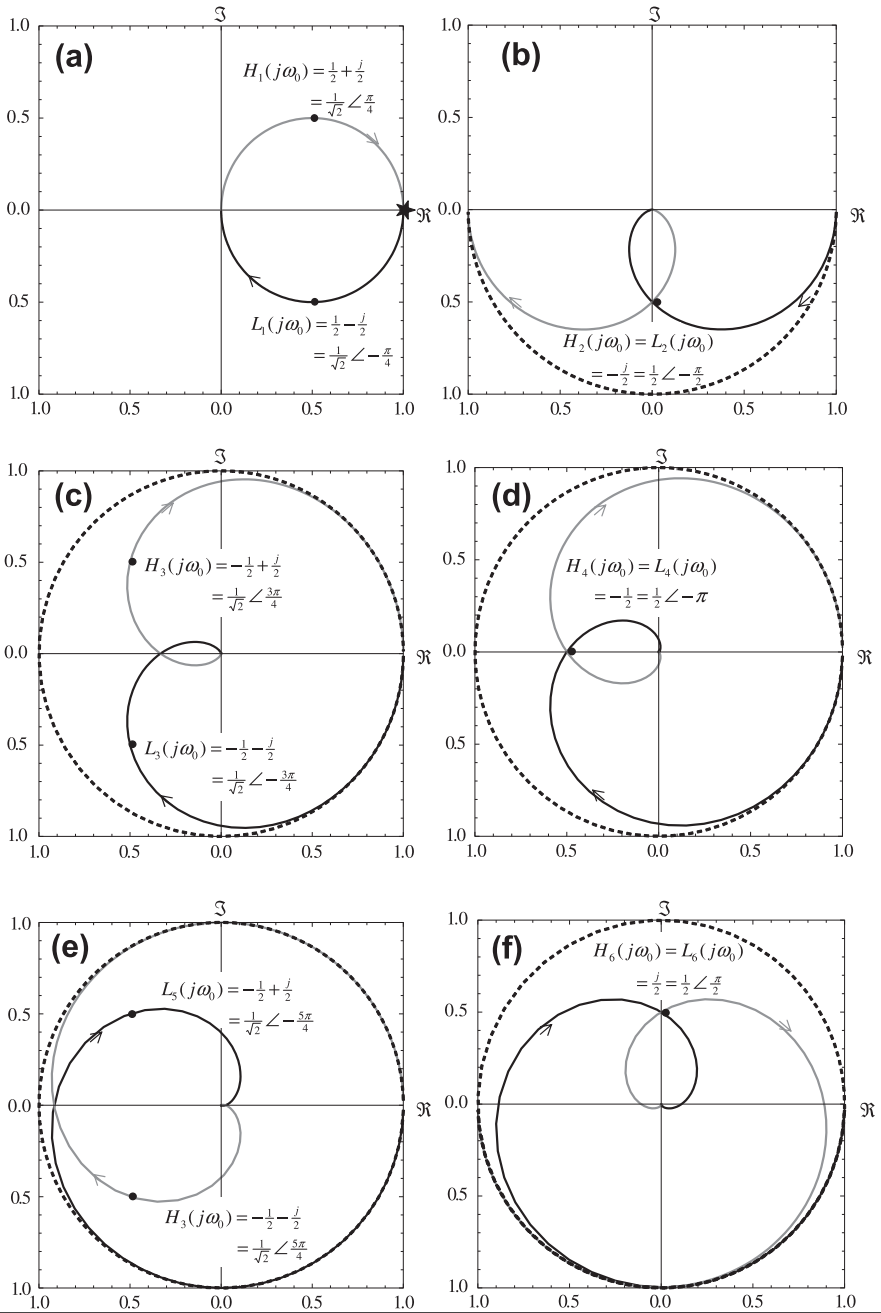
(a)
$H_1(j\omega_0) = \frac{1}{2} + \frac{j}{2}$
$= \frac{1}{\sqrt{2}} \angle \frac{\pi}{4}$
$L_1(j\omega_0) = \frac{1}{2} - \frac{j}{2}$
$= \frac{1}{\sqrt{2}} \angle -\frac{\pi}{4}$
(b)
$H_2(j\omega_0) = L_2(j\omega_0)$
$= -\frac{j}{2} = \frac{1}{2} \angle -\frac{\pi}{2}$
(c)
$H_3(j\omega_0) = -\frac{1}{2} + \frac{j}{2}$
$= \frac{1}{\sqrt{2}} \angle \frac{3\pi}{4}$
$L_3(j\omega_0) = -\frac{1}{2} - \frac{j}{2}$
$= \frac{1}{\sqrt{2}} \angle -\frac{3\pi}{4}$
(d)
$H_4(j\omega_0) = L_4(j\omega_0)$
$= -\frac{1}{2} = \frac{1}{2} \angle -\pi$
(e)
$L_5(j\omega_0) = -\frac{1}{2} + \frac{j}{2}$
$= \frac{1}{\sqrt{2}} \angle -\frac{5\pi}{4}$
$H_3(j\omega_0) = -\frac{1}{2} - \frac{j}{2}$
$= \frac{1}{\sqrt{2}} \angle \frac{5\pi}{4}$
(f)
$H_6(j\omega_0) = L_6(j\omega_0)$
$= \frac{j}{2} = \frac{1}{2} \angle \frac{\pi}{2}$
ℑ
ℜ
1.0
0.5
0.0

3rd-order high-pass filter with a series capacitor. The simplest high-pass filter is just a series capacitor, as shown in Fig. 7.48. Using the same methodology as in Secs. 7.6 and 7.12, we can write the following expression for the radiated sound:

$$\tilde{p}(r) = \frac{\tilde{e}_g BIS_D \rho_0}{(R_g + R_E)M_{MS}} \cdot \frac{e^{-jkr}}{4\pi r} G(s) \tag{7.142}$$

where the 3rd-order frequency-response function $G(s)$ is given by

$$G(s) = \frac{s^3}{s^3 + P_2 s^2 + P_1 s + P_0} \tag{7.143}$$

and the coefficients of the denominator polynomial in $s = j\omega$ are given by

$$P_2 = \frac{\omega_C}{Q_{TC}} + \omega_E \tag{7.144}$$

$$P_1 = \left(\omega_C + \frac{\omega_E}{Q_{MC}}\right)\omega_C \tag{7.145}$$

$$P_0 = \omega_C^2 \omega_E \tag{7.146}$$

where ω_C is the angular resonant-frequency of the tweeter in its closed-box enclosure, Q_{MC} is its mechanical Q factor, Q_{TC} is its total Q factor, and ω_E is the cut-off frequency of the electrical filter comprising the external capacitor C and coil resistance R_E:

$$\omega_E = \frac{1}{R_E C} \tag{7.147}$$

The electrical Q factor is given by

$$Q_{EC} = \frac{Q_{MC} Q_{TC}}{Q_{MC} - Q_{TC}} \tag{7.148}$$

The transfer function of a 3rd-order Butterworth high-pass filter is shown in Fig. 7.46(c) so that

$$P_2 = 2\omega_0 \tag{7.149}$$

FIG. 7.47 Nyquist plots for classical crossover filters in the complex plane: (a) 1st-order; (b) 2nd-order; (c) 3rd-order; (d) 4th-order; (e) 5th-order; (f) 6th-order.

Black solid curves show the low-pass transfer functions $L_n(s)$, gray solid curves the high-pass transfer functions $H_n(s)$, and black dotted curves the resultant all-pass transfer functions $F_n(s) = L_n(s) + H_n(s)$, where $s = j\omega$ is the complex frequency and n is the order of the crossover. Note that for the 1st-order crossover, there is no dotted curve because the resultant is always $+1$, marked by a pentagram. Black dots indicate the crossover frequencies at which $\omega = \omega_0$ and arrows show the direction of increasing frequency. The maximum phase shift of $F_n(s)$ is 0 for $n = 1$, π for $n = 2$, 2π for $n = 3$, 4, 5, and 3π for $n = 6$.

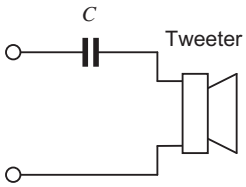

FIG. 7.48 3rd-order high-pass filter in which the native response of tweeter provides the 2nd-order part of the transfer function and the series capacitor provides the 1st-order part.

$$P_1 = 2\omega_0^2 \tag{7.150}$$

$$P_0 = \omega_0^3 \tag{7.151}$$

where ω_0 is the angular crossover frequency. Equating Eqs. (7.144) to (7.146) with Eqs. (7.149) to (7.151) and solving for ω_0, ω_E, and Q_{TC} gives

$$\omega_0^3 - 2Q_{MC}\omega_C\omega_0^2 + Q_{MC}\omega_C^2 = 0 \tag{7.152}$$

which has to be solved for ω_0. Then

$$\omega_E = \frac{\omega_0^3}{\omega_C^2} \tag{7.153}$$

and

$$Q_{TC} = \frac{\omega_C}{2\omega_0 - \omega_E} \tag{7.154}$$

Numerical values for these solutions are given in Table 7.5. A tweeter unit should be chosen which has Q_{MC} and Q_{EC} values that match, as closely as possible, those in one of the rows of the table,

Table 7.5 Parameters for 3rd-order Butterworth high-pass crossover filter using a series capacitor

Q_{MC}	Q_{EC}	Q_{TC}	f_0/f_C	f_E/f_C
1.0	∞	1.0000	1.0000	1.0000
1.2	4.1510	0.9309	0.8921	0.7099
1.5	2.3729	0.9191	0.8318	0.5754
2.0	1.7039	0.9201	0.7892	0.4916
3.0	1.3392	0.9259	0.7564	0.4327
4.0	1.2112	0.9297	0.7424	0.4091
5.0	1.1457	0.9322	0.7346	0.3964
10	1.0343	0.9374	0.7202	0.3735
∞	0.9428	0.9428	0.7071	0.3535

remembering that the Q_{EC} value will be modified by any series resistance added to match the sensitivity of the tweeter to that of the woofer. Then the crossover frequency f_0 is given as a multiple of f_C. For example, if the Q_{MC} and Q_{EC} values are 2 and 1.7 respectively and the resonance frequency is $f_C = 2$ kHz, we use the 4th row of Table 7.5 to arrive at a crossover frequency of

$$f_0 = 0.7892 \times 2 = 1.56 \text{ kHz}$$

and an electrical cut-off frequency of

$$f_E = 0.4916 \times 2 = 0.98 \text{ kHz}$$

If the coil resistance is 6 Ω, the value of the capacitor is then given by

$$C = \frac{1}{2\pi f_E R_E} = \frac{1}{2 \times 3.14 \times 980 \times 6} = 27 \ \mu\text{F}$$

Unfortunately, choosing a tweeter to use with this type of filter is not so easy, as few manufacturers provide much information about their tweeters, which is strange considering that woofers now come with a full set of Thiele–Small parameters practically as standard (Thiele–Small parameters are discussed in Sec. 6.5). Let this be considered as a plea to manufacturers to rectify the situation and provide all the data necessary to design the crossover filter.

Note that for higher values of Q_{MC}, the crossover frequency f_0 is about half an octave below the resonance frequency f_C. Hence the working range of the tweeter is extended. In fact many commercial closed-box loudspeakers have a capacitor in series with the woofer in order to augment the bass response [30]. However, this advantage is reduced as Q_{MC} approaches unity.

4th-order high-pass filter with a series capacitor and shunt inductor. The 4th-order high-pass filter is shown in Fig. 7.49. Using the same methodology as in Secs. 7.6 and 7.12, we can write the following expression for the radiated sound:

$$\tilde{p}(r) = \frac{\tilde{e}_g B I S_D \rho_0}{(R_g + R_E) M_{MS}} \cdot \frac{e^{-jkr}}{4\pi r} \, G(s) \tag{7.155}$$

where the 4th-order frequency-response function $G(s)$ is given by

$$G(s) = \frac{s^4}{s^4 + P_3 s^3 + P_2 s^2 + P_1 s + P_0} \tag{7.156}$$

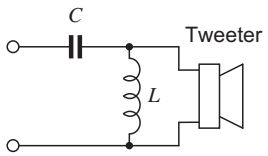

FIG. 7.49 4th-order high-pass filter in which the native response of tweeter provides one 2nd-order part of the transfer function and the series capacitor and shunt inductor provide the other.

and the coefficients of the denominator polynomial in $s = j\omega$ are given by

$$P_3 = \frac{\omega_C}{Q_{TC}} + \frac{\omega_E}{Q_E} \tag{7.157}$$

$$P_2 = \omega_C^2 + \omega_E^2 + \frac{\omega_C \omega_E}{Q_{MC} Q_E} \tag{7.158}$$

$$P_1 = \left(\frac{\omega_E}{Q_{TC}} + \frac{\omega_C}{Q_E}\right)\omega_C \omega_E \tag{7.159}$$

$$P_0 = \omega_C^2 \omega_E^2 \tag{7.160}$$

where ω_C is the angular resonant-frequency of the tweeter in its closed-box enclosure, Q_{MC} is its mechanical Q factor, Q_{TC} is its total Q factor, and ω_E is the cut-off frequency of the electrical filter comprising the external capacitor C and inductor L:

$$\omega_E = \frac{1}{LC} \tag{7.161}$$

The electrical Q factor of the filter is given by

$$Q_E = \omega_E R_E C \tag{7.162}$$

The electrical Q factor of the tweeter is given by

$$Q_{EC} = \frac{Q_{MC} Q_{TC}}{Q_{MC} - Q_{TC}} \tag{7.163}$$

The transfer function of a 4th-order Linkwitz-Riley or $B2^2$ high-pass filter is shown in Fig. 7.46(d), so that

$$P_3 = 2\sqrt{2}\omega_0 \tag{7.164}$$

$$P_2 = 4\omega_0^2 \tag{7.165}$$

$$P_1 = 2\sqrt{2}\omega_0^3 \tag{7.166}$$

$$P_0 = \omega_0^4 \tag{7.167}$$

where ω_0 is the angular crossover frequency. Equating Eqs. (7.157) to (7.160) with Eqs. (7.164) to (7.167) and solving for ω_0, ω_E, and Q_{TC} gives

$$\omega_0^6 - 3\omega_C^2 \omega_0^2 + \frac{2\sqrt{2}\omega_C^3 \omega_0^3}{Q_{MC}} - 3\omega_C^4 \omega_0^2 + \omega_C^6 = 0 \tag{7.168}$$

which has to be solved for ω_0. Then

$$\omega_E = \frac{\omega_0^2}{\omega_C} \tag{7.169}$$

$$Q_E = \frac{\omega_0^2\omega_C^2}{Q_{MC}(4\omega_0^2\omega_C^2 - \omega_0^2 - \omega_C^2)} \tag{7.170}$$

and

$$Q_{TC} = \frac{Q_E\omega_C^2}{\omega_0(2\sqrt{2}Q_E\omega_C - \omega_0)} \tag{7.171}$$

Numerical values for these solutions are given in Tables 7.6 and 7.7. In Table 7.6, the crossover frequency f_0 if *below* the tweeter's resonance frequency f_C and in Table 7.7 f_0 is *above* f_C. The latter is

Table 7.6 Solution 1 parameters for 4th-order Linkwitz–Riley ($B2^2$) high-pass crossover filter using a series capacitor and shunt inductor

Q_{MC}	Q_{EC}	Q_{TC}	f_0/f_C	f_E/f_C	Q_E
$1/\sqrt{2}$	∞	0.7071	1.0000	1.0000	0.7071
1.0	3.2743	0.7660	0.6666	0.4444	0.7660
2.0	1.3924	0.8209	0.5712	0.3263	0.8209
3.0	1.1604	0.8368	0.5506	0.3031	0.8368
4.0	1.0703	0.8444	0.5415	0.2932	0.8444
5.0	1.0224	0.8489	0.5363	0.2876	0.8489
10	0.9380	0.8576	0.5266	0.2773	0.8576
∞	0.8660	0.8660	0.5176	0.2679	0.8660

In this solution the crossover frequency f_0 *is below* the tweeter resonance frequency f_C.

Table 7.7 Solution 2 parameters for 4th-order Linkwitz–Riley ($B2^2$) high-pass crossover filter using a series capacitor and shunt inductor

Q_{MC}	Q_{EC}	Q_{TC}	f_0/f_C	f_E/f_C	Q_E
$1/\sqrt{2}$	∞	0.7071	1.0000	1.0000	0.7071
1.0	3.2743	0.7660	1.5001	2.2502	0.7660
2.0	1.3924	0.8209	1.7506	3.0646	0.8209
3.0	1.1604	0.8368	1.8161	3.2985	0.8368
4.0	1.0703	0.8444	1.8468	3.4107	0.8444
5.0	1.0224	0.8489	1.8646	3.4767	0.8489
10	0.9380	0.8576	1.8989	3.6061	0.8576
∞	0.8660	0.8660	1.9318	3.7321	0.8660

In this solution the crossover frequency f_0 is *above* the tweeter resonance frequency f_C.

a safer solution as it is less likely to lead to excessive diaphragm excursion or a dip in the input impedance. A tweeter unit should be chosen which has Q_{MC} and Q_{EC} values that match, as closely as possible, those in one of the rows of the table, remembering that the Q_{EC} value will be modified by any series resistance added to match the sensitivity of the tweeter to that of the woofer. Then the crossover frequency f_0 is given as a multiple of f_C. For example, if the Q_{MC} and Q_{EC} values are 3 and 1.2 respectively and the resonance frequency is $f_C = 2$ kHz, we use the 4th row of Table 7.7 to arrive at a crossover frequency of

$$f_0 \;=\; 1.8161 \times 2 \;=\; 3.63\ \text{kHz}$$

and an electrical cut-off frequency of

$$f_E \;=\; 3.2985 \times 2 \;=\; 6.60\ \text{kHz}$$

If the coil resistance is 6 Ω, the value of the capacitor is then given by

$$C \;=\; \frac{Q_E}{2\pi f_E R_E} \;=\; \frac{1}{2 \times 3.14 \times 6600 \times 6} \;=\; 3.9\ \mu\text{F}$$

and the value of the inductor is given by

$$L \;=\; \frac{1}{(2\pi f_E)^2 C} \;=\; \frac{1}{(2 \times 3.14 \times 6600)^2 \times 3.9 \times 10^{-6}} \;=\; 150\ \mu\text{H}$$

Effect of phase delay of 2nd-order crossover on time-domain response to square waves. Although we have already discounted the use of a 2nd-order crossover when taking into account the frequency response of the tweeter, this serves as a relatively simple example of what the phase delay of a crossover does to the shape of a square wave. Obviously, the effects will only be more pronounced in higher order crossover filters. A square wave $W(t)$ can be described by an infinite series of sinusoidal waves:

$$W(t) \;=\; \frac{4}{\pi} \sum_{n=0}^{\infty} \frac{\sin \omega_n t}{2n+1} \tag{7.172}$$

where $\omega_n = (2n+1)\omega$ are *odd* harmonics. According to Table 6.2, the Laplace transform of the square wave is

$$W(s) \;=\; \frac{4}{\pi} \sum_{n=0}^{\infty} \frac{\omega_n}{(2n+1)(s^2+\omega_n^2)} \tag{7.173}$$

Thus the frequency domain response of the 2nd-order filter to a square wave is

$$\begin{aligned} G(s) \;&=\; (L_2(s) + H_2(s)) \cdot W(s) \\ &=\; F_2(s) \cdot W(s) \;=\; \frac{\omega_0^2 - s^2}{(\omega_0 + s)^2} \cdot \frac{4}{\pi} \sum_{n=0}^{\infty} \frac{\omega_n}{(2n+1)(s^2+\omega_n^2)} \end{aligned} \tag{7.174}$$

In other words, $G(s)$ is the sum of the outputs of the low-pass and high-pass filters and thus constitutes an all-pass filter. Taking the inverse Laplace transform then gives us the time-domain response to a square wave:

$$g(t) = \frac{1}{2\pi j}\int_{\gamma-j\infty}^{\gamma+j\infty} G(s)e^{st}ds = \frac{4}{\pi}\sum_{n=0}^{\infty}\frac{2\omega_0\omega_n\left(e^{-\omega_0 t}-\cos\omega_n t\right)+\left(\omega_0^2-\omega_n^2\right)\sin\omega_n t}{\left(2n+1\right)\left(\omega_0^2+\omega_n^2\right)} \tag{7.175}$$

The distortion of a square wave produced by the phase delay of a 2nd-order all-pass crossover filter is shown in Fig. 7.50, where the square wave frequency is $f = 1$ kHz and the crossover frequency is $f_0 = 4$ kHz. Clearly, the output waveform is radically different from the input one.

What we have is an imperfect time delay filter. If it were ideal, the phase would increase linearly with frequency in Fig. 7.47 so that it would keep wrapping round indefinitely, whereas in reality it stops at π for $n = 2$, 2π for $n = 3$, 4, 5 and 3π for $n = 6$. Hence the time delay τ decreases above the crossover frequency according to

$$\tau = \frac{\angle F_2(s)}{\omega} = -\frac{2}{\omega}\arctan\frac{\omega}{\omega_0}$$

The effect of this is to delay the low frequencies relative to the high ones so that the sound from the tweeter arrives at the listener before that from the woofer.

The audibility of phase distortion has provoked a lively debate over the years [31–35], but why not design the loudspeaker correctly in the first place so that there need not be any doubt about its accuracy? As we shall see in the next section, the solution to this problem need not be complicated if we approach it holistically and take into account all the factors that affect the response of the loudspeaker, including the baffle effect.

Crossover filters with zero phase shift. In the previous section we studied the waveform distortion produced by classical crossover networks. We also saw that the simplest high-pass filter $H(s)$ is a series capacitor (see Fig. 7.48). Let us now take its transfer function and deduce what low-pass filter $L(s)$ when summed with it will produce an output which is real and constant at all frequencies, that is, simply unity:

$$L(s) + H(s) = 1 \tag{7.176}$$

where

$$H(s) = \frac{s^3}{(s+\omega_0)(s^2+\omega_0 s+\omega_0^2)} \tag{7.177}$$

Hence

$$L(s) = 1 - H(s) = \frac{\omega_0}{s+\omega_0}\cdot\frac{2s^2+2\omega_0 s+\omega_0^2}{s^2+\omega_0 s+\omega_0^2} \tag{7.178}$$

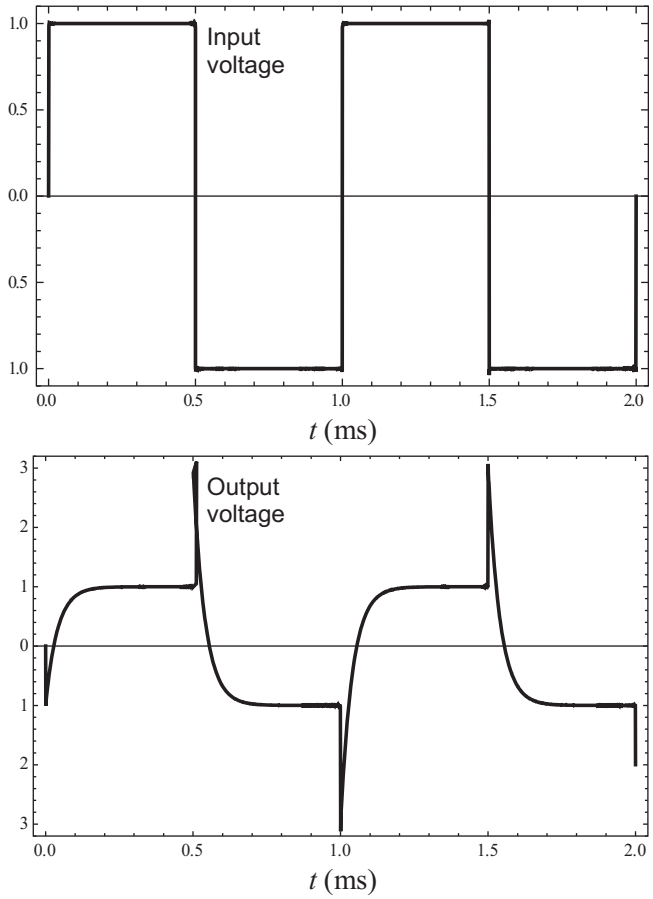

FIG. 7.50 Distortion of a square wave produced by the phase delay of a 2nd-order all-pass crossover filter, where the output voltage is the sum of the output voltages of the low-pass and high-pass filters.

The square wave frequency is 1 kHz and the crossover frequency is 4 kHz.

The first part of this transfer function is just simple 1st-order low-pass filter. The second part is a shelf with a 6 dB boost at frequencies above the crossover frequency ω_0. As it happens, such a boost is provided by the baffle effect whereby the woofer acts as a point source when the wavelength is large compared with the dimensions of the box but behaves like a piston in an infinite baffle when the wavelength is small. Comparing Eq. (7.178) with Eq. (7.38) for the on-axis response of a closed-back piston in free space, we deduce that the ideal crossover frequency is

$$f_0 = c/(2\pi a) \tag{7.179}$$

It should be noted that the methods developed in this chapter are by no means perfect, because of the assumptions we have made about the baffle effect and the drive units behaving as perfectly rigid flat pistons. However, computer algorithms have been developed [36] which can optimize the crossover component values taking into account the measured responses of the drivers.

Example 7.4. Crossover for woofer of Example 7.2. In this example we shall implement a 3rd-order Butterworth high-pass filter using a series capacitor. Because the tweeter will be mounted in a sphere, we shall design a network to compensate for the 6 dB lift associated with a point source in a sphere (see Fig. 7.14). The low-pass section will be designed to give an all-pass overall response with zero phase shift, as discussed in the previous section. Hence the low-pass section will use just a series inductor together with the 6 dB lift due to the baffle effect, using a closed-back piston as a model (see Fig. 7.15). Since the woofer occupies almost the full width of the box, we will take a as 9.4 cm which, using Eq. (7.179), gives us a crossover frequency of

$$f_0 = 344.8/(2 \times 3.14 \times 0.094) = 584 \text{ Hz}$$

Hence the value of the series inductance needed is

$$L_1 = \frac{R_E}{2\pi f_0} = \frac{6.27}{2 \times 3.14 \times 584} = 1.71 \text{ mH}$$

However, the coil inductance is 0.71 mH, so to make up the difference we will use an inductor with a value of $1.71 - 0.71 = 1.0$ mH. Next we need to choose a tweeter suitable for a crossover frequency of 584 Hz. The SEAS model 27TTFNC/GW has a resonance frequency of $f_C = 750$ Hz and its 27 mm titanium dome has a very high stiffness to mass ratio, which gives an extended flat frequency response. The effective area of the dome is $S_D = 7$ cm^2. The maximum sound pressure of the woofer has already been specified as 99 dB SPL at a distance of $r = 1$ m. At the crossover frequency f_0, the sound pressure produced by the tweeter is 3 dB less than this, that is 96 dB SPL, and decreases at a rate of 18 dB/octave below f_0. The peak displacement at f_0 is obtained from Eq. (6.35), except that here we double the result because at f_0 the tweeter is radiating omnidirectionally rather than into half-space from an infinite baffle

$$\eta_{\text{peak}} = \frac{2\sqrt{2}r \times 10^{\frac{\text{SPL}}{20}-5}}{\pi f^2 \rho_0 S_D} = \frac{2 \times 1.414 \times 1 \times 10^{\frac{96}{20}-5}}{3.14 \times 584^2 \times 1.18 \times 7 \times 10^{-4}} = 2\text{mm}$$

Although this is stretching the tweeter to its absolute limit, this limit is unlikely to be reached under normal listening conditions as, at frequencies above and below f_0, the displacement is reduced. Using the method described in Sec. 6.10 for measuring the Thiele–Small parameters, we estimate the Q factors from the manufacturer's impedance curve to be

$$Q_{EC} = 1.2$$

$$Q_{MC} = 2.1$$

Also, the quoted sensitivity is 91.5 dB SPL in a baffle at 1 m with an input voltage of 2.83 Vrms or 85.5 dB SPL in free space. However, the woofer has a sensitivity of 80.2 dB SPL in free space, so the

tweeter needs a series resistance to match its sensitivity to that of the woofer. If $R_E = 4.9\ \Omega$, then the series resistor value is

$$\begin{aligned} R_1 &= R_E\left(10^{(\textit{Tweeter Senitivity}-\textit{Woofer Sensitivity})/20} - 1\right) \\ &= 4.9 \times \left(10^{(85.5-80.2)/20} - 1\right) = 4.1\ \Omega \approx 3.9\ \Omega \end{aligned}$$

This will modify the value of Q_{EC} as follows:

$$Q_{EC} = \left(1 + \frac{R_1}{R_E}\right) Q_{EC} = \left(1 + \frac{3.9}{4.9}\right) \times 1.2 = 2.2$$

The values of Q_{MC} and Q'_{EC} are close enough to those of the 4th row of Table 7.5 for us to establish the optimum crossover and electrical cut-off frequencies f_0 and f_E respectively:

$$f_0 = 0.789 \times f_C = 0.789 \times 750 = 592\ \text{Hz}$$

$$f_E = 0.492 \times f_C = 0.492 \times 750 = 369\ \text{Hz}$$

from which we determine the series capacitor value:

$$C_1 = \frac{1}{2\pi f_E(R_E + R_1)} = \frac{1}{2 \times 3.14 \times 369 \times (4.9 + 3.9)} = 49\ \mu\text{F} \approx 47\ \mu\text{F}$$

Happily, the value of f_0 practically coincides with that which we determined from Eq. (7.179) at the beginning of this example. Finally, we need to correct for the 6 dB lift in the response of the tweeter due to the baffle effect. We will simplify this by mounting the tweeter on a wooden sphere so that we can model it as a point source on a sphere of radius $R = 7.5$ cm. We then equalize the 6 dB lift using the shelf filter involving L_2 in parallel with R_2. In order to produce a 6 dB cut, we set

$$R_2 = R_1 + R_E = 3.9 + 4.9 = 8.8\ \Omega \approx 8.2\ \Omega$$

Then the transfer function of the point source on a sphere (producing a 6 dB lift) is the inverse of the transfer function of the shelf filter:

$$D(0) = \frac{2s + R_2/L_2}{s + R_2/L_2}$$

Comparing this with Eq. (7.36) for the point source on a sphere yields

$$L_2 = \frac{R_2 R}{2c} = \frac{8.2 \times 0.075}{2 \times 344.8} = 0.89\ \text{mH} \approx 1\ \text{mH}$$

Thus the 6 dB transition takes place between $f_1 = R_2/(2\pi L_2) = 1.3$ kHz and $f_2 = R_2/(\pi L_2) = 2.6$ kHz, which is far enough above the crossover frequency of $f_0 = 592$ Hz for this network not to interfere significantly with the operation of the crossover network. The network is shown in Fig. 7.51.

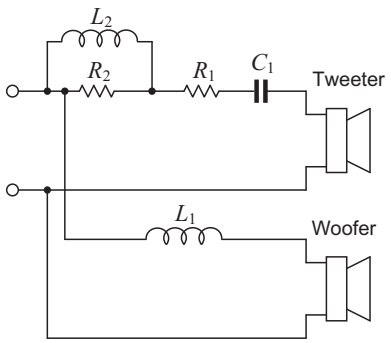

FIG. 7.51 Crossover network of Example 7.4 with a crossover frequency of $f_0 = 592$ Hz.

The values of the crossover circuit elements are $R_1 = 3.9\ \Omega$ (25 W), $R_2 = 8.2\ \Omega$ (15 W), $L_1 = L_2 = 1$ mH, and $C_1 = 50\ \mu$F. The woofer is a Bandor type 100DW/8A mounted in a closed-box baffle as described in Example 7.2 and shown Fig. 7.18. The tweeter is a SEAS type 27TTFNC/GW mounted in a 15 cm diameter sphere.

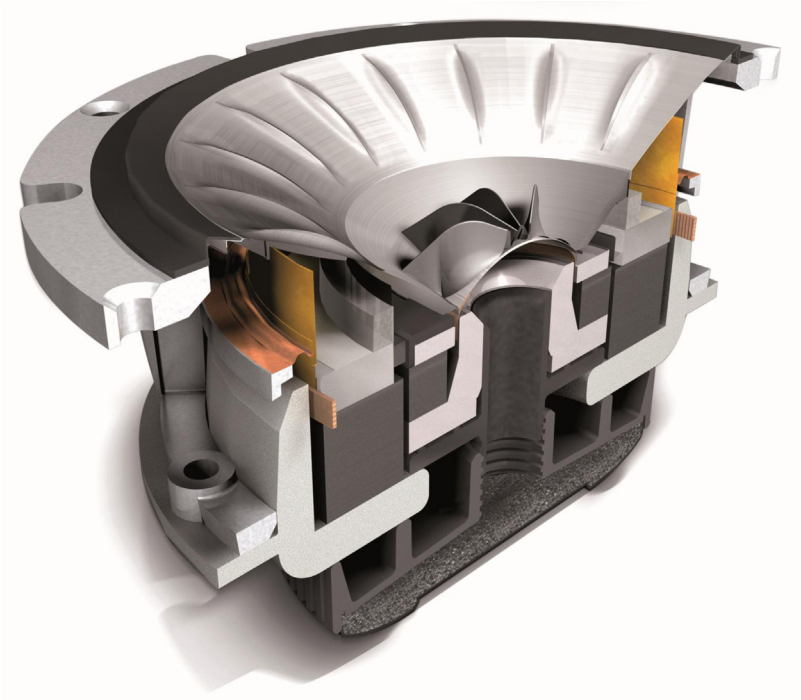

FIG. 7.52 Section view of a Blade UniQ two-way drive unit.

The tweeter is located at the center of the woofer behind a "tangerine" phase plug and has its own independent voice coil. Note that the woofer diaphragm is driven half way along its radius in order to eliminate the first radial mode together with its odd-order harmonics.

Courtesy of KEF.

7.21 DUAL CONCENTRIC DRIVE UNITS

A difficulty with mounting a woofer and tweeter side by side or one above the other is that the path that the sound has to travel from each of the loudspeakers to a listener will be different in different parts of the listening room. Hence, in the vicinity of the crossover frequencies, cancellation of the sound will result at some parts of the room, and addition will occur at others.

To avoid this effect, the loudspeakers are sometimes mounted *concentrically* i.e., the tweeter is placed behind and on the axis of the woofer (see Fig. 7.52). In this arrangement, the diaphragm of the woofer acts as a horn and the tweeter usually has a phase plug in front of it. Horn loudspeakers will be discussed in greater detail in Chapter 9.

References

[1] Small RH. Closed-Box Loudspeaker Systems Part I: Analysis. J Audio Eng Soc 1972;20(10):798–808.
[2] Small RH. Closed-Box Loudspeaker Systems Part II: Synthesis. J Audio Eng Soc 1973;21(1):11–8.
[3] Backman J. Improvement of One-Dimensional Loudspeaker Models, in the 123rd AES Convention 2007. paper no. 7253.
[4] Attenborough K. Acoustical Characteristics of Porous Materials. Phys Rep 1982;82(2):179–227.
[5] Zarek JHB. Sound Absorption in Flexible Porous Materials. J Sound Vib 1978;61(2):205–34.
[6] Delany ME, Bazley EN. Acoustical Properties of Fibrous Absorbent Materials. Appl Acoust 1970;3: 105–16.
[7] Miki Y. Acoustical Properties of Porous Materials, Modification of Delany-Bazley Models. J Acoust Soc Jpn 1990;11:19–24(E).
[8] Sides DJ, Attenborough K, Mulholland KA. Application of a Generalized Acoustic Propagation Theory of Fibrous Absorbents. J Sound Vib 1971;19:49–64.
[9] At 1000 Hz, a wavelength at 22°C is about 35 cm; at 500 Hz, 70 cm; at 2000 Hz, 17.5 cm; and so on.
[10] Backman J. Computation of Diffraction for Loudspeaker Enclosures. J Audio Eng Soc 1989;37(5): 353–62.
[11] Vanderkooy J. A Simple Theory of Cabinet Edge Diffraction. J Audio Eng Soc 1991;39(12):923–33.
[12] Svensson UP. Line Integral Model of Transient Radiation from Planar Pistons in Baffles. Acta Acust Acust 2001;87:307–15.
[13] Thuras AL. U.S. Patent No. 1,869,178. Sound Translating Device July, 1932 (filed 1930).
[14] Locanthi BN. Applications of Electric Circuit Analogies to Loudspeaker Design Problems, IRE Trans. Audio, PGA-6: 15 (1952); republished in. J Audio Eng Soc 1971;19(9):778–85.
[15] Novak JF. Performance of enclosures for high-compliance loudspeakers. J Audio Eng Soc 1959;7(1): 29–37.
[16] Thiele AN. Loudspeakers in Vented Boxes, Proc. IREE 22: 487 (1961); republished in J Audio Eng Soc 1971;19(5):382–92 and 1971;19(6):471–83.
[17] Small RH. Vented-Box Loudspeaker Systems Part I: Small-Signal Analysis. J Audio Eng Soc 1973;21(5):363–72.
[18] Small RH. Vented-Box Loudspeaker Systems Part II: Large-Signal Analysis. J Audio Eng Soc 1973;21(6):438–44.
[19] Small RH. Vented-Box Loudspeaker Systems Part III: Synthesis. J Audio Eng Soc 1973;21(7):549–54.
[20] Small RH. Vented-Box Loudspeaker Systems Part IV: Appendices. J Audio Eng Soc 1973;21(8):635–9.
[21] Mellow TJ. A New Set of Fifth and Sixth-Order Vented-Box Loudspeaker System Alignments using a Loudspeaker-Enclosure Matching Filter: Part I, in the 112th AES Convention 2002. paper no. 5505.

[22] Mellow TJ. A New Set of Fifth and Sixth-Order Vented-Box Loudspeaker System Alignments using a Loudspeaker-Enclosure Matching Filter: Part II, in the 112th AES Convention 2002. paper no. 5506.
[23] Linkwitz SH. Active Crossover Networks for Noncoincident Drivers. J Audio Eng Soc 1976;24(1):2–8.
[24] Linkwitz SH. Passive Crossover Networks for Noncoincident Drivers. J Audio Eng Soc 1978;28(3): 149–50.
[25] Bullock III RM. Loudspeaker-Crossover Systems: An Optimal Crossover Choice. J Audio Eng Soc 1982;30(7/8):486–95.
[26] Vanderkooy J, Lipshitz SP. Power Response of Loudspeakers with Noncoincident Drivers – the Influence of Crossover Design. J Audio Eng Soc 1986;34(4):236–44.
[27] Hawksford MOJ. Asymmetric All-Pass Crossover Alignments. J Audio Eng Soc 1993;41(2):123–34.
[28] Thiele AN. Passive All-Pass Crossover System of Order 3 (Low Pass) + 5 (High Pass), Incorporating Driver Parameters. J Audio Eng Soc 2002;50(12):1030–8.
[29] Thiele AN. Implementing Asymmetrical Crossovers. J Audio Eng Soc 2007;55(10):819–32.
[30] Recklinghausen DR. Low-Frequency Range Extension of Loudspeakers. J Audio Eng Soc 1985;33(6): 440–6.
[31] Mathes RC, Miller RL. Phase Effects in Monaural Perception. J Acoust Soc Am 1947;19(5):780–97.
[32] Craig JH, Jeffress LA. Effect of Phase on the Quality of a Two-Component Tone. J Acoust Soc Am 1962; 34(11):1752–60.
[33] Cabot RC, Mino MG, Dorans DA, Tackel IS, Breed HE, Detection. of Phase Shifts in Harmonically Related Tones. J Audio Eng Soc 1976;24(7):568–71.
[34] J.R. Ashley, Group and Phase Delay Requirements for Loudspeaker Systems, Proc. IEEE Int. Conf. on Acoustics, Speech, and Signal Processing (Denver, CO, 1980 Apr. 9–11), 1980;3:1030–33.
[35] Lipshitz SP, Pocock M, Vanderkooy J. On the Audibility of Midrange Phase Distortion in Audio Systems. J Audio Eng Soc 1982;30(9):580–95.
[36] Schuck PL. Design of Optimized Loudspeaker Crossover Networks Using a Personal Computer. J Audio Eng Soc 1986;34(3):124–42.
[37] Villchur EM. Problems of bass reproduction in loudspeakers. J Audio Eng Soc 1957;5(3):122–6.
[38] See IEC 60268–5, ed. 3.1, "Sound system equipment - Part 5: Loudspeakers," available from http://webstore.iec.ch/. For example, for a nominal 8-in (200 mm) diameter loadspeaker, the baffle size would be 1.65 m long by 1.35 m wide, with the loadspeaker offset from the center by 22.5 cm lengthways and 15 cm widthways.
[39] Thiele AN. Estimating the loudspeaker response when the vent output is delayed. J Audio Eng Soc 2002;50(3):173–5.
[40] Wright JR. The virtual loudspeaker cabinet. J Audio Eng Soc 2003;51(4):244–7.
[41] Venegas R, Umnova O. Acoustical properties of double porosity granular materials. J Acoust Soc Am. 2011;130(5):2765–76.
[42] Werner RE. Effect of negative impedance source on loudspeaker performance. J Audio Eng Soc 1957;29(3):335–40.